APPLICATION OF COMPUTER TECHNIQUES TO SOME PROBLEMS IN LINEAR VISCOELASTICITY

Joseph W. Sell

William C. Forsman

A technical report to the National Aeronautics and Space Administrations on research under Grant No. NsG 667.

Contractor: UNIVERSITY OF PENNSYLVANIA

Address: The School of Chemical Engineering
University of Pennsylvania
Philadelphia, Pennsylvania 19104

Principal Investigator: William C. Forsman
Assistant Professor
School of Chemical Engineering

Associate Investigators: R. I. Wolkowicz, J. W. Sell,
H. S. Grand and A. P. Sikri

Date Submitted: June 21, 1967

FORWARD

Contract NsG 667 was initiated to study molecular mechanisms of flow of concentrated polymer solutions and polymer melts. Considerable evidence has now been presented suggesting that the rapidly decreasing (non-Newtonian) viscosity of polymer melts and solutions with increasing shear rate is a result of disentanglement of polymer chains.* Since entanglement density can be determined from measurements of linear viscoelastic behavior, we are planning to make such measurements on polymer melts and solutions subjected to varying rates of steady state shear. We thus expect to measure directly entanglement density and viscosity as functions of shear rate. This technical report gives computer solutions to some of the problems associated with analysis of experimental data and interpretation of results in terms of molecular theories of linear viscoelasticity. This report, is, in essence, the M.S. thesis of one of the associate investigators, Mr. Joseph W. Sell.

In addition to support from NASA, we would like to acknowledge additional support from the Ford Foundation and the Computer Center of the University of Pennsylvania.

---

*Porter, Roger S. and Johnson, Julian F., Chem. Rev., 66, 1 (1966).

Table of Contents

Appendices

List of Figures

List of Tables

Abstract

In Part A of this thesis, we examine the affect on calculated viscoelastic functions of gradually introducing entanglement coupling in the Williams, Landel, and Ferry (WLF) modification of Rouse's theory of viscoelasticity. An empirical equation is proposed that makes the segmental friction factor a function of the molecular weight and the critical chain length between entanglement points. This device bridges the gap between entangled and unentangled modes of motion in the distribution of relaxation times by placing some relaxation times in the void created by the WLF modification. The value selected for the adjustable parameter in our empirical equation affects the viscoelastic functions only in the plateau region. Calculated loss moduli and loss compliances are most notably altered by this extension of the theory and are brought into closer correspondence with experimentally determined functions.

Part B of this thesis uses the data from Part A to test the validity of a number of approximate equations for the interconversion of the various viscoelastic functions. These equations generally approximate well

the viscoelastic functions in regions where the relaxation spectrum has a slope of about -1/2 on a log-log plot. Where the relaxation spectrum exhibits a plateau region, a number of the interconversion equations gave poor approximations. None of the interconversion equations are applicable in regions where the relaxation spectrum is discrete.

PART A

The Influence of Entanglements on Several Linear Viscoelastic Functions Using an Empirical Entanglement Coupling Function.

Definitions

A number of inter-related functions characterize the linear viscoelastic behavior of polymers. We will consider only shear deformation and define the following parameters:

(1.) γ_o , a constant strain;

(2.) $\gamma(t)$, a time varying strain;

(3.) γ^*, a strain varying sinusoidally with time at an angular frequency of ω radians per second;

(4.) τ_o , a constant stress;

(5.) $\tau(t)$, a varying stress;

(6.) τ^*, a stress varying sinusoidally with time at an angular frequency of ω radians per second.

The viscoelastic functions of interest in this thesis are listed below.

(1.) The stress relaxation modulus, G(t), is the proportionality between the stress and a constant strain and is given by

$$\tau(t) = G(t)\gamma_o \mathcal{U}(t) \qquad (A.1)$$

where $\mathcal{U}(t)$ is the unit step function, i.e., $\mathcal{U}(t) = 1$ if $t > 0$ and $\mathcal{U}(t) = 0$ if $t < 0$.

(2.) The dynamic modulus, $G^*(\omega)$, is the ratio of the response stress to the imposed sinusoidally varying strain

$$G^* = \tau^*/\gamma^*. \qquad (A.2)$$

The dynamic modulus is usually written as

$$G^* = G' + i\,G'' \qquad (A.3)$$

where

$$i = \sqrt{-1}\,. \qquad (A.4)$$

The real part, G', is called the storage modulus; the imaginary part, G", is the loss modulus.

(3.) The creep compliance, J(t), is the proportionality between the strain and a constant stress and is expressed as

$$\gamma(t) = J(t)\tau_o\mathcal{U}(t). \qquad (A.5)$$

Usually $J(t) \neq G(t)$.

(4.) The dynamic compliance, $J^*(\omega)$, is the ratio of the response strain to the imposed sinusoidally varying stress

$$J^* = \gamma^*/\tau^*. \qquad (A.6)$$

The dynamic compliance is usually written as

$$J^* = J' - i\,J''. \qquad (A.7)$$

The real part, J', is called the storage compliance and the imaginary part, J", is the loss compliance. The dynamic compliance equals the reciprocal of the dynamic modulus

$$J^* = 1/G^*. \qquad (A.8)$$

(5.) The dynamic viscosity, η^*, relates the rate of strain, $\dot{\gamma}^*$, with the sinusoidally varying stress and is expressed as

$$\eta^* = \tau^*/\dot{\gamma}^*. \qquad (A.9)$$

It can be shown that

$$\eta^* = G^*/(i\omega). \qquad (A.10)$$

The real part of the dynamic viscosity, η', equal to G''/ω and its imaginary part, η'', equal to G'/ω .

To fit experimental observations, a set of relaxation processes can be used to describe viscoelastic moduli such as

$$G(t) = \sum_i G_i \, EXP(-t/\tau_i) + G_e \qquad (A.11)$$

and

$$G^*(\omega) = \sum_i \left[G_i \omega^2 \tau_i^2/(1 + \omega^2\tau_i^2)\right] + G_e + i \sum_i \left[G_i \omega \tau_i/(1 + \omega^2\tau_i^2)\right] \qquad (A.12)$$

for the discrete set of relaxation processes. The equilibrium modulus, G_e. is equal to the limit of G(t) as t approaches infinity and G'(ω) as ω approaches zero. The G_i are the spring constants and the τ_i, which are equal to η_i/G_i, are the relaxation times associated with the elements of a generalized Maxwell model (see Figure 1).

If the relaxation times are sufficiently close together, linear viscoelastic behavior would be appropriately characterized by a continuous distribution of relaxation processes. The summations are then replaced by integrations as follows:

$$G(t) = \int_{-\infty}^{\infty} H(\tau)\ EXP(-t/\tau)\ d(\ln\tau) + G_e \qquad (A.13)$$

and

$$G^*(\omega) = \int_{-\infty}^{\infty} \left[H(\tau)\ \omega^2\tau^2/(1+\omega^2\tau^2)\right] d(\ln\tau) + G_e$$
$$i\int_{-\infty}^{\infty} \left[H(\tau)\omega\tau/(1+\omega^2\tau^2)\right] d(\ln\tau) \qquad (A.14)$$

where $H(\tau)$ is the distributiin of relaxation times.

A set of retardation processes is a convenient representation of the observed experimental behavior of viscoelastic compliances. Using a discrete set of retardation processes, the creep compliance is found to be

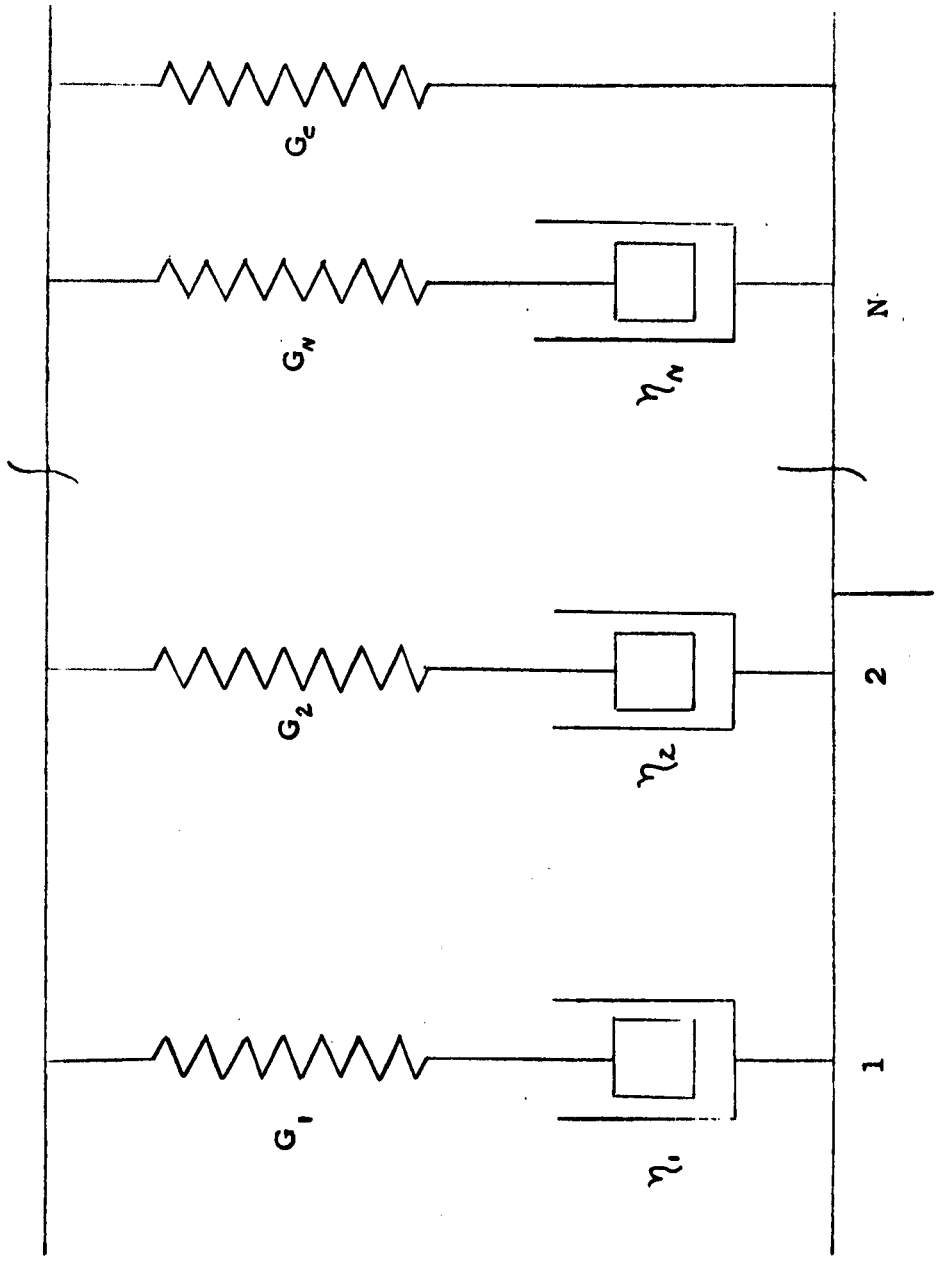

FIGURE 1 MAXWELL MODEL

$$J(t) = \sum_i J_i \left[1 - EXP(-t/\tau_i)\right] + Jg + t/\eta \qquad (A.15)$$

and dynamic compliance is

$$J^*(\omega) = Jg + \sum_i \left[J_i/(1 + \omega^2\tau_i^2)\right] - i\left\{\sum_i \left[J_i\omega\tau_i/(1 + \omega^2\tau_i^2)\right] + 1/(\omega\eta)\right\} . \qquad (A.16)$$

The glassy compliance, Jg, is the limit of J(t) as t approaches zero and the limit of J'(ω) as ω approaches infinity. The J_i are the spring constants and τ_i, which are equal to $\eta_i J_i$, are the retardation times of the elements of a generalized Voigt model (see Figure II). The term η is the steady-state viscosity of the polymer and can be shown to equal $\sum_i \eta_i$.

If the retardation times are sufficiently close together, the summations may be replaced by integrations as follows:

$$J(t) = Jg + \int_{-\infty}^{\infty} L(\tau)\left[1 - EXP(-t/\tau)\right] d(\ln\tau) + t/\eta \qquad (A.17)$$

and

$$J^*(\omega) = Jg + \int_{-\infty}^{\infty} \left[L(\tau)/(1 + \omega^2\tau^2)\right] d(\ln\tau) - i\left\{\int_{-\infty}^{\infty} \left[L(\tau)\omega\tau/(1 + \omega^2\tau^2)\right] d(\ln\tau) + 1/(\omega\eta)\right\} \qquad (A.18)$$

where $L(\tau)$ is the retardation spectrum.

The relaxation and retardation spectra are related by the expressions (2.a)

VOIGT MODEL FIGURE 2

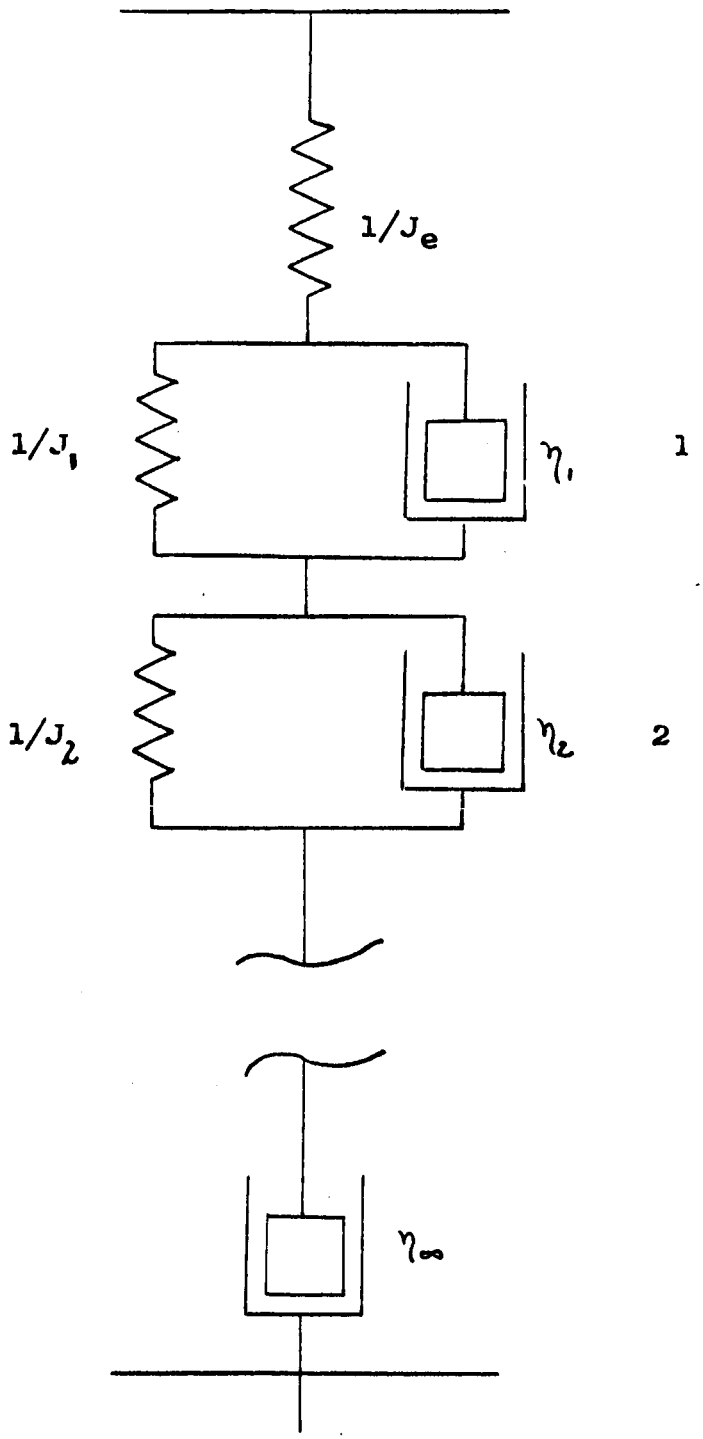

$$L = H/\left[\left\{ G_e - \int_{-\infty}^{\infty} \left[H(u)/(\tau/u-1) \right] \, d(\ln u) \right\}^2 + \pi^2 H^2 \right] \quad (A.19)$$

and

$$H = L/\left[\left\{ J_g + \int_{-\infty}^{\infty} \left[L(u)/(1-u/\tau) \right] \, d(\ln u) - \tau/u \right\}^2 + \pi^2 L^2 \right] \quad (A.20)$$

Background and Theory

The treatment of linear viscoelastic behavior of polymers will be introduced by a discussion of experimental observations and a qualitative explanation of the observed phenomenon. A discussion of Rouse's and Bueche's theories of linear viscoelastic behavior is presented, followed by the combination of these theories by Williams, Landel, and Ferry. These theoretical considerations are related to the observed experimental results. The theoretical developments of viscosity (we mean zero shear rate viscosity) of Bueche and Chikahisa are described.

I. Experimental Linear Viscoelastic Behavior

Molecular motion gives rise to viscoelastic behavior. The viscoelastic functions characteristic of this behavior can be explained in terms of molecular mechanics. These functions of amorphous, uncrosslinked polymers exhibit four characteristic regions which are explained by their corresponding molecular behavior.

(1.) The glassy zone, where moduli are of the order of magnitude of 10^{10} dynes/cm^2 and compliances of 10^{-10} cm^2/dyne, occurs at small times or high

frequencies where the local molecular motion is bond bending and stretching in the chain backbone and pendant groups. Here, viscoelastic behavior is nearly molecular weight independent.

(2.) The transition zone occurs at greater times or lower frequencies than the glassy zone with moduli of the order of 10^8 dynes/cm.^{2} and compliances of the order of 10^{-8} cm.^{2}/dyne. In this region, viscoelastic behavior depends on various degrees of cooperative backbone motion of the polymer molecule and is independent of molecular weight if it is sufficiently high.

(3.) The plateau or rubbery zone occurs at even larger times or lower frequencies. Typical values of the moduli are about 10^7 dynes/cm.^{2} and of compliances about 10^{-7} cm.^{2}/dyne. Here, configurational backbone rearrangements involving molecular entanglements are prevalent. Polymers of sufficiently

high molecular weight exhibited this behavior.

(4.) The terminal or viscous flow zone occurs after nearly all the coordinated motion of the macromolecule is completed and results from the steady-state motion of the independent polymer molecules. The steady-state viscosity, η , which determines this viscoleastic behavior, is molecular weight dependent. (1.a, 2.a)

Viscoelastic behavior of polymers is often characterized by a distribution of relaxation times. A simplified description of the log(H) - log(τ) plot for sufficiently high molecular weight polymers is a "box" and a "wedge" (see Figure 3.A). The "box" section appears at the long time end of the spectrum and determines behavior in the plateau and terminal zones. Its width was found to be molecular weight dependent and its nature is thought to be determined by molecular entanglements. The "wedge" section appears at the short end of the spectrum and determines behavior in the glassy transition zone. It has a slope of approximately -1/2 and its nature is interpreted as being due to coordinated motion of the polymer chain (3., 4., 5., 6., 7.).

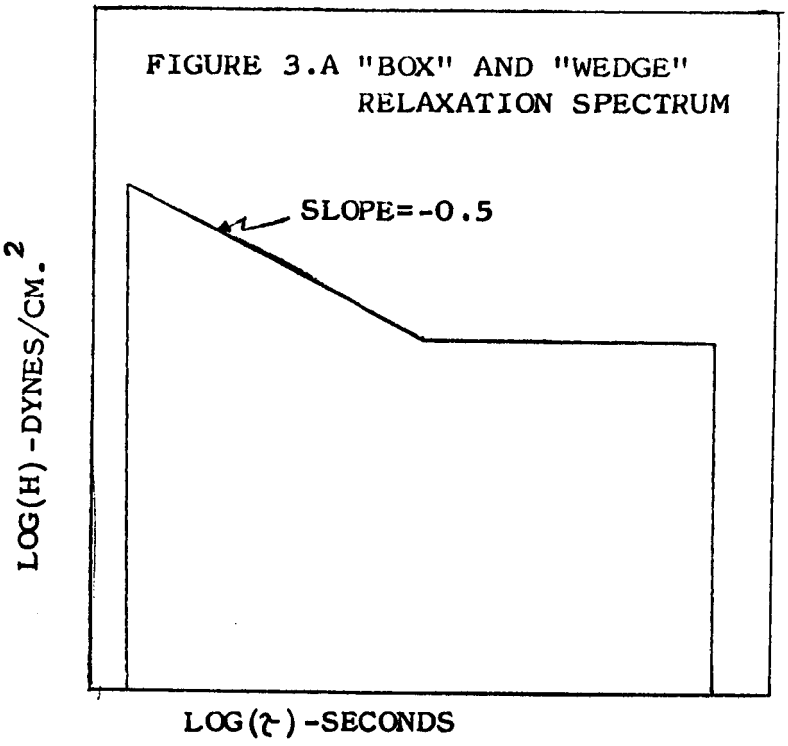

FIGURE 3.A "BOX" AND "WEDGE" RELAXATION SPECTRUM

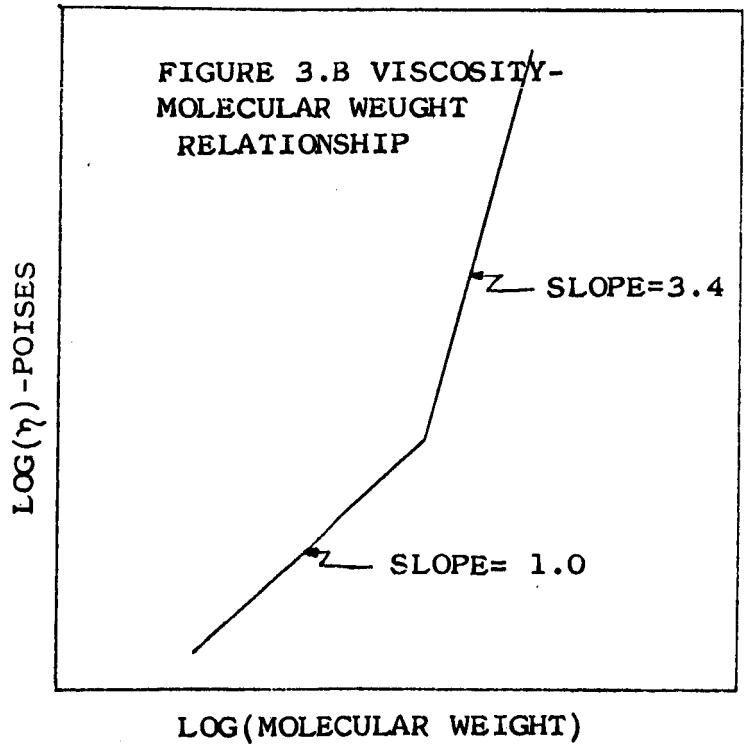

FIGURE 3.B VISCOSITY-MOLECULAR WEUGHT RELATIONSHIP

In studies of viscosity as a function of molecular weight, various experimenters (1.c, 2.a, 8., 9., 10.) havenoted that the plot log (η) versus log (M) for polymers in bulk and concentrated solution consisted of two straight lines which intersect at a critical molecular weight (see Figure 3.B). For lower molecular weights, the line has a slope between 1 and 2; for higher molecular weights, a slope of 3.4. The break in the log (η)- log (M) curve defines the critical molecular weight, Mc.

At the higher molecular weights, it is assumed that polymer systems exhibit long relaxation times enhanced by the coordinated flow through chain entanglements. This produces the observed abrupt increase in the viscosity dependence on the molecular weight and the onset of a rubbery region (3.). The flow behavior above the critical molecular weight is dependent on a slippage factor for the intermolecular couplings (i.e., entanglements)(11.).

Polystyrene at 217^{o}C illustrates these experimental results. Fox and Flory (12.) found the following pair of equations represented their data on fractionated

polystyrene samples at 217°C:

$$\log(\eta) = 1.65 \log(M) - 5.38 \qquad 38{,}000 > M \geq 4{,}000 \qquad (A.21)$$

$$\log(\eta) = 3.4 \log(M) - 13.40 \qquad M > 38.000. \qquad (A.22)$$

Herman et al (9.) report an empirical viscosity-molecular relationship for isotatic polystyrene at 281°C. We converted their equation to 217°C and their equation became

$$\log(\eta) = 3.4 \log M - 13.43 \qquad M \geq 40{,}000. \qquad (A.23)$$

Above a critical molecular weight of 40,000, it is generally agreed that the viscosity is proportion to $M^{3.4}$ (10., 13., 14.).

Nevertheless, there are some conflicting data which demonstrated that viscosity is proportional to $M^{3.14}$ for monodispersed polystyrene (15.). The same samples as Tobolsky et al (14.), who reported that viscosity was proportional to $M^{3.4}$, were used. Tobolsky and Aklonsis (7.) found that the viscosity becomes proportional to $M^{4.0}$ above a molecular weight considerably greater than Mc.

II. Molecular Theories on Linear Viscoelasticity

A. Rouse's Theory

To describe the complicated motion of polymer

molecules, Rouse (16.) assumed that the randomly coiled macromolecules can be mathematically divided into N submolecules of equal length. The submolecules were of sufficient length to assure that the distribution of end-to-end distances was approximately Guassian, but short enough that the mass of each submolecule could be considered concentrated at the end of the subchain. When the submolecule obeyed these restrictions, the theory of rubber elasticity showed that each segment would act as a Hookean spring. Thus, Rouse's model reduced the macromolecule to a series of N + 1 beads connected by N Hookean springs. The root-mean-square end-to-end distance of each segment, σ', equalled the unstressed length of the spring. The spring constant was equal to $3kT/(2\sigma^2)$ where k is Boltzman's constant and T is the absolute temperature (17.). A friction factor, f_o, characterized the resistance to motion of a submolecule. With this model, Rouse considered the mechanics of a single polymer molecule. Its environment was imagined as a continuum consisting of other polymer and solvent molecules in the system. Thus, the only hydrodynamic interaction considered was the frictional

drag on the masses as they moved through this continuum. Rouse wrote the equations of motion for each of the N + 1 masses in a sinusoidally varying force field including the forces exerted by the N springs. The equation of motion of each mass included the position coordinates of the two adjacent masses. Rouse's N + 1 simultaneous differential equations were, thus, impossible to solve in the original coordinate system. An orthogonal transformation to a set of normal coordinates resolved the cooperative motions of the molecule into a series of independent normal modes with relaxation times, τ_p , given by

$$\tau_p = \sigma^2 f_o / \left\{ 24k\ T\ \mathrm{SIN}^2 \left[P\pi/(2N + 2) \right] \right\} . \qquad (A.24)$$

The integer index, P, runs from unity to N and specifies the normal mode of motion and its associated relaxation time. The normal mode of motion with P equal to unity corresponded to motion of the entire chain; with P equal two, the coordinated motion of half of the chain. Subsequent values of the index have a corresponding meaning. The relaxation spectrum comes directly from the relaxation times and is discrete. It is given by

$$H = n\ k\ T \sum_{i=1}^{N} \tau_p\ \delta (\tau - \tau_p) \qquad (A.25)$$

where n is the number of molecules per unit volume and δ is the Dirac delta function. Since the mathematical subdivision of the polymer molecule was arbitrary, Rouse's theory would not be expected to be valid for very short relaxation times (i.e., the relaxation spectrum above 10^7 dynes/cm^2). At short times, the details of the backbone structure, not coordinated chain motion, determine the viscoelastic behavior of the polymer molecule. Thus, Rouse's theory breaks down as the relaxation times approach τ_N (18., 19.).

When P is much less than N, the SIN term in Equation A.24 becomes nearly equal to the argument of the SIN (2.a). Replacing the SIN with its argument and using the relationship

$$\sigma^2 f_o N^2 = a^2 Z_1^2 \zeta_o \qquad (A.26)$$

reduces the expression for the relaxation times to

$$\tau_p = a^2 Z_1^2 \zeta_o / (6\pi^2 p^2 k T). \qquad (A.27)$$

The effective root-mean-square end-to-end distance of one repeat unit, a, is defined by

$$\sigma\sqrt{N} = a\sqrt{Z_1} \qquad (A.28)$$

with Z_1, the degree of polymerization. ζ_o is the monomer friction factor. This expression is a close approximation

for $P \leq N/3$, which is the region where Rouse's theory is valid.

Rouse's theory predicts that slope of $\log(H) - \log(\dot{\gamma})$ plot is -0.5 which is the "wedge" portion of the relaxation spectrum (see Appendix VII). This theory cannot explain the "box" segment of the spectrum.

B. Bueche's Theory

Bueche (20., 21.) applied dilute solution viscosity theory to bulk polymers noting that the environment of each macromolecule is the same, i.e., the polymer molecules are themselves the solvent. In this case, $\eta_s \equiv 0$. He assumed that the polymer molecules were completely entangled, i.e., that all of the modes of motion were enhanced by entanglements. Bueche considered that the force resisting motion consists of: the slippage of polymer segments past one another; the dragging of entangled molecules; and the circulation of the molecules. Employing a transformation of coordinates similar to Rouse, Bueche solved for the relaxation times of the normal modes of motion and obtained

$$\tau_p = \sigma^* f / \left\{ 36\ k\ T\ \mathrm{SIN}^2 \left[P\pi/(2N+2) \right] \right\} \qquad (A.29)$$

where f is the friction factor enhanced by entanglements.

Bueche's theory predicts that f is proportional to $M^{3.5}$.

C. WLF Combination of Rouse-Bueche Theories

The normal modes of motion which correspond to segment lengths less than the length required for entanglements should remain unaffected by the entanglements. Thus, these relaxation times should be given by Rouse's theory. The normal modes of motion of segments longer than the length necessary for entanglements have their relaxation times enhanced by the entanglements and should be given by Bueche's theory. Thus, Ferry, Landel, and Williams (i.e., WLF modification) (2.a, 22.) combined the Rouse and Bueche theories. They defined an entanglement coupling function, Qe, as

$$Qe = \left[M/(2\ Me)\right]^{3.4} \qquad P > Pe \qquad (A.30)$$

$$Qe = 1 \qquad P \leq Pe \qquad (A.31)$$

where Pe is called the critical index and Me is the molecular weight between entanglements and equal to Mc/2. The critical index is

$$Pe \equiv M/(2\ Me). \qquad (A.32)$$

To obtain the relaxation times for the unentangled modes of motion, it was necessary to divide Equation A.29 by Qe and this yielded

$$\tau_p = \zeta^2 f / \left\{ 24\, Qe\, k\, T\, SIN^2 \left[P\pi/(2N+2) \right] \right\} . \qquad (A.33)$$

The resultant relaxation spectrum consists of two segments on a log-log plot (see Figure 4) with each having a slope of -1/2. The spectrum vanishes between the relaxation time given when the index equals Pe and Pe + 1.

The other viscoelastic functions calculated from the modification of the Rouse-Bueche theories exhibited the characteristic behavior observed experimentally for entangled polymer systems.

III. Theories of Viscosity

A. Rouse's Theory of Viscosity

The relationship between viscosity and molecular weight for bulk polymer was derived using Rouse's model (see Rouse's theory) for a polymer molecule. It was assumed to behave as a sequence of beads distributed along a flexible random flight chain. The environment of chains was a continuum composed of other polymer and solvent molecules with the system subjected to a linear velocity gradient. The average torque on the chain was set equal to zero (Zero rate of shear is

FIGURE 4

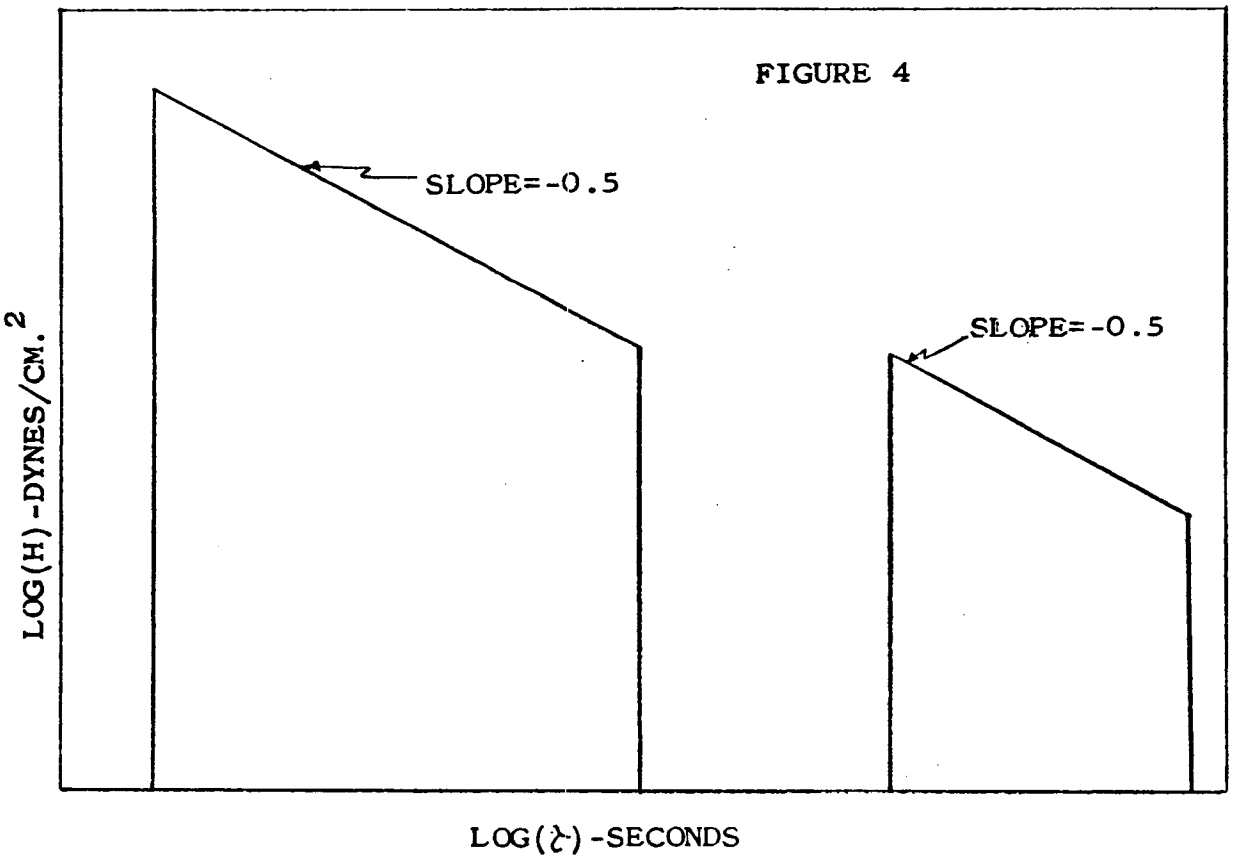

assumed so that the polymer chains are not perturbed from their random configuration). Thus, the torque due to the shear field (i.e., that which keeps the molecule rotating) was equated to the torque due to the frictional forces (i.e., that which attempts to retard rotation). The relationship between viscosity and molecular weight, then, is

$$\eta = \rho \, N_A \, a^2 \xi_o \, M/(36 \, M_o^2) \qquad (A.34)$$

where N_A is Avogadro's number and M_o is the molecular weight per monomer unit (23.).

From Equation A.34, the viscosity is shown to be proportional to $\xi_o M$. The monomer friction factor, ξ_o, depends on the density of free chain ends which at low molecular weight increases. Thus, since ξ_o is a function of molecular weight, the viscosity is not just proportional to M for $M < Mc$ (2.a, 23.).

B. Bueche's Theory of Viscosity

The viscosity of entangled polymer systems was derived from Bueche's model (see Bueche's theory) for entangled polymers (20., 21.). This model yielded the viscosity proportional to $M^{3.5}$ as shown by

$$\eta = N_A \rho a^2 M^{3.5} \xi_o \, /(36 \, M_o \, Me^{2.5}) . \qquad (A.35)$$

C. WLF Modification of Rouse-Bueche Theory of Viscosity

Using Equation A.34 to represent the viscosity below Mc and Equation A.35 to describe the viscosity above Mc, Ferry, Landel, and Williams described the two segments of $\log(\eta)$ - $\log(M)$ curve by (2.a)

$$\eta = \rho N_A a^2 \zeta_o M Qe/(36 M_o^2). \quad (A.36)$$

Here

$$Qe = \left[M/(2Me) \right]^{2.4} \qquad M > 2Me \quad (A.37)$$

and

$$Qe = 1 \qquad M \leq 2Me. \quad (A.38)$$

The molecular weight was raised to the 3.4 power to correspond to observed experimental behavior rather than the 3.5 power as predicted by Bueche. Below Mc, a slope of approximately unity was still found.

D. Molecular Weight Dependence of Viscosity

Fox and Allen (26.) employed the viscosity relation

$$\eta = (N_A/6) \left[(\langle s_o^2 \rangle_{AV.}/M) (Z_1/v) \right]^{\alpha} Qe \zeta_o \quad (A.39)$$

$$Qe = (M/Mc)^{\alpha} \quad (A.40)$$

$$\alpha = 2.4 \nu (M-Mc) \quad (A.41)$$

where s is the radius of gyration. Including the molecular dependence of the monomeric friction factor, they were

able to describe the non-linear relationship between viscosity and molecular weight below Mc (see Appendix I).

E. Chikahisa Theory of Viscosity

Chikahisa (24.) viewed an entangled polymer system from a different view. He assumed that the intermolecular forces between two polymer molecules consisted of the interaction of their potential fields and the frictional forces required for slippage of the macromolecules past one another. The segmental conformations of the polymer molecules were assumed to be in equilibrium by considering only a slowly relaxing phenomena (i.e., steady-state zero shear rate viscosity). Thus, the inter-chain relaxation processes were dominant. The viscosity is, then, given by

$$\eta = b_1 M + b_2 M^3 \qquad (A.42)$$

where b_1 and b_2 are constants for a given polymer and temperature and

$$b_1 \gg b_2 . \qquad (A.43)$$

At low molecular weights, the first term predominates and the viscosity is proportional to the M; at high molecular weights, the second term overwhelms and the viscosity becomes proportional to $M^{3.0}$.

Model of a Continuous Entanglement Function

A. Relaxation Spectrum

The WLF modification of Rouse's theory introduces the effects of entanglements abruptly. This sudden and discontinuous influence of entanglements causes the relaxation spectrum to vanish between the Pe and Pe + 1 relaxation times. The WLF entanglement coupling function may be written as

$$Qe = \left[M/(2\ Me) \right]^{\kappa} \qquad (A.44)$$

where κ is a function of the index of the mode of motion and is defined as

$$\kappa = 2.4\ \mathcal{U}(P - Pe + 1). \qquad (A.45)$$

The limits of the entanglement coupling function vary from 0 to 2.4 to correspond to experimentally observed facts.

A more reasonable model to introduce entangled modes of motion would allow the importance of entanglements to build continuously. Thus, a region is created in the relaxation spectrum where the modes of motion vary smoothly between being completely entangled and completely unentangled. (This zone will be referred to as the partial entanglement region.) Effectively, a number of relaxation times would be placed in the void created by the WLF

modification.

In Bueche's (25.) theory of entangled polymers, he defined a slippage factor, describing the flow of polymer chains past one another, and was able to relate the monomeric friction factor to the molecular weight. Since the viscosity is directly proportional to the monomeric friction factor

$$\eta - \eta_s = n a^2 Z^2 \xi_o / 36 \ , \qquad (A.46)$$

the viscosity-molecular weight relationship was thus determined. For molecular weights much less than Mc, the viscosity was predicted to be proportional to M. At molecular weights much greater than Mc, the viscosity was predicted to be proportional to $M^{3.5}$. In the range of molecular weights between these limiting cases, the proportionality between viscosity and molecular weight was predicted to change rapidly and continuously from $M^{1.0}$ to $M^{3.5}$. Bueche's equation involves an infinite series to describe the influence of molecular weight on viscosity which makes this relationship difficult to use.

Two analytical expressions which continuously increase the importance of entanglements are

$$K = 2.4 \ EXP\left[E_1 (P - Pe)\right] \ / \ \left\{1 + EXP\left[E_1 (P-Pe)\right]\right\} \qquad (A.47)$$

and

$$\kappa = (2.4/\pi)\ \mathrm{TAN}^{-1}\left\{(2\,E_2P/Pe)/\left[1-(P/Pe)^2\right]\right\}. \qquad (A.48)$$

Equation A.47 will be referred to as the exponential modification and Equation A.48 as the arc tan modification. The constants, E_1 and E_2, which appear in the above equations, control the rate at which the functions change from 0 to 2.4 in the neighborhood of Pe. The slower this change, the greater is the number of relaxation times involved in the partial entanglement region. The effect of these functions is to distribute the passage from entangled to unentangled modes of motion over several relaxation times. In the limit as E_1 goes to infinity and as E_2 goes to zero, Equations A.47 and A.48 approach the step function. Thus, the limiting form of these equations yield the WLF modification.

B. Viscosity

The relationship between viscosity and molecular weight from Bueche's theory of viscosity (12.) can be written for temperature, T, as

$$\eta = K_T\, M\, (M/Mc)^{\alpha} \qquad (A.49)$$

where K_T is a constant at any given temperature and α is

defined by a WLF-type relationship as

$$\alpha = 2.4\,\eta\,(M - Mc). \qquad (A.50)$$

This equation is consistent with the generally observed result that viscosity is proportional to M below Mc and proportional to $M^{3.4}$ above Mc. The equation abruptly introduces the effects of entanglements and causes a sharp break in the log (η)-log (M) curve at Mc.

It is reasonable to assume that the entanglements would not produce a sudden break in this curve. Indeed, Bueche's (25.) derivation of the effect of entanglements on the friction factor predicts a smooth transition of the proportionality from M to $M^{3.5}$. However, his expression is difficult to employ.

To introduce the influence of entanglements gradually by means of an entanglement coupling which has ease of use would be an improvement over Bueche's expression. Replacing the step function of Equation A.50 with relationships similar to Equations A.47 and A.48 alters the equation for α to

$$\alpha = 2.4\ \mathrm{EXP}\left[E_1(M-Mc)\right] \Big/ \left\{1 + \mathrm{EXP}\left[E_1(M-Mc)\right]\right\} \qquad (A.51)$$

or

$$\alpha = (2.4/\pi)\ \mathrm{TAN}^{-1}\left\{(2\,E_2 M/Mc)/\left[1-(M/Mc)^2\right]\right\}. \qquad (A.52)$$

As before, the constants, E_1 and E_2, control the extent of the transition from being completely entangled to completely unentangled.

The same values of the constants E_1 and E_2 would be expected to characterize the partial entanglement region whether considering viscoelastic behavior or the molecular weight dependence of viscosity. This can be demonstrated from phenomenological viscoelasticity since

$$\eta = \text{Constant} \sum_p \tau_p . \qquad \text{(A.53)}$$

With the longest relaxation times given approximately by

$$\tau_p = \tau_1 / p^2 , \qquad \text{(A.54)}$$

the first few relaxation times almost completely determine the sum of Equation A.53 and thus, the viscosity.

Results and Discussion

The relaxation times using Rouse's theory with Equation A.47 describing the influence of entanglements were investigated for three cases. Case I was polystyrene of 154,000 molecular weight for which the experimental relaxation spectrum had already been reported (6.) (see Appendix II). Case II was a polystyrene of 750,000 molecular weight (26.) (see Appendix II). Case III was a polymer with properties equivalent to polystyrene of 85,600 molecular weight but with a value of 1,650 employed for Me (see Appendix III).

If Rouse's theory is valid, the calculated viscoelastic functions should agree with the experimentally determined functions. Generally, however, there is a lack of experimental data on monodisperse polymer; such data is necessary to validate critically Rouse's theory.

Figures 5 and 6 illustrate the difference between the WLF entanglement coupling function and Equations A.47 and A.48, in accounting for the influence of entanglements for Case III. Figure 5 shows for the exponential modification (Equation A.47) the log (Qe) versus the index for various values of E_1. Figure 6 illustrates the influence

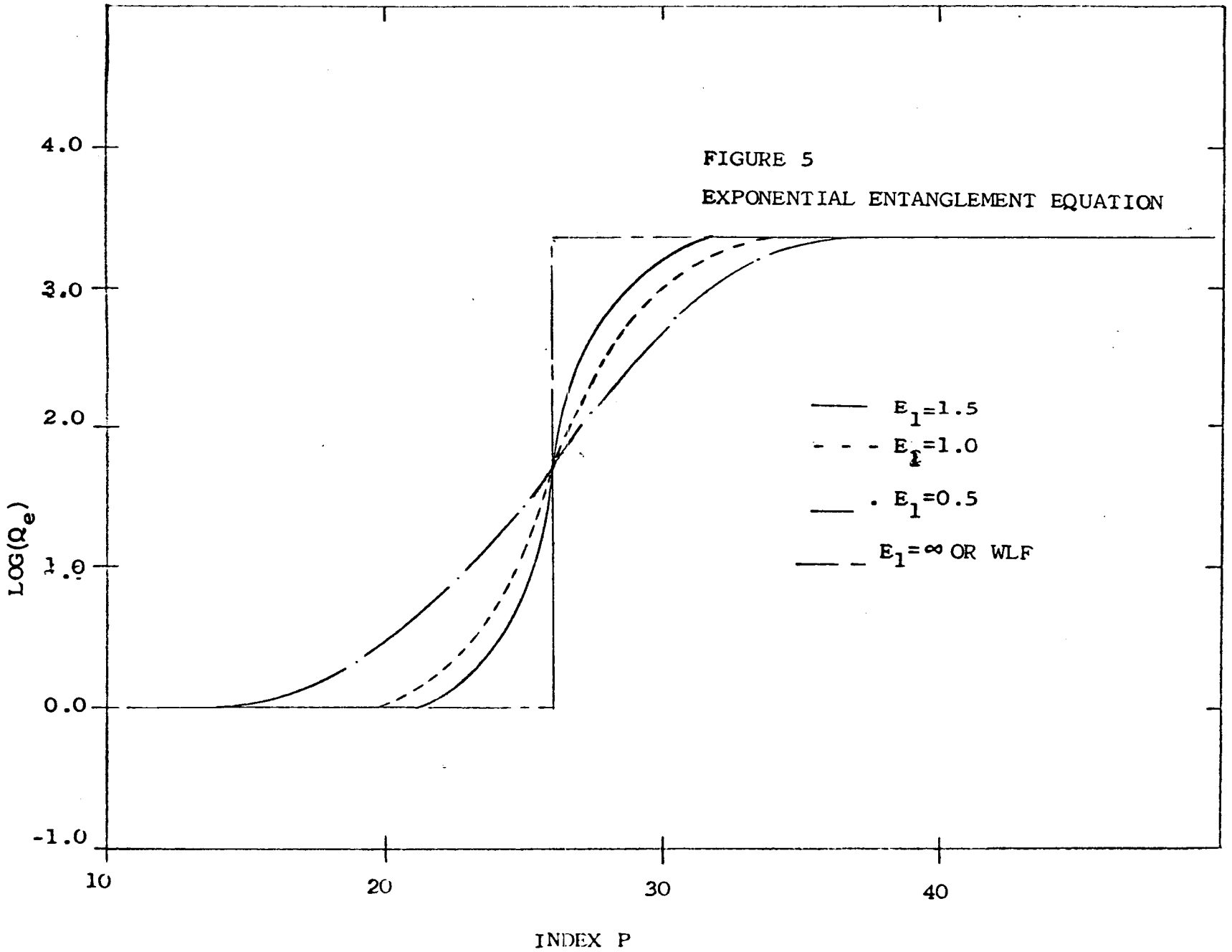

FIGURE 5

EXPONENTIAL ENTANGLEMENT EQUATION

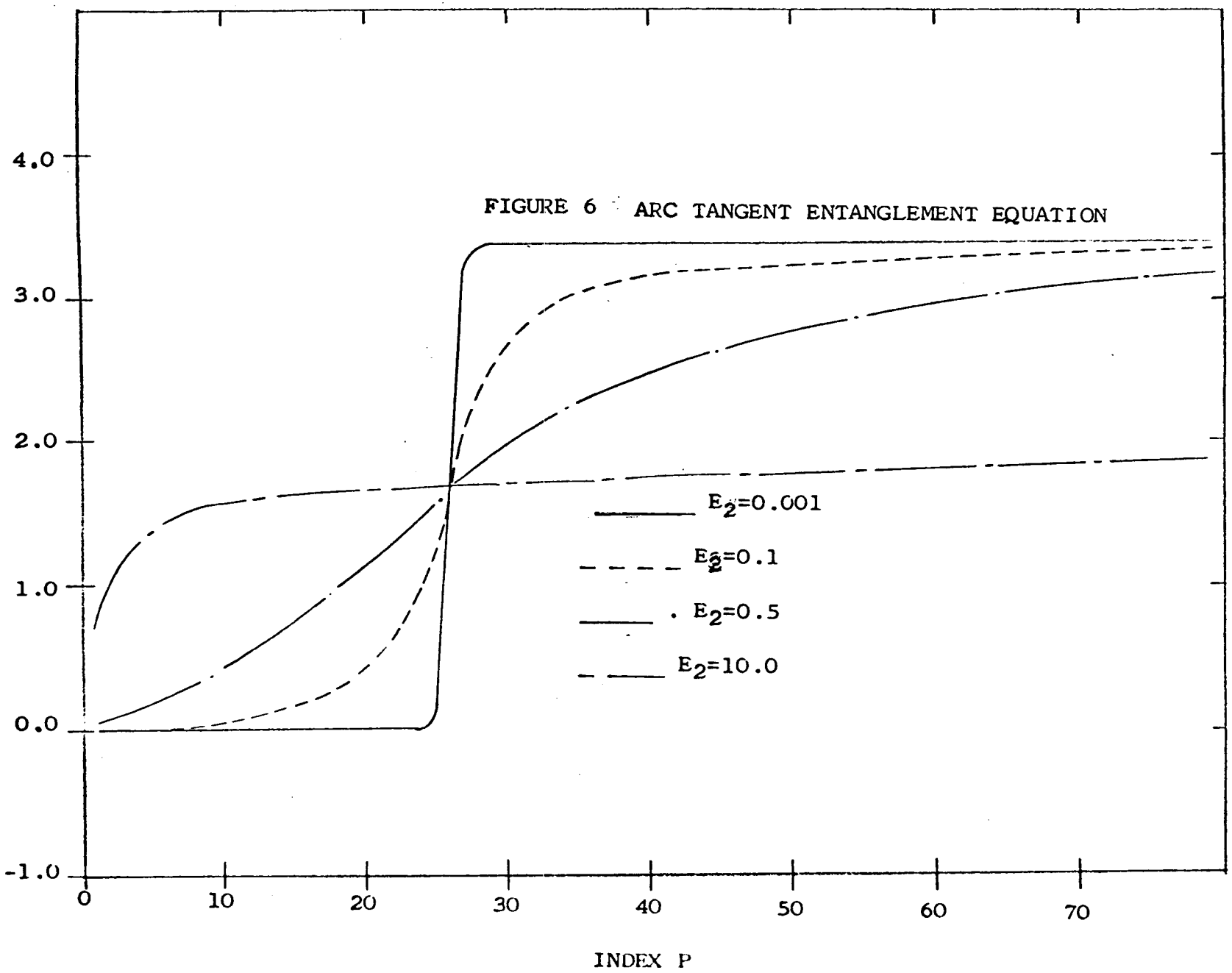

FIGURE 6 ARC TANGENT ENTANGLEMENT EQUATION

of the arc tan modification (Equation A.48) for this case. As E_1 approaches infinity and E_2 approaches zero, these equations approach the WLF coupling function. Decreasing E_1 or increasing E_2 increases the number of relaxation times in the partial entanglement region. Thus, the parameter E_1 or E_2 controls the rate of transition between completely entangled modes of motion and completely unentangled.

To calculate H from the relaxation times for these cases, the Dirac delta functions of Equation A.25 were approximated by sharp normalized Guassian distributions. The relaxation spectrum was then expressed as

$$H(\tau) = n\,k\,T \sum_{\rho} (C/\sqrt{\pi})\,EXP\left\{\left[(\tau/\tau_\rho)-1\right]^2 C^2\right\} \quad . \quad (A.53)$$

For our calculations, C was set equal to 4 which leads to very sharp distributions (see Appendix III). Since the spikes of the Dirac delta functions have been replaced by Guassian distributions, each relaxation time was replaced by a sharp distribution of relaxation times. This procedure seems reasonable since slight heterogeneity of molecular weight is always present. This causes each relaxation process to be characterized by a distribution of relaxation times. If the molecular weight distribution can be

represented as a Gaussian distribution, the relaxation spectrum may be calculated by the proper selection of the value for the parameter C.

Case I.

For this case, Tobolsky et al (6.) reported the relaxation spectrum. Rouse's theory modified to include the influence of entanglements by Equation A.47, was employed to predict the relaxation spectrum. Figure 7 illustrates both of these spectra. The discrete relaxation spectrum obtained from our exponential modification of the Rouse theory cannot be approximated as a continuous function at the longest times since the relaxation times are too far apart. Thus, for log (τ) greater than 2.9, the predicted relaxation spectrum consists of six discrete relaxation times. The predicted relaxation spectrum does exhibit a definite "wedge" section; however, the "box" section, which is the partial entanglement region, is composed of discrete elements.

To compare the relaxation spectra for log (τ) greater than 2.9, the predicted spectrum was approximated

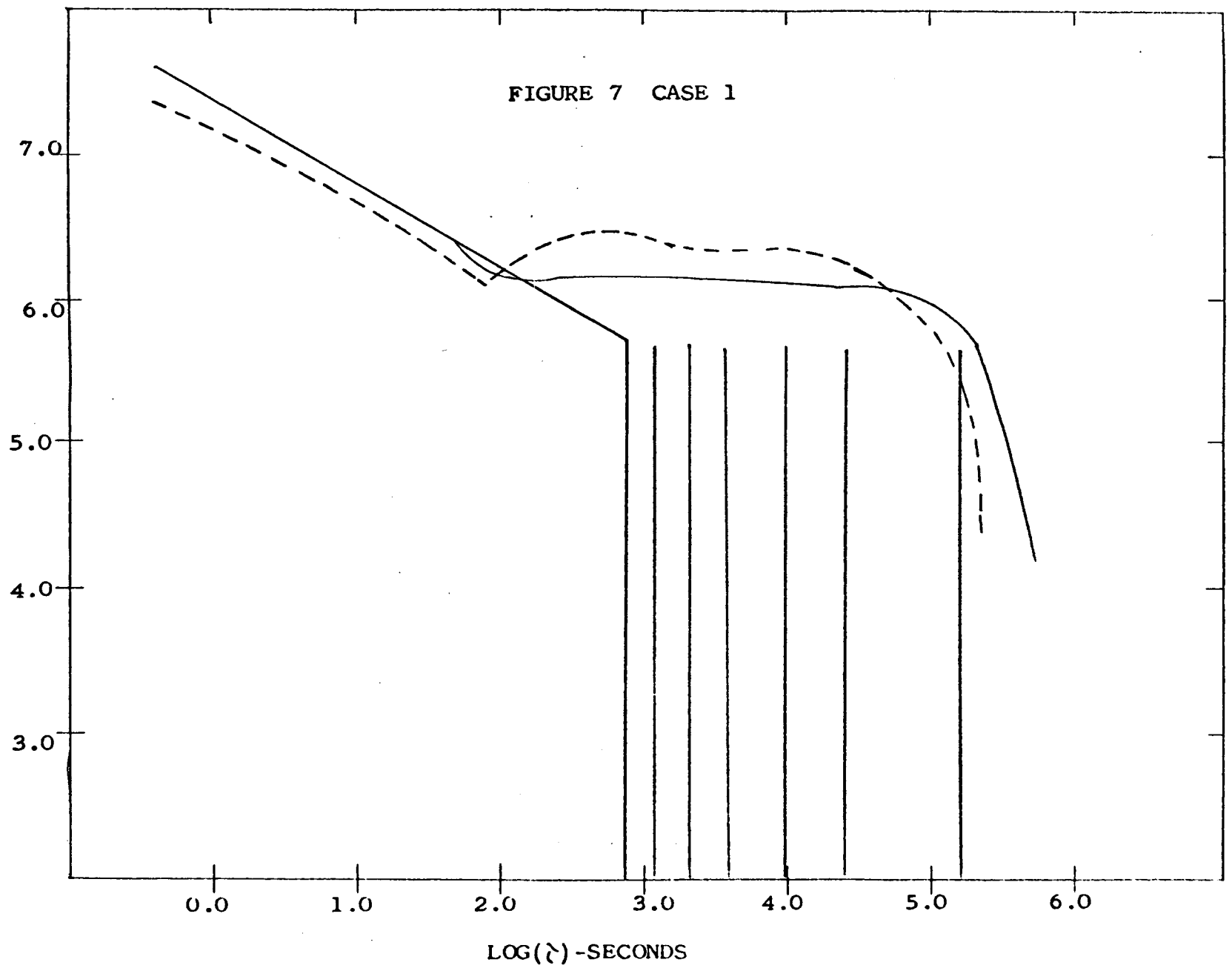
FIGURE 7 CASE 1
7.0
6.0
5.0
4.0
3.0
LOG(H)-DYNES/CM.2
0.0
1.0
2.0
3.0
4.0
5.0
6.0
LOG(τ)-SECONDS

from the relaxation modulus by

$$H(\tau) = -dG(t)/d(\ln t) + d^2 G(t)/d(\ln t)^2 \Big|_{t=2\tau} . \qquad (A.54)$$

This was similar to the method employed by Tobolsky in calculating the experimental spectrum. This approximation technique yielded the "box" portion of the predicted spectrum. The approximate interconversion of the relaxation modulus into the spectrum predicted a continuous spectrum where Rouse's theory predicted a discrete one for long relaxation times.

Each of the two relaxation spectra exhibit the same characteristic regions: (1) at shortest times, a region of -1/2 slope; (2) at moderate times, a flat region; and (3) at longest times, a sudden drop. An extended region of -1/2 slope at the longest relaxation times does not occur because the molecular weight is too low. The critical index was only 2.47. For the prediction of extended region of -1/2 slope at these times requires the critical index to be considerably higher.

The differences between the experimental spectrum of Tobolsky and the calculated spectrum in the plateau and transition region are primarily due to the molecular weight distribution and the deficiency of

the approximate interconversion technique. The calculated spectrum assumed that the polymer was monodispersed; however, the sample of Tobolsky possessed a narrow spread of molecular weights. This introduced slight differences in the spectrum by replacing a single relaxation time by a narrow distribution of relaxation times. It is impossible to quantitatively to predict these differences. Since the approximate interconversion formula possesses some error, the formula inserted this error into the spectrum. Considering these sources of inexactness, the agreement between the spectra is satisfactory.

Case II.

Case II is a typical entangled high molecular weight polymer. Figure 8 shows the relaxation spectrum for this case which was calculated using Equation A.47 to describe the influence of entanglements by the Rouse theory. The spectrum consists of: (1) the three longest relaxation times which must be considered discrete; (2) the partial entanglement region where the slope is nearly zero; (3) the region of unentangled modes of motion where the slope equals -1/2; and (4) the glassy region where the

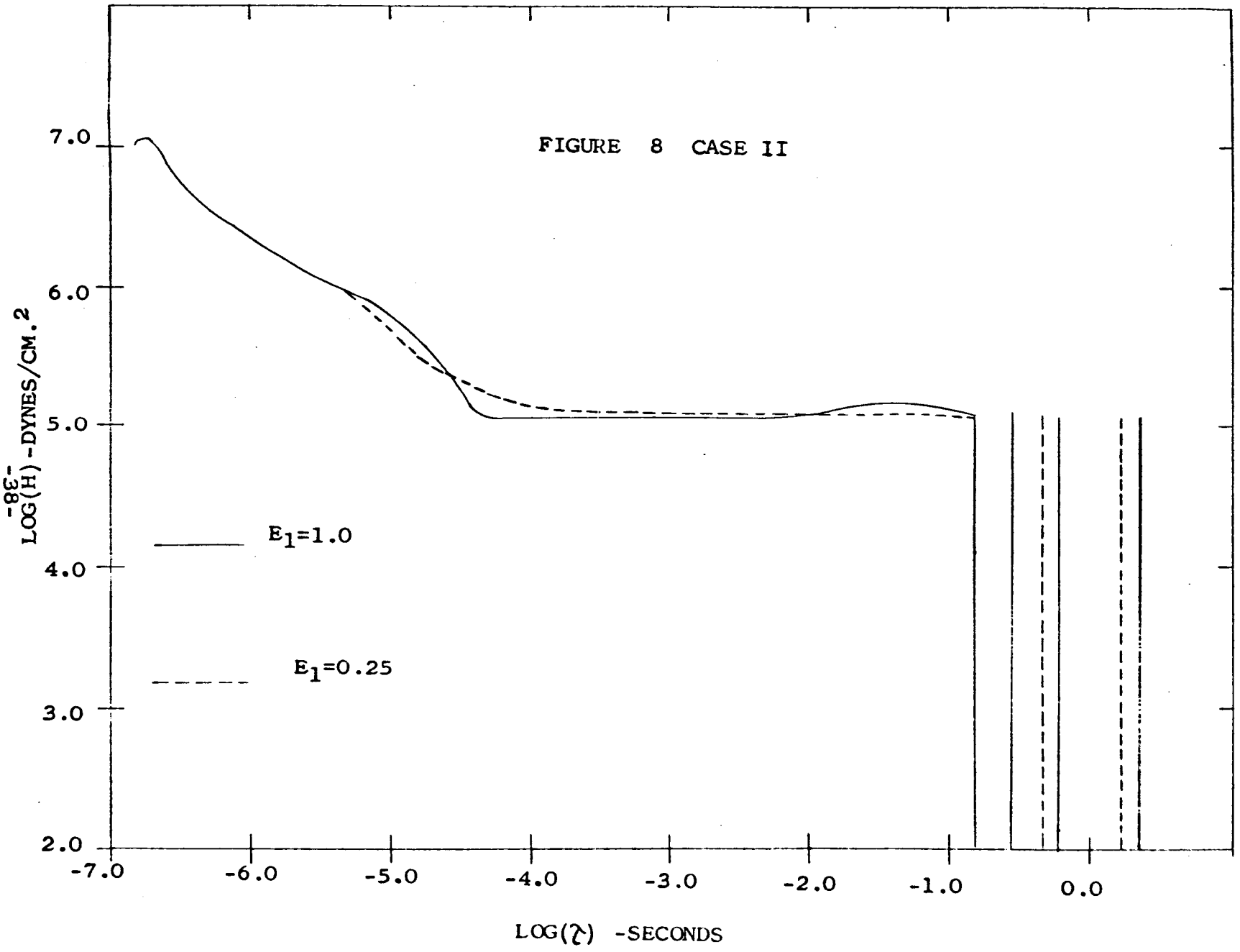
FIGURE 8 CASE II
7.0
6.0
5.0
4.0
3.0
2.0
-7.0
-6.0
-5.0
-4.0
-3.0
-2.0
-1.0
0.0
LOG(H) -DYNES/CM.2
-38-
LOG(τ) -SECONDS
E1=1.0
E1=0.25

results of the theory are invalid.

A feature of the Rouse theory is the arbitrary subdivision of the polymer molecule. To illustrate the influence of altering the number of submolecules, this number was varied for this case. Appendix VI shows that the only difference caused by changing this number occurs in the glassy region where the theory is not valid.

The spectrum in the partial entanglement region exhibited fluctuations of a few percent; for this portion of the curve, Figure 8 shows the best curve drawn through these variations. The spread between relaxation times in this region of the spectrum was sufficient to introduce these slight variances in the spectrum.

The spectrum does exhibit very definite "box" and "wedge" sections. Equation A.47 gradually reduced the influence of entanglements by spreading the relaxation times further apart than the approximate $1/\rho^2$ relationship, which is valid if modes of motion are entirely entangled or unentangled, producing the partial entanglement region. Thus, the spectrum became a "box". The value of Equation A.47 became essentially constant for a relaxation time greater than the Pe time and the slope of $\log(H) - \log(\tau)$

plot became -1/2 which is the "wedge" section.

The relaxation modulus for Case II is shown in Figure 9. Employing our modification of Rouse's theory and varying the value of E_1 slightly alters the width of the plateau region of this curve by decreasing to a small extent the slope of the plateau region. An interesting point is that the various values of the parameter cause the curve to cross at a single point in the plateau region (i.e., point of inflection) where the modulus is equal to 5.63×10^5 dynes/cm^2. This point is called the pseudo-equilibrium modulus.

For this case, the relaxation moduli for the values of E_1 greater than 0.5 for Equation A.47 are indistinguishable from the WLF entanglement coupling function (Equation A.45). This means that the variation of the number of relaxation times in the partial entanglement region for this condition has only slight influence on the relaxation modulus. For E_1 less than 0.5, the relaxation modulus predicted from the exponential modification of Rouse's theory differs from the WLF entanglement coupling function for this theory in the partial entanglement and terminal regions.

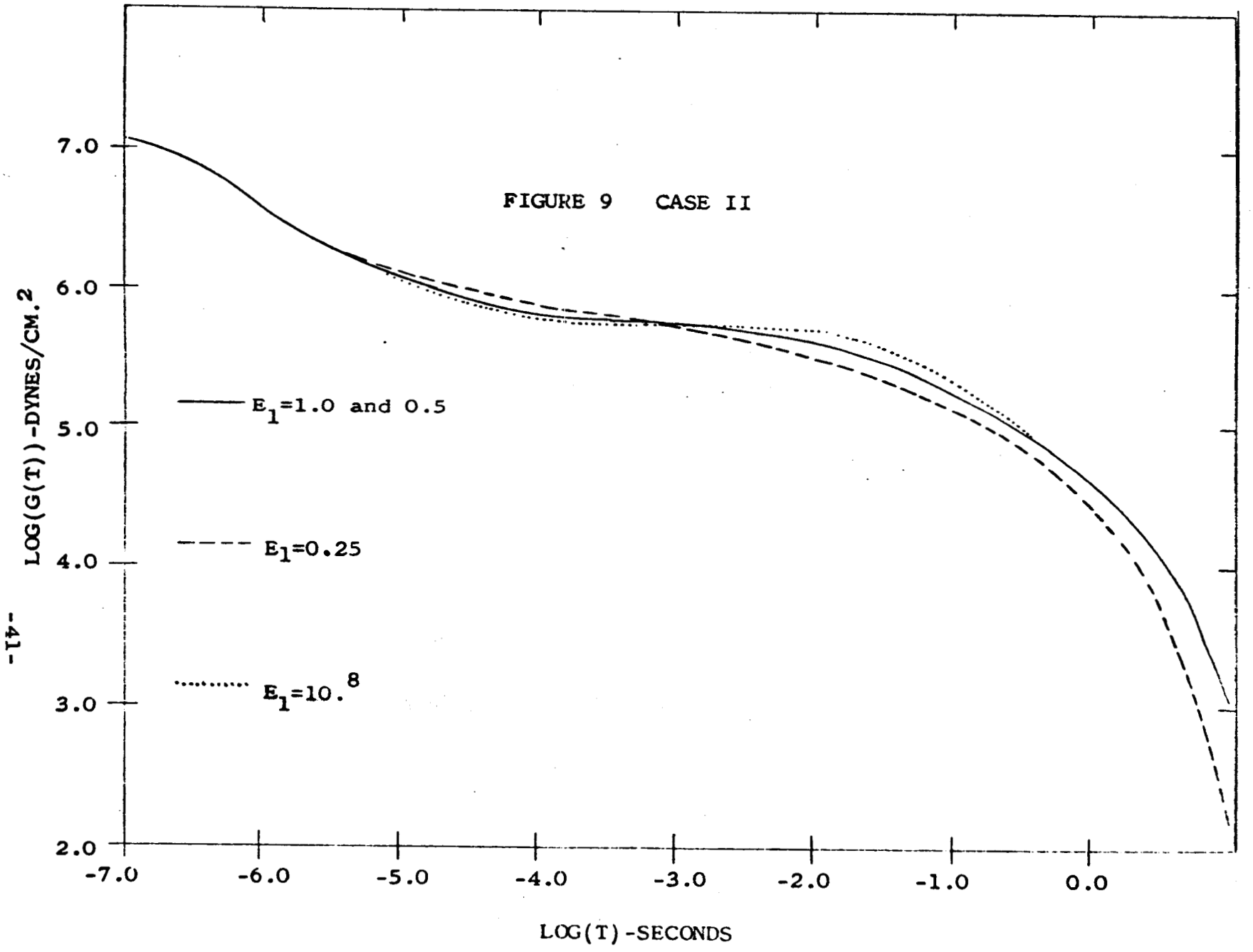
FIGURE 9 CASE II
7.0
6.0
5.0
4.0
3.0
2.0
LOG(G(T))-DYNES/CM.2
E_1=1.0 and 0.5
E_1=0.25
E_1=10.^{8}
-7.0
-6.0
-5.0
-4.0
-3.0
-2.0
-1.0
0.0
LOG(T)-SECONDS

Case III.

This hypothetical polymer differs from Case II primarily by having a considerably higher critical index. Figure 10 is the relaxation spectrum for Case III. The spectrum consists of: (1) the three longest relaxation times which are discrete; (2) the entangled modes of motion region with a -1/2 slope; (3) the partial entanglement or plateau region, which is nearly flat; (4) the unentangled modes of motion region with a -1/2 slope; and (5) the glassy region where the results of the Rouse theory are invalid.

The most noticeable difference in the spectrum between Case II and Case III is the region of entangled modes of motion with a slope of -1/2. In Case II, the value of the critical index was insufficient for the discrete relaxation times for the entangled modes of motion to be represented as a continuum before the partial entanglement region was encountered. For this case, the value of the critical index was adequate to allow the relaxation times for the entangled modes of motion to produce the region of -1/2 slope at these times.

The relaxation spectrum remains unaffected for the

exponential form of the entanglement coupling function for the range of value of E_1 studied. As E_1 approaches infinity, the WLF entanglement coupling function is approximated. As this occurs, the spectrum in the region of the Pe relaxation time becomes discrete and eventually it will vanish between Pe and Pe + 1 relaxation times.

Figures 11 through 15 show the relaxation modulus, dynamic modulus, and the dynamic compliance for the relaxation spectrum of Case II. In the terminal and transition regions of these figures, the various viscoelastic functions are independent of the value selected for E_1 . The loss modulus and loss compliance exhibit the largest variation in their mid-range depending on the value chosen for E_1 . Figure 13 compares the loss modulus calculated using E_1 equal to 0.25, 0.50, and 1.0 and the loss modulus calculated using the WLF modification, i.e., E_1 equal to ∞ . Using the first three of these values for E_1 gave results that were equivalent within the resolution of Figure 13 and they are all displayed as the solid line. It is unlikely

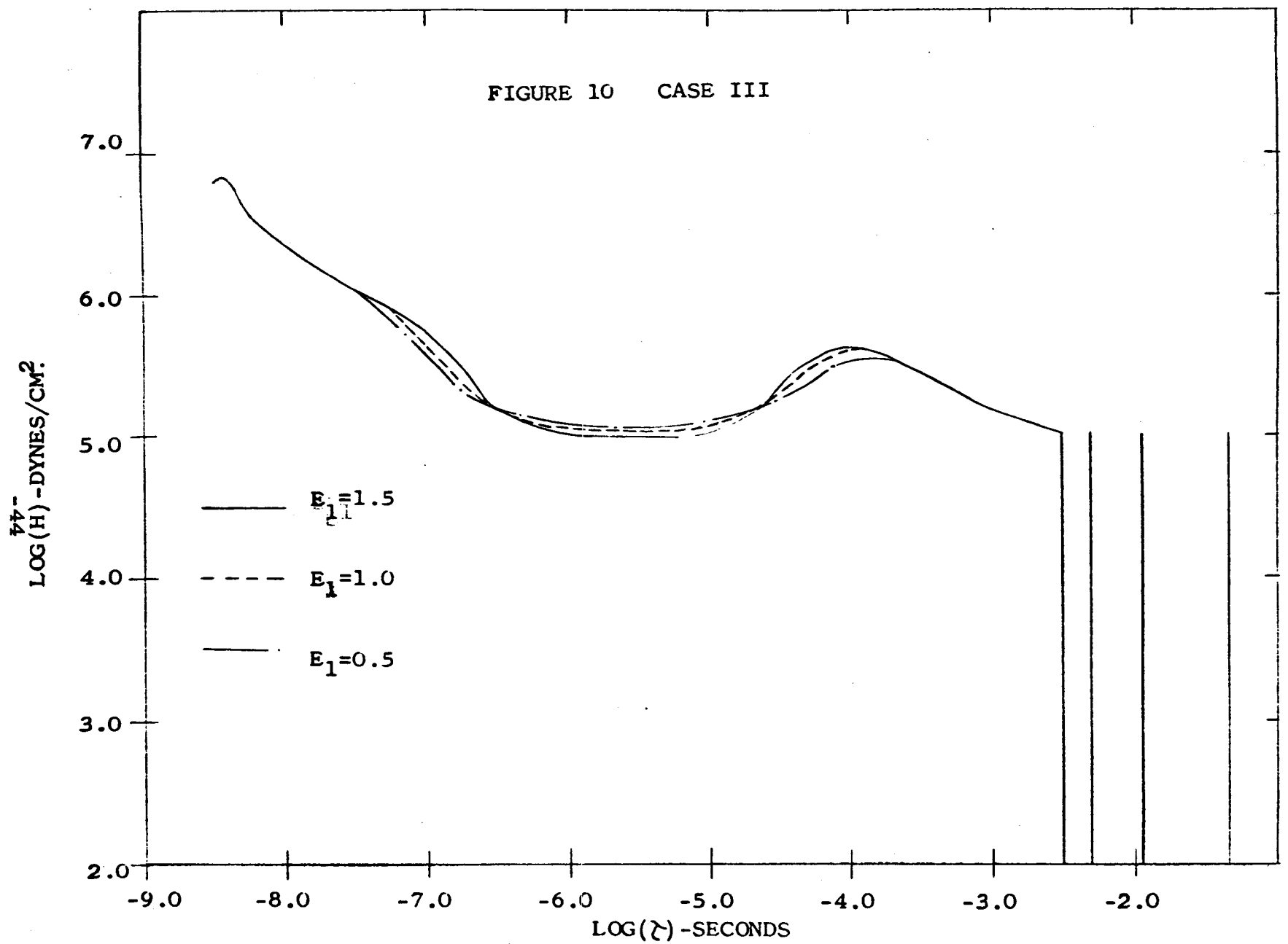
FIGURE 10 CASE III
7.0
6.0
5.0
4.0
3.0
2.0
LOG(H)-DYNES/CM.-44
E1=1.5
E1=1.0
E1=0.5
-9.0
-8.0
-7.0
-6.0
-5.0
-4.0
-3.0
-2.0
LOG(τ)-SECONDS

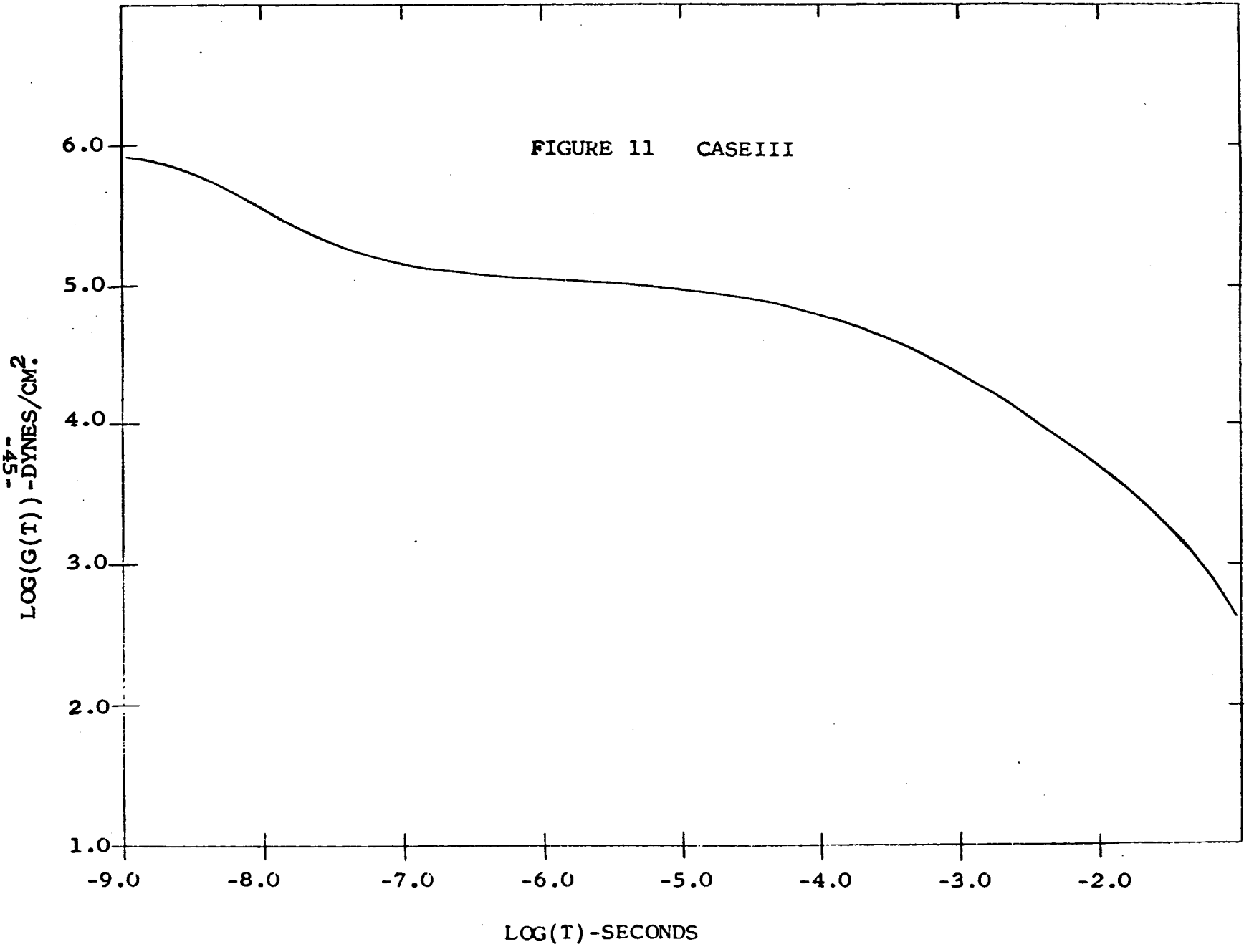
FIGURE 11 CASEIII
6.0
5.0
4.0
3.0
2.0
1.0
-9.0
-8.0
-7.0
-6.0
-5.0
-4.0
-3.0
-2.0
LOG(G(T)) -DYNES/CM.2
-45-
LOG(T)-SECONDS

FIGURE 12 CASE II

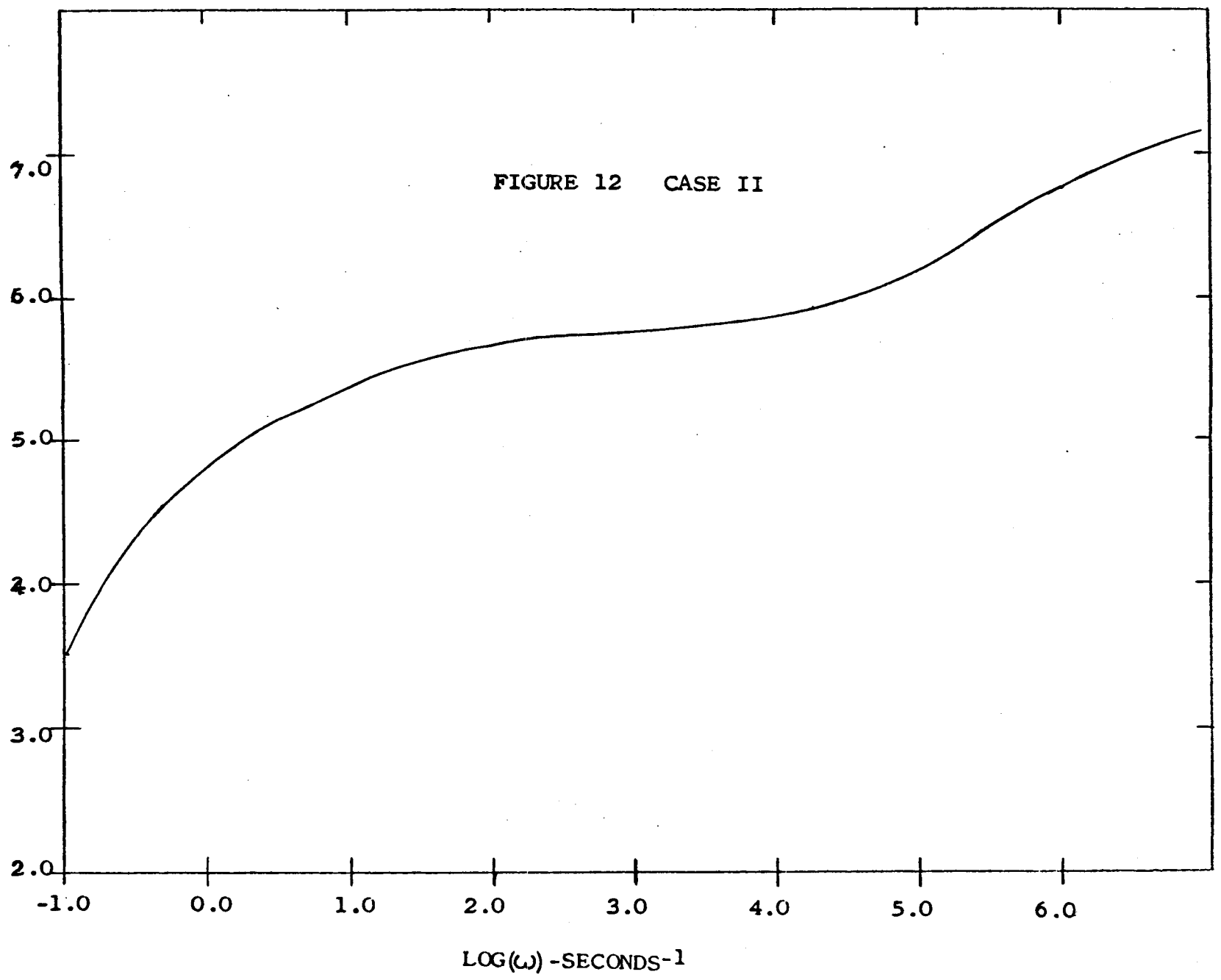

FIGURE 13 CASE II

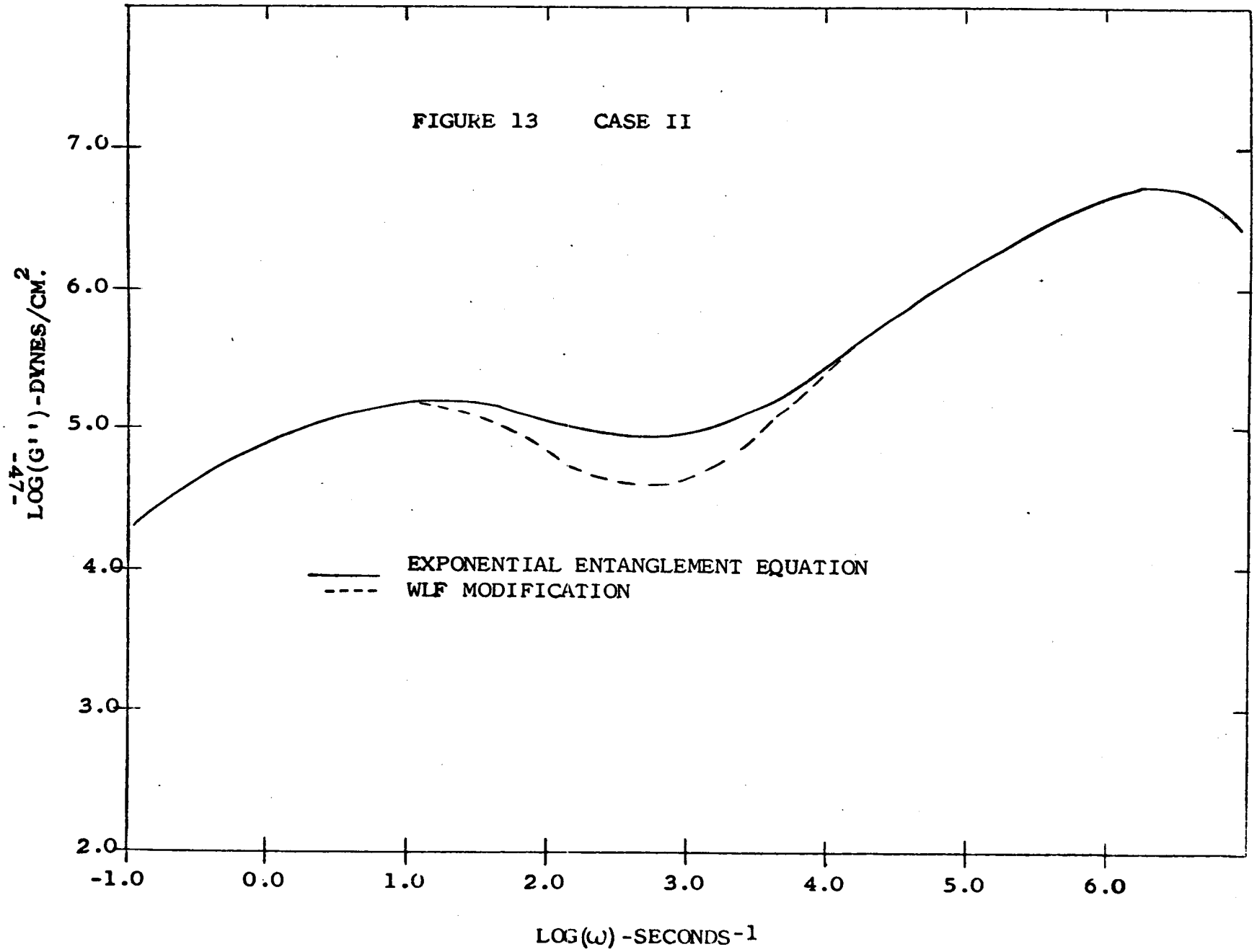

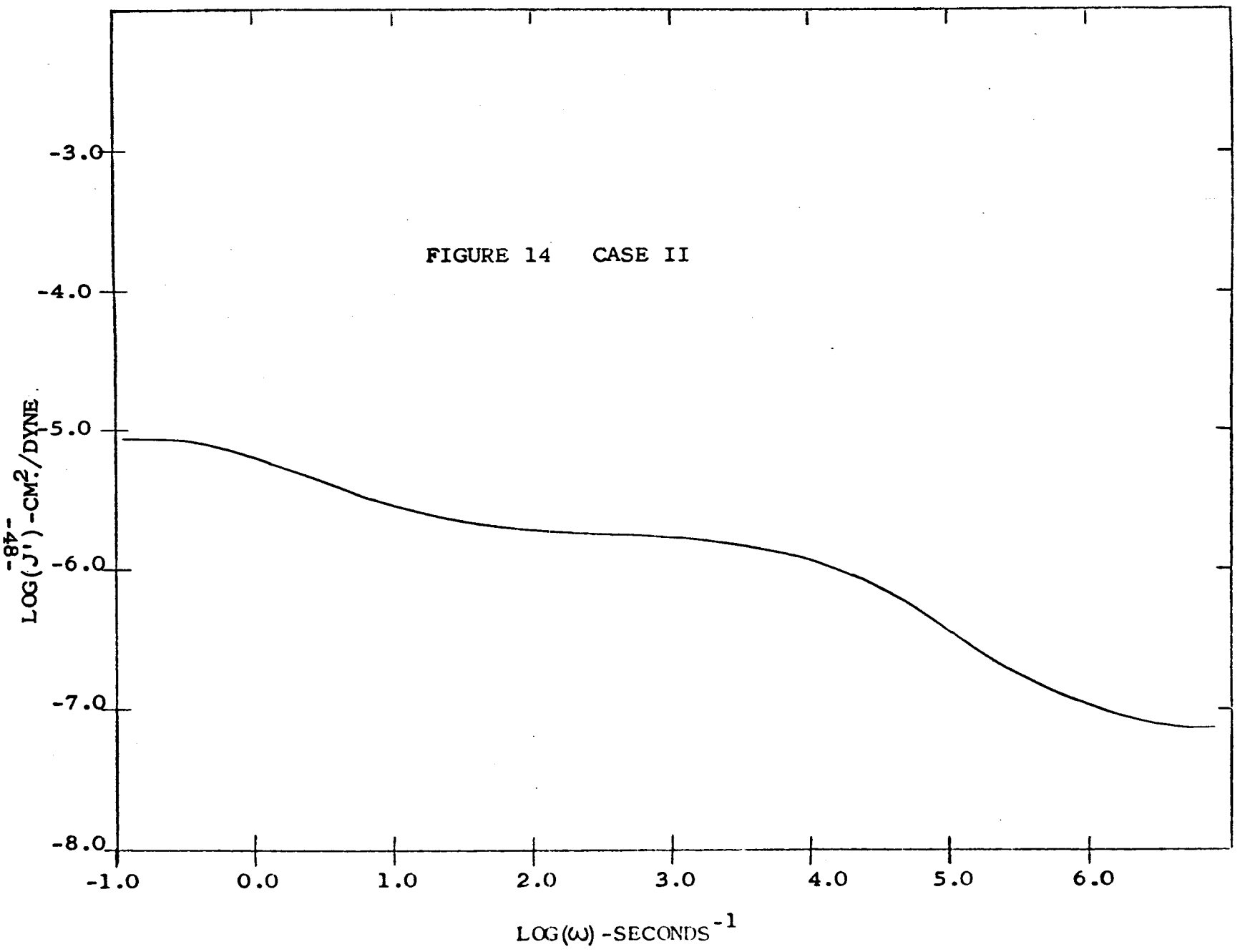

FIGURE 14 CASE II

FIGURE 15 CASE II

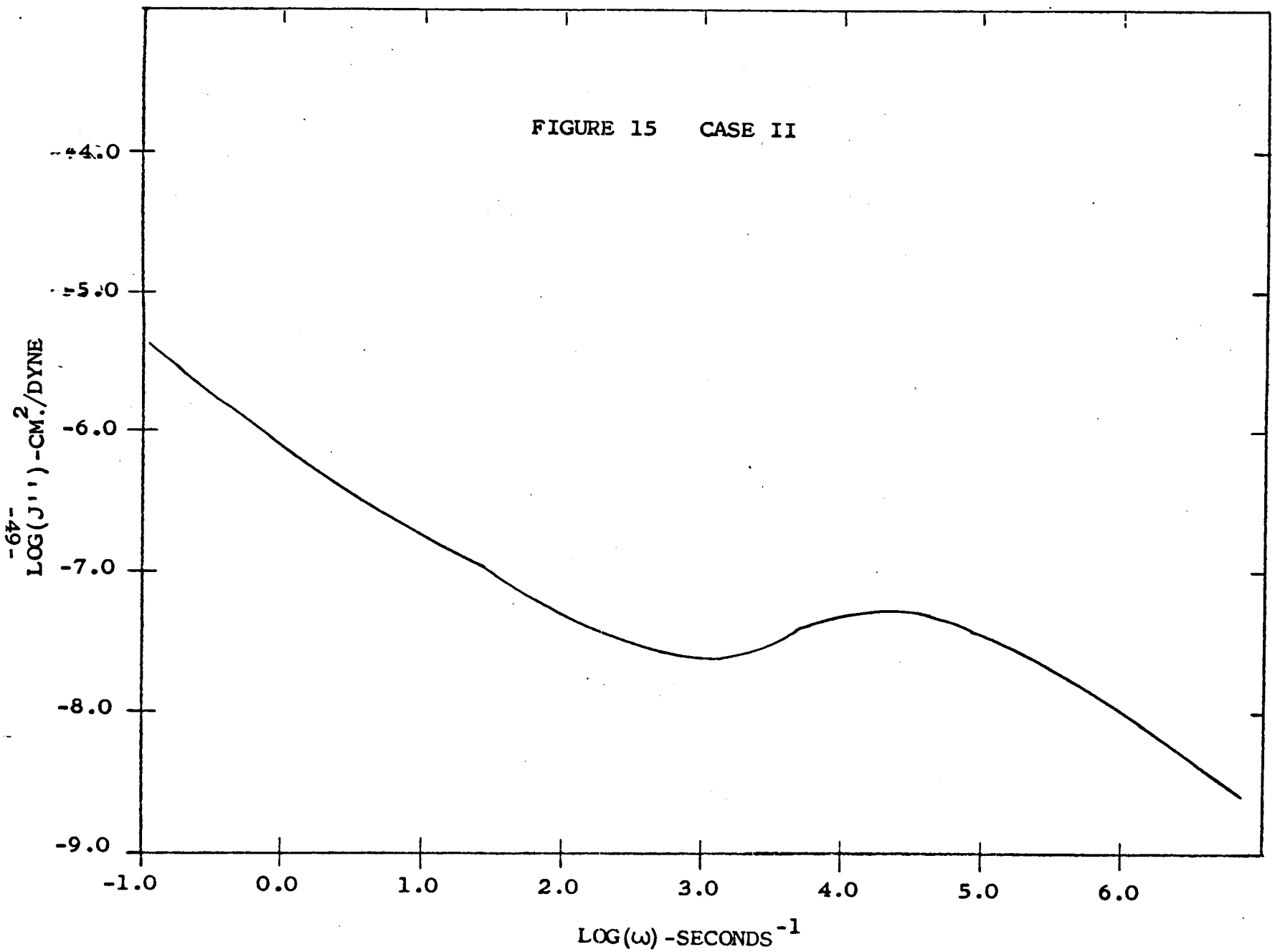

that such differences could be detected by present experimental methods. There is, however, a noticeable difference between the curves calculated using the small finite values of E_1 and the WLF modification. The latter gives a deeper minimum in the plateau region. It is clear that the behavior predicted by the WLF modification could be distinguished experimentally from the behavior predicted by small values of E_1 . The calculated storage modulus and the storage compliance were insensitive to the various values of the parameter. Thus, these viscoelastic functions were nearly independent of the fine details of the partial entanglement region of the relaxation spectrum.

Molecular Weight Between Entanglements

Entanglements among polymer chains alter the shape of the various viscoelastic functions. The relaxation modulus for both Cases II and III (Figures 9 and 11) shows the plateau region characteristic of high molecular weight, amorphous polymers. The real part of their

dynamic moduli (Figures 12 and 16) are approximately a mirror image of the relaxation moduli. For each case, the pseudo-equilibrium modulus is the same whether from either the relaxation or storage modulus. The imaginary part of their dynamic moduli (Figures 13 and 17) pass through a minimum which is distinctive of an entangled polymer. The real part of their dynamic compliance (Figures 14 and 18) exhibits a plateau region. Their equilibrium compliances are approximately equal to the reciprocal of their pseudo-equilibrium moduli. The imaginary part of their dynamic compliance (Figures 15 and 19) illustrates the broad maximum which distinguishes a network structure induced by entanglements.

These characteristic features of the various viscoelastic functions for entangled, amorphous polymers are directly related to the molecular weight between entanglements by the following equations (2.a):

(1.) from the relaxation spectrum by

$$\Delta = 2.4 \log\left[M/(2\ Me)\right] \qquad \text{(A.55)}$$

where Δ is the width of the transition region;

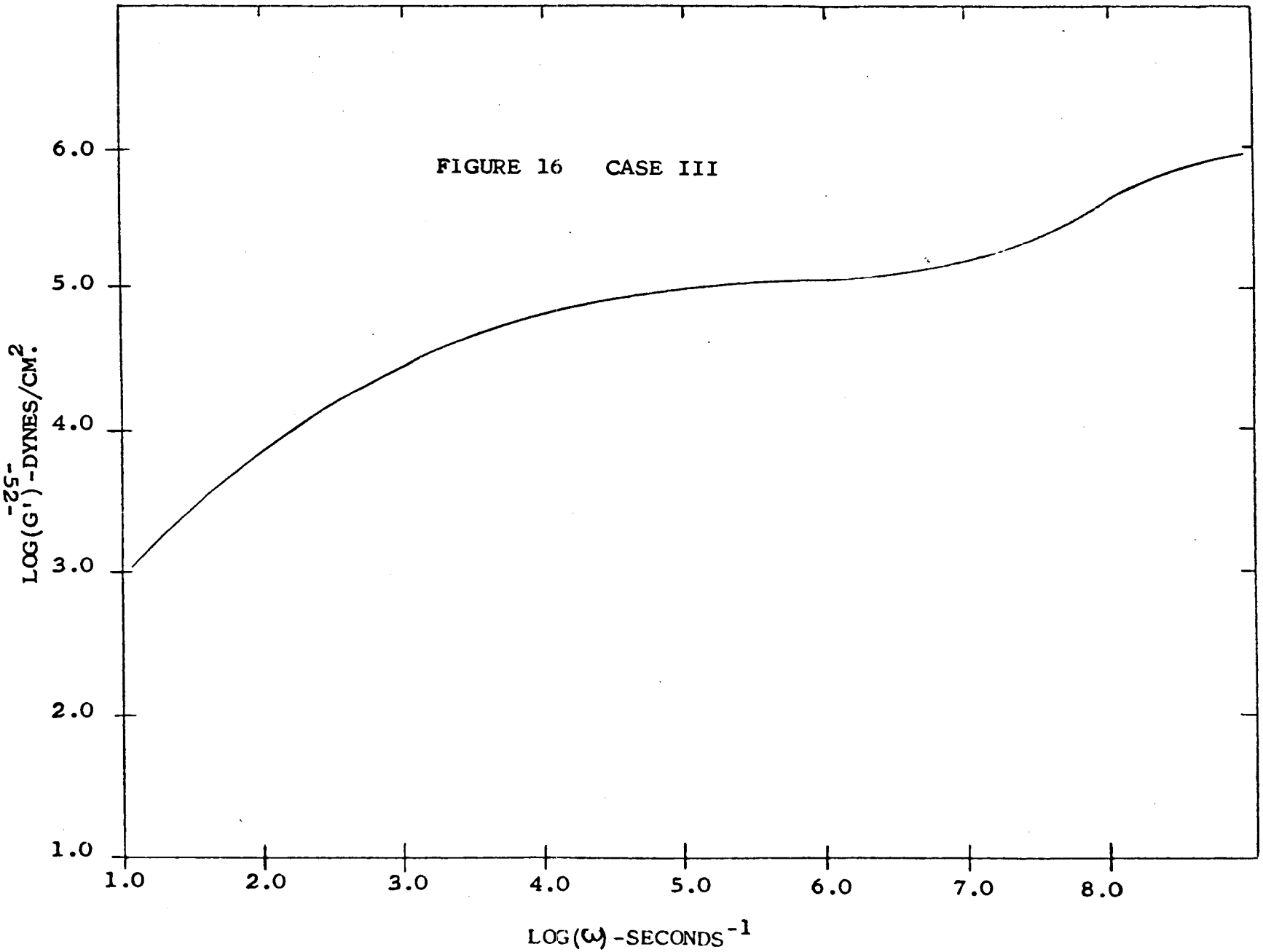
FIGURE 16 CASE III
6.0
5.0
4.0
3.0
2.0
1.0
LOG(G')-DYNES/CM.2
-52-
1.0
2.0
3.0
4.0
5.0
6.0
7.0
8.0
LOG(ω)-SECONDS-1

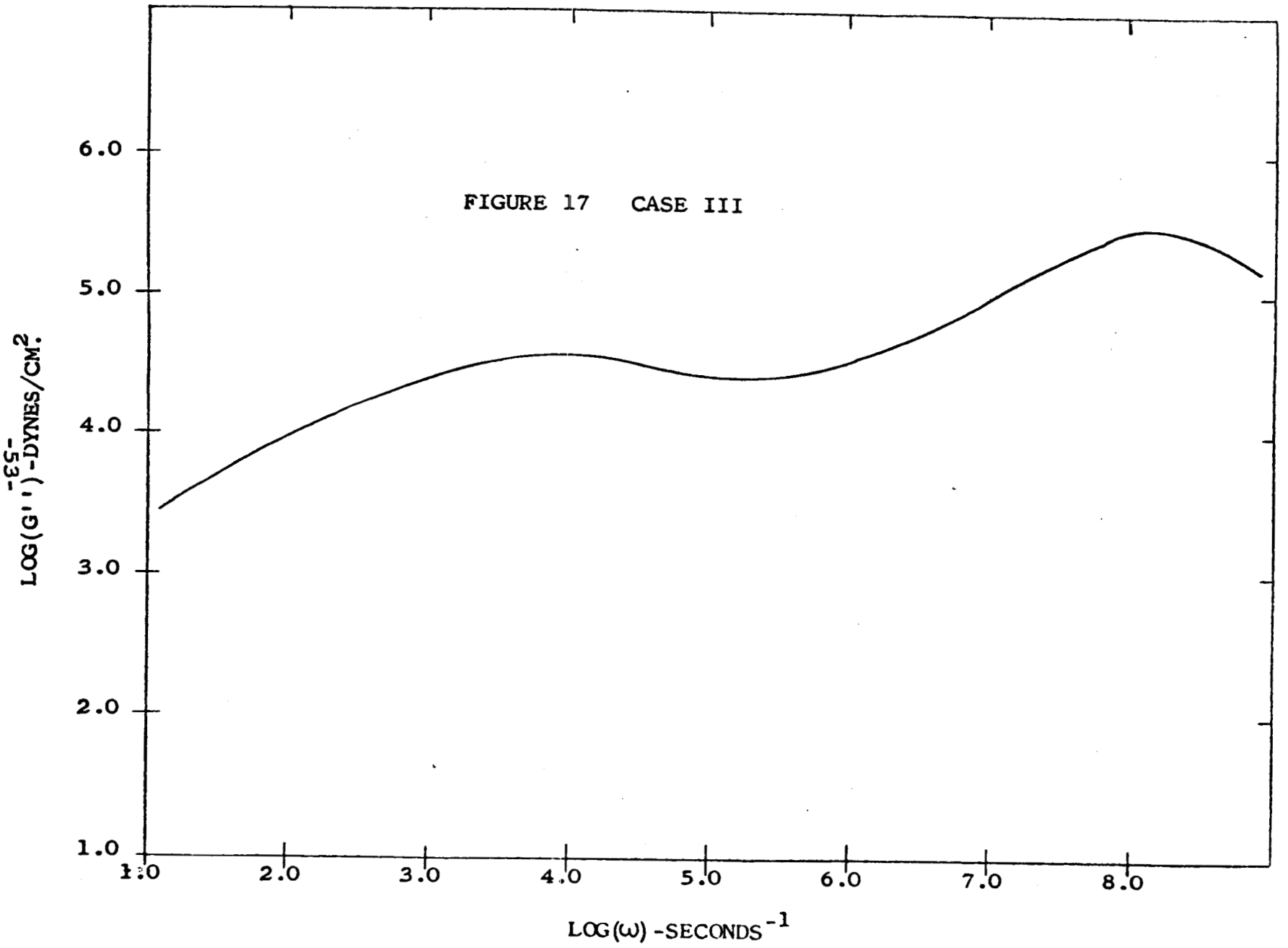
FIGURE 17 CASE III
6.0
5.0
4.0
3.0
2.0
1.0
1.0
2.0
3.0
4.0
5.0
6.0
7.0
8.0
LOG(G'') -DYNES/CM.2
-53-
LOG(ω) -SECONDS-1

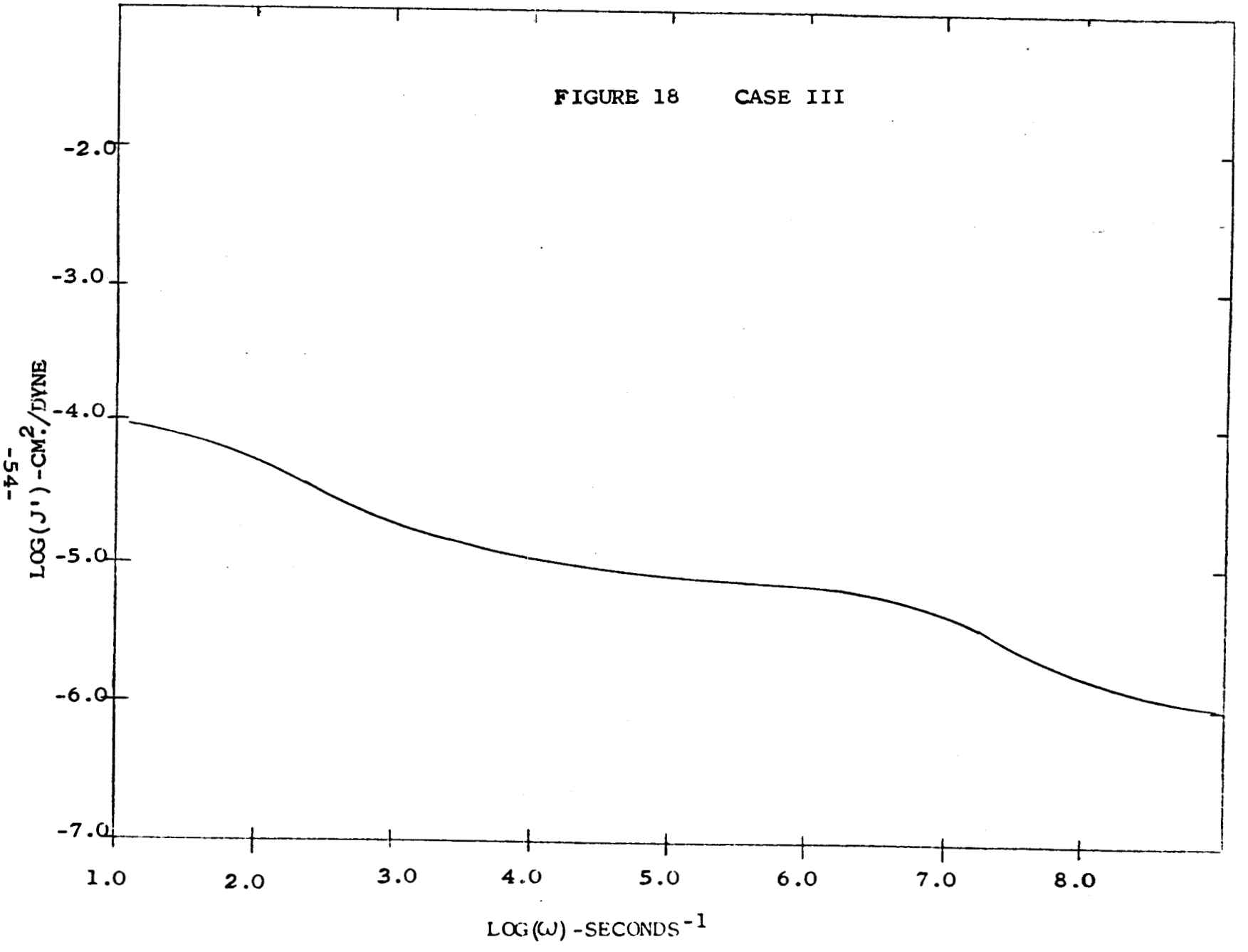
FIGURE 18 CASE III
-2.0
-3.0
-4.0
-5.0
-6.0
-7.0
LOG(J') -CM.2/DYNE
1.0
2.0
3.0
4.0
5.0
6.0
7.0
8.0
LOG(ω) -SECONDS-1

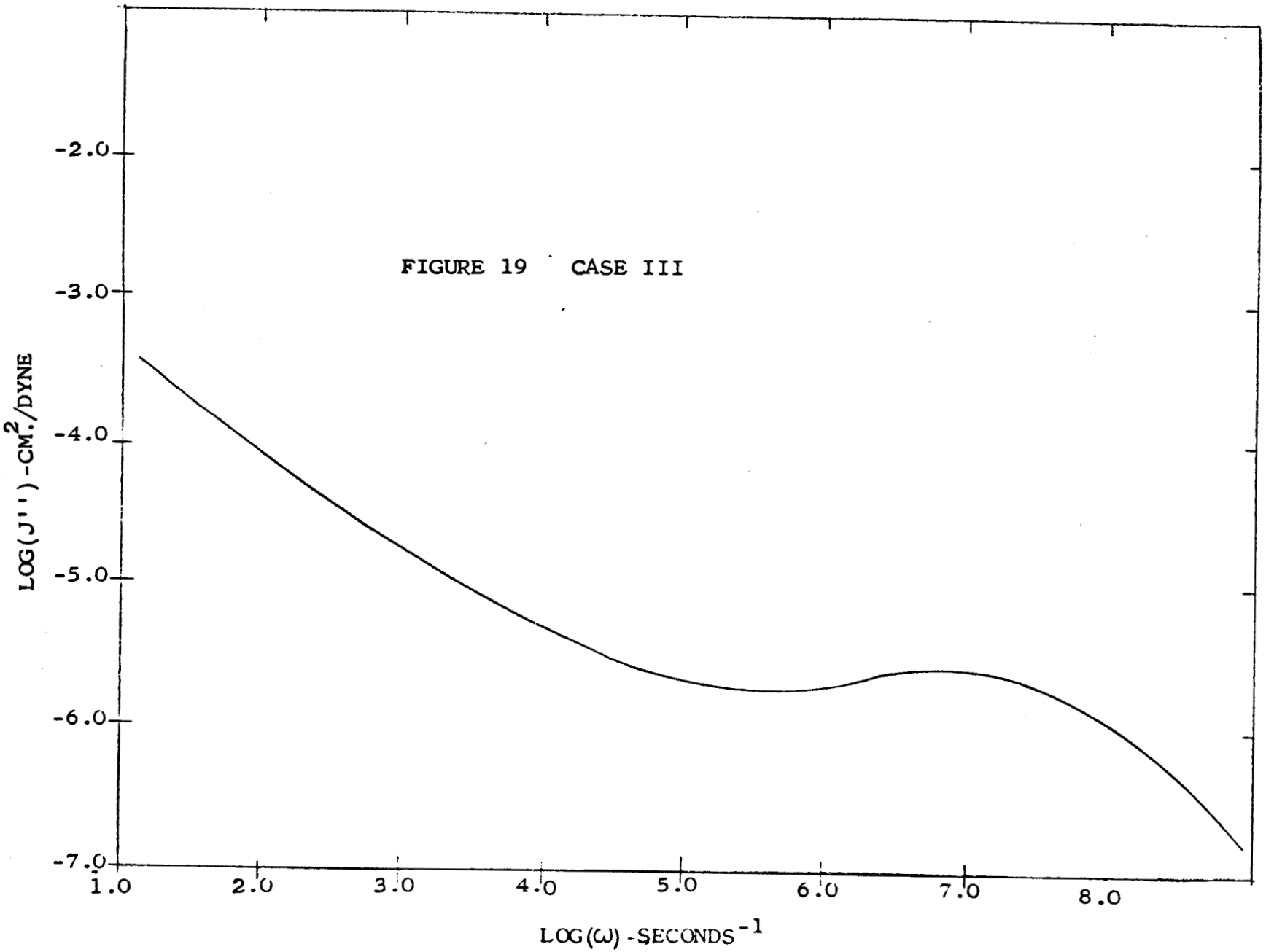

FIGURE 19 CASE III

(2.) from the loss compliance by

$$(J'')_{MAX.} = 0.32\ Me/(\rho\ RT); \qquad (A.56)$$

(3.) from the loss modulus by

$$(G'')_{MAX} = 0.32\ \rho\ RT/Me; \qquad (A.57)$$

and (4.) from the relaxation modulus, storage modulus and the storage compliance by

$$J_e = 1/G_e = 2\ Me/(\rho\ RT). \qquad (A.58)$$

Table I shows the results of using these equations.

For Case II, the calculated Me depends on the viscoelastic function selected for its evaluation. Me calculated from relaxation and storage moduli and the storage compliance are close to the actual molecular weight between entanglements employed in the computation of these functions. The relaxation spectrum does not give Me accurately since there is no extended region of -1/2 slope for the entangled modes of motion. The maxima in the loss modulus and the loss compliance probably do not give an accurate Me because of lack of this region in the spectrum.

For Case III, the various methods for calculation of Me give a close approximation of Me used for computing the viscoelastic functions. The apparent reason for the success

Table I: Molecular Weight Between Entanglements

Case Number	$H(\tau)$	$G(t)$	$G'(\omega)$	$G''(\omega)$	$J'(\omega)$	$J''(\omega)$	Actual Molecular Weight between Entanglements
II	21,300	36,500	36,500	77,300	36,500	8,360	31,150
III	1,800	1,850	1,850	1,980	1,530	1,980	1,650

of the relaxation spectrum, the loss modulus, and the loss compliance predicting Me for Case III is that the spectrum has a definite extended region of -1/2 slope for the entangled modes of motion.

Viscosity-Molecular Weight Relationship

Molecular weight of a polymer was found to influence directly its viscosity. To illustrate the viscosity-molecular weight relationship, polystyrene was selected.

Figure 20 shows experimental viscosity-molecular weight data on monodisperse polystyrene from a number of laboratories (15., 26.). As mentioned previously, the data can be represented by the two characteristic line segments. Below a critical molecular weight of about 40,000, the often used empirical relationship of Fox and Flory (which gives the viscosity as proportional to $M^{1.65}$) fits the data poorly. The experimental data below the critical molecular weight shows a marked deviation from a straight line indicating that the viscosity is a more complex function of the molecular weight. Considering the sizeable scatter in the experimental viscosities, above

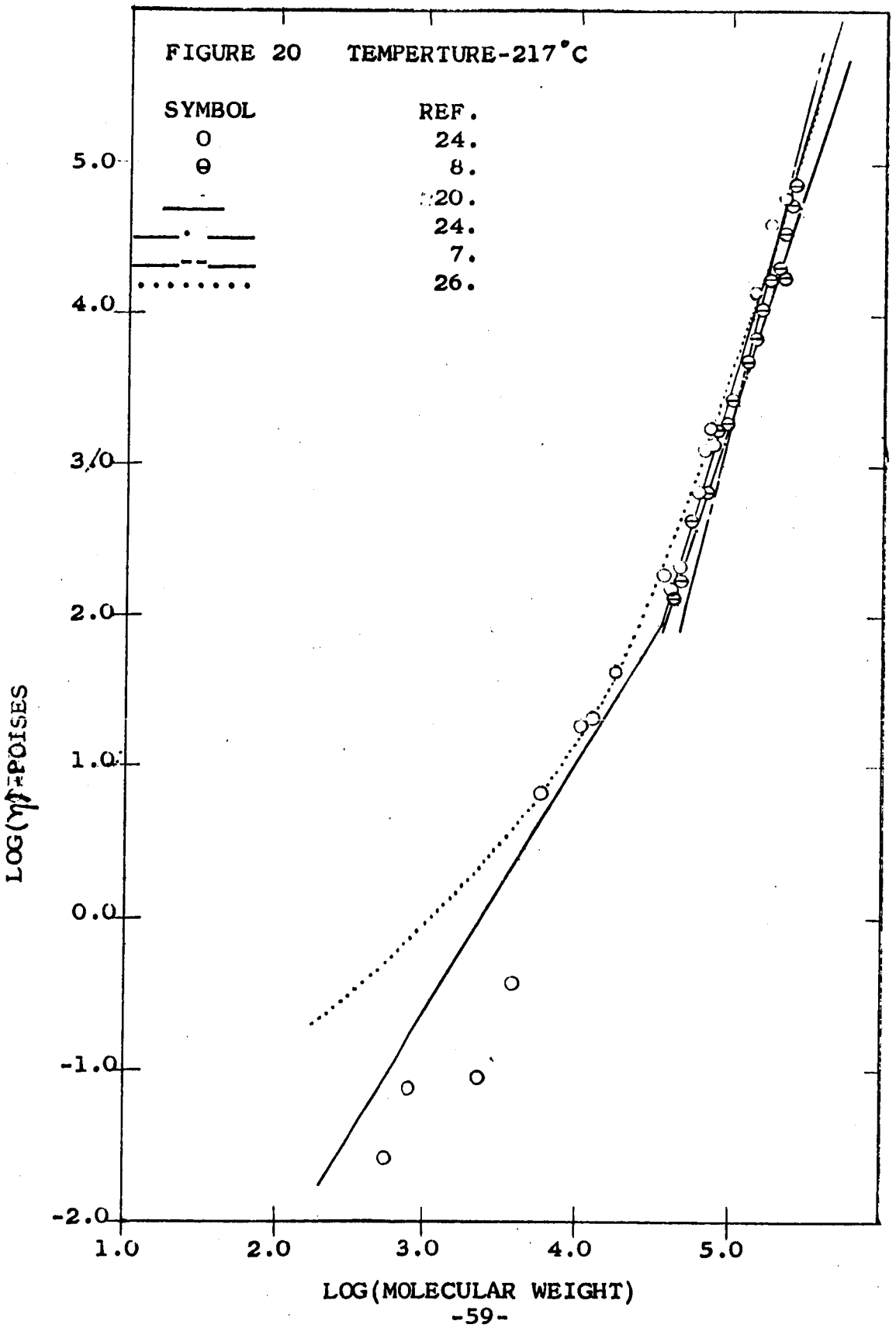
FIGURE 20 TEMPERTURE-217°C
SYMBOL
REF.
O
24.
Θ
8.
20.
24.
7.
26.
5.0
4.0
3.0
2.0
1.0
0.0
-1.0
-2.0
1.0
2.0
3.0
4.0
5.0
LOG(η)-POISES
LOG(MOLECULAR WEIGHT)

the critical molecular weight, viscosity-molecular weight data follow equally well the predictions of the several empirical equations. These relationships have the slope of the log (η) - log (M) plot ranging from 3 to 4.

In Figure 20, the curve for Chiakahisa (24.) was obtained by using b_1 and b_2 as adjustable parameters to best fit the experimental data. As with the empirical equations of Fox and Flory, Chiakahisa's theory does not predict the complicated molecular weight dependence below the critical molecular weight. Above the critical molecular weight, Chiakahisa's theory predicts that the slope will approach three and the data fall close to this line.

The failure below the critical molecular weight of the Fox and Flory empirical equation and Chiakahisa's theory was due to neglecting the effect of the chain ends. For the low molecular weights, there is a relatively high density of chain ends which greatly influence the viscous behavior of the polymer. Fox and Allen (26.) modified Bueche's viscosity equation to include the influence of chain ends and entanglements and obtained good agreement with their experimental data.

Our two modifications (Equations A.51 and A.52) of Bueche's viscosity equation which Fox and Allen included the affects of chain ends allow for a gradual introduction of the influence of entanglements. Figures 21.A and 21.B show the prediction of our modifications. Each curve is only very slightly influenced by the choice of value for its parameter. The precision of the viscosity data does not allow one to determine which equation best describes the effect of entanglements.

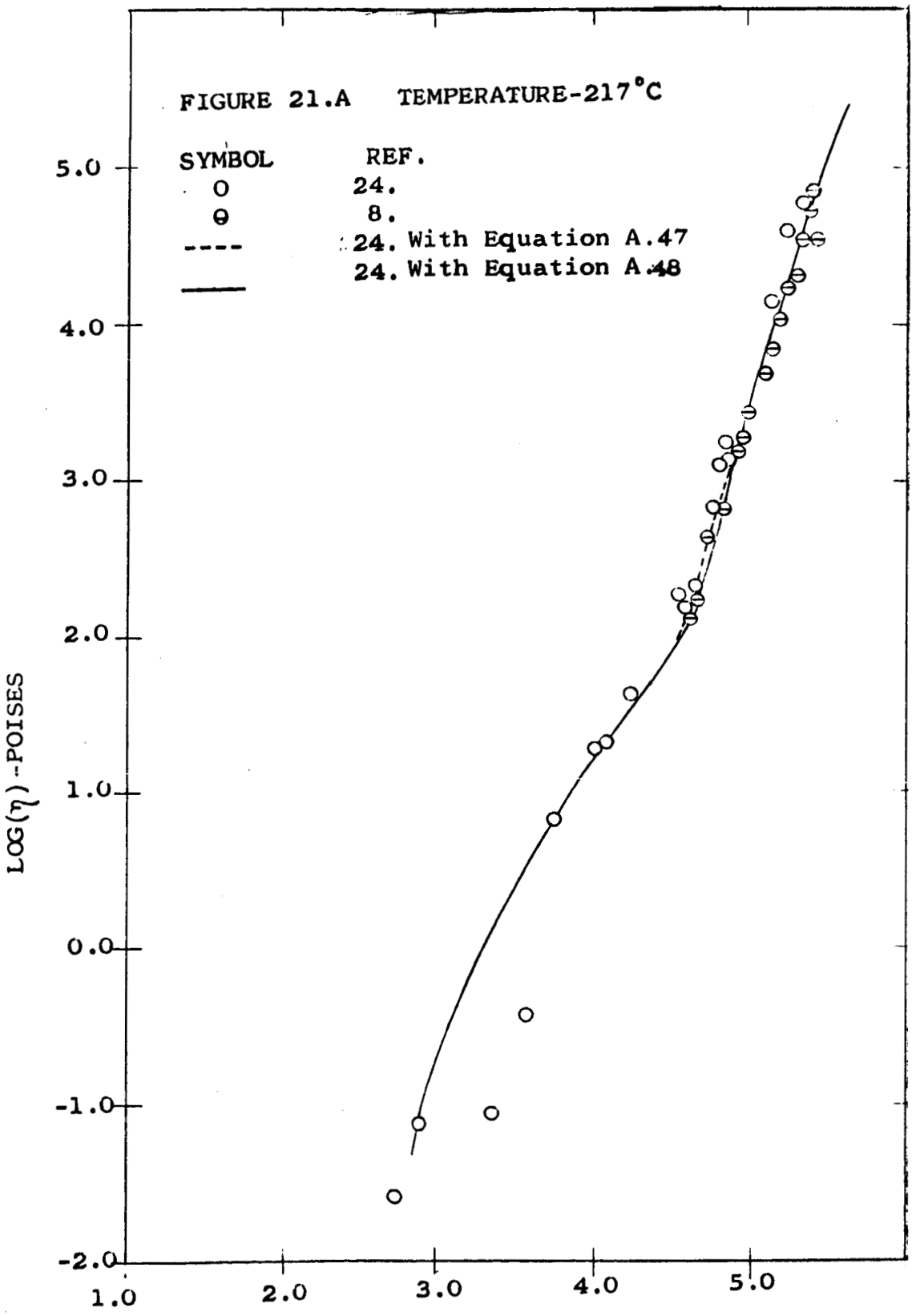
FIGURE 21.A TEMPERATURE-217°C
SYMBOL REF.
O 24.
Θ 8.
---- 24. With Equation A.47
—— 24. With Equation A.48
5.0
4.0
3.0
2.0
1.0
0.0
-1.0
-2.0
1.0
2.0
3.0
4.0
5.0
LOG(η)-POISES
LOG(MOLECULAR WEIGHT)

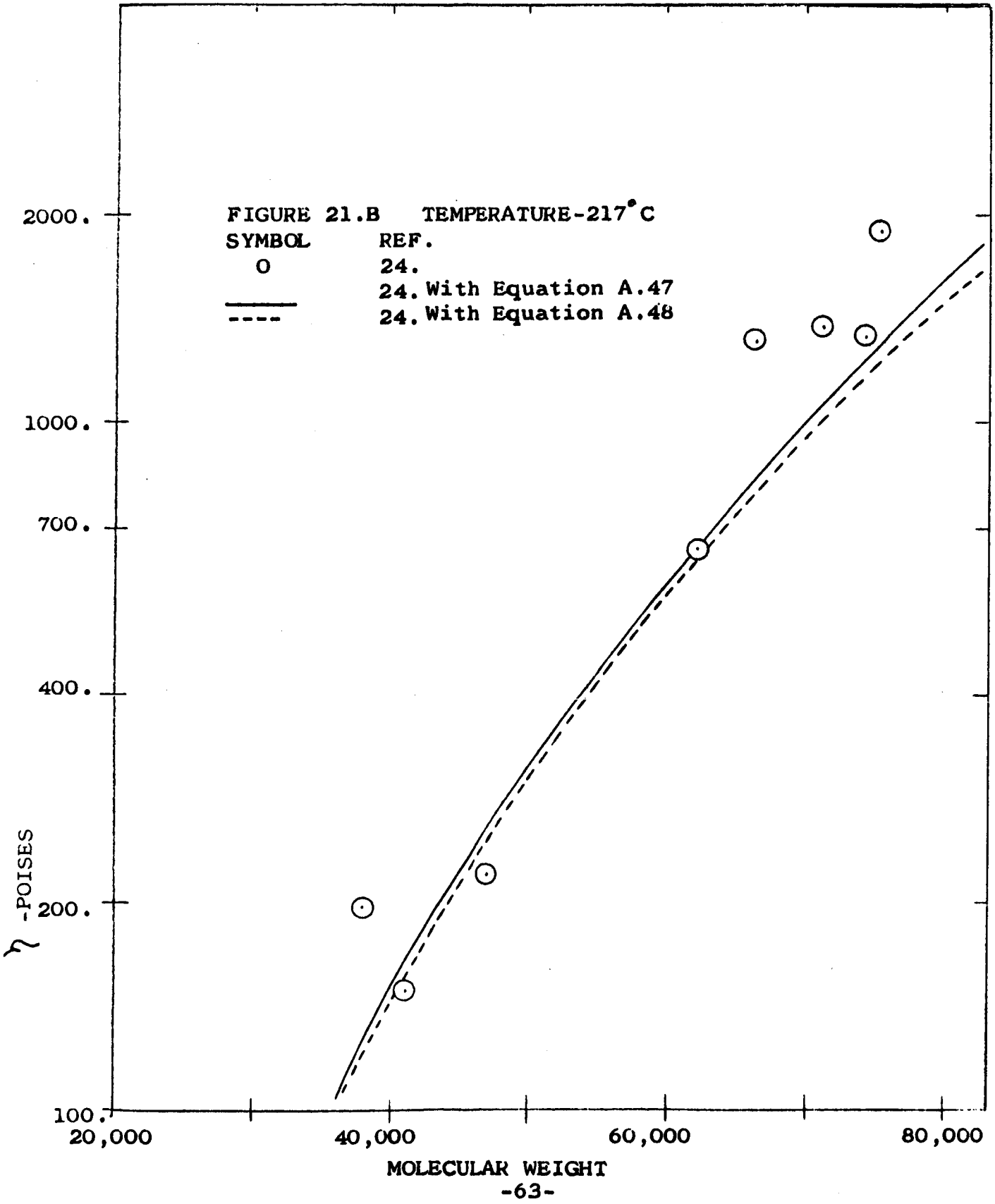
FIGURE 21.B TEMPERATURE-217°C
SYMBOL REF.
O 24.
24. With Equation A.47
24. With Equation A.48
2000.
1000.
700.
400.
200.
100.
η -POISES
20,000
40,000
60,000
80,000
MOLECULAR WEIGHT

Conclusions

The viscoelastic functions calculated from the WLF modification of Rouse's theory using the exponential entanglement coupling function (Equation A.47) illustrate generally observed experimental behavior. The loss modulus is the most sensitive of the viscoelastic functions to the nature of entanglement coupling. The minimum exhibited by this function depends on the number of relaxation times bridging the region between totally unentangled and totally entangled modes of chain motion. We thus propose that the loss modulus is the viscoelastic function to measure in order to study the details of entanglement couplings.

The viscosity-molecular weight relationship calculated from the exponential entanglement function is in good agreement with experiment.

Part B

Testing Approximate Interconversion Formulas for Various Viscoelastic Functions

Background and Theory

Exact methods for transformation from any linear viscoelastic function to any other have been developed from analytic function theory (2.b). These methods, however, are not practical for conversion of experimentally determined functions because their use requires integrations over times from 0 to $+\infty$ whereas experimental data can be obtained only over finite time intervals. To alleviate this difficulty, various approximate equations for interconversion between functions have been developed (1.b, 2.c, 27., 28.).

Using published experimental data determined for samples of National Bureau of Standards polyisobutylene, Smith (28.) interconverted many viscoelastic functions using several approximate equations. The magnitude of deviations of the calculated results from the experimental data indicated that the generally accepted approximate equations give only fair interconversion results. In addition, the interpretation of Smith's results on the validity of these equations is complicated due to the experimental error which is inherent in the data employed. A possible source of error is non-linear response because one is never sure that the data are taken in the range of linear viscoelasticity. Thus, there is no completely

reliable way of assessing the influence of experimental error and the approximate technique on the deviation of any of the interconversion formulas.

There is, however, no need to rely on experimental data to critically test interconversion formulas. Linear viscoelasticity is a mathematical formalism and thus it is possible to calculate completely consistent sets of linear viscoelastic functions. In part A of this thesis, just such mathematical data were generated which were typical of the behavior of high molecular weight amorphous polymers. In part B of this thesis, these viscoelastic functions are employed to test the generally used interconversion formulas.

Leaderman (1.b) discussed the calculation of the relaxation spectrum from either the relaxation or dynamic moduli and he proposed that:

$$H(t/2) = -\left[d/d(\ln t) - d^2/d(\ln t)^2\right] G(t) \qquad (B.1)$$

and

$$H(1/\omega) = \left[d/d(\ln\omega) - (1/4)d^3/d(\ln\omega)^3\right] G'(\omega). \qquad (B.2)$$

These equations require numerical differentiation of experimental data to obtain first, second, and third derivatives of moduli with respect to $\ln(t)$ or $\ln(\omega)$ with the concommitant increase in the error of the result. In fact,

since original experimental data usually contain considerable error, second or higher derivatives are often little more than crude approximations. Since the first terms in Equation B.1 and Equation B.2 usually predominate, they are often used as first approximations for the relaxation spectrum. For such first approximations, Leaderman concluded that Equation B.2 gives the more accurate result.

An approximate relation between relaxation spectrum and dynamic modulus proposed by Marin (35.) is

$$H(1/\omega) = (2/\pi)\, G''(\omega). \qquad (B.3)$$

This equation has ease of use; however, he reports that it approximates the relaxation spectrum poorly with best results occurring when $G''(\omega)$ changes gradually with frequency.

The relaxation spectrum can also be calculated approximately from the storage modulus by

$$H(1/\omega) = \left[e^2/2\pi \right] \left[d/d \ln\omega - (1/2) d^2/d(\ln\omega) \right] G'(\omega) \qquad (B.4)$$

which Okano and Fujita (1.b) proposed. This equation is similar to Equation B.2.

A relationship between the relaxation and dynamic moduli given by Ninomeya and Ferry is (2.c,29.)

$$G(\omega) = G'(\omega) - 0.40G''(0.40\omega) + 0.014G''(10\omega). \qquad (B.5)$$

The loss modulus can be estimated from the relaxation spectrum by means of (2.c)

$$G''(1/\tau) = (\pi/2)\, H(\tau)\, \sec(m\,\tau/2) \qquad (B.6)$$

and

$$G''(1/\tau) = H(\tau)/\left[\, B(1 - |m|\,)\right] \qquad (B.7)$$

where m is the negative slope of the log-log plot of the relaxation spectrum versus relaxation time and B is defined by

$$B \equiv (1 + |m|)/\left[2\,\Gamma(3/2 - |m|/2)\,\Gamma(3/2 + |m|/2)\right] . \qquad (B.8)$$

New Approximate Interconversion Formula

Ferry (2.b) reports many interconversion formulas for viscoelastic functions including several equations which allow the calculation of the loss modulus from the relaxation spectrum. However, there is no corresponding approximate equation for the calculation of the storage modulus. In this section, we derive such an interconversion formula. This new formula was tested along with the previously discussed equations and the results reported later in this thesis. With this relationship, the experimental determination of the loss modulus would be sufficient to estimate

all the other viscoelastic functions except G_e.

From analytic function theory (1.b),

$$G'(\omega) = \int_{-\infty}^{\infty} \left\{ H(\tau)\omega^2\tau^2 / \left[1 + \omega^2\tau^2\right] \right\} d(\ln \tau) . \qquad (B.9)$$

Changing the variable to Z where

$$Z \equiv \ln(\omega\tau) \qquad (B.10)$$

and

$$dZ = d(\ln\tau), \qquad (B.11)$$

Equation B.9 becomes

$$G'(\omega) = \int_{-\infty}^{\infty} \left\{ H\left[\mathrm{EXP}(Z)/\omega\right] \mathrm{EXP}(2Z)\,dZ \right\} \Big/ \left[1 + \mathrm{EXP}(2Z)\right] . \qquad (B.12)$$

Assuming that the relaxation spectrum can be approximated over a reasonable range of relaxation times by

$$H(\tau) = \beta \tau^{-m} \qquad (B.13)$$

and with

$$\tau = \mathrm{EXP}(Z)/\omega , \qquad (B.14)$$

the relaxation spectrum in the Z variable becomes

$$H\left[\mathrm{EXP}(Z)/\omega\right] = \beta \left\{ \mathrm{EXP}(Z)/\omega \right\}^{-m} . \qquad (B.15)$$

Using this relationship for the relaxation spectrum, the storage modulus becomes equal to

$$G'(\omega) = \beta\omega^m \int_{-\infty}^{\infty} \left[\mathrm{EXP}\ (2-m)Z\right]\ dZ / \left[1 + \mathrm{EXP}(2Z)\right] . \qquad (B.16)$$

If $H(\tau)$ is given adequately by Equation B.13 over a sufficiently range of relaxation times, then it is noted

that the integrand is effectively non-zero only when Z is near zero (i.e., $\tau = 1/\omega$) if m is between 0 and 2. Thus, Equation B.16 can be written as

$$G'(1/\tau) = \rho \tau^{-m} I(m) \qquad (B.17)$$

or

$$G'(1/\tau) = H(\tau) I(m) \qquad (B.18)$$

where I(m) is defined by

$$I(m) \equiv \int_{-\infty}^{\infty} \text{EXP}\left[(2-m)Z\right] dZ / \left[1 + \text{EXP}(2Z)\right] \quad . \qquad (B.19)$$

It should be noted that if m is not between 0 and 2, the integral of Equation B.19 will not converge and this inter-conversion formula will not apply. The function I(m) was evaluated numerically for values of m from 0.1 to 0.8 and is shown in Figure 22.

This equation has limited applicability since the slope of the relaxation spectrum must change gradually within a restricted range of m. We could expect, for example, that Equation B.18 should be useful for conversion of the relaxation spectrum into the storage modulus in the region where Rouse's theory adequately describes the spectrum. However, this approximate interconversion equation will break down in the plateau region since the slope approaches zero there.

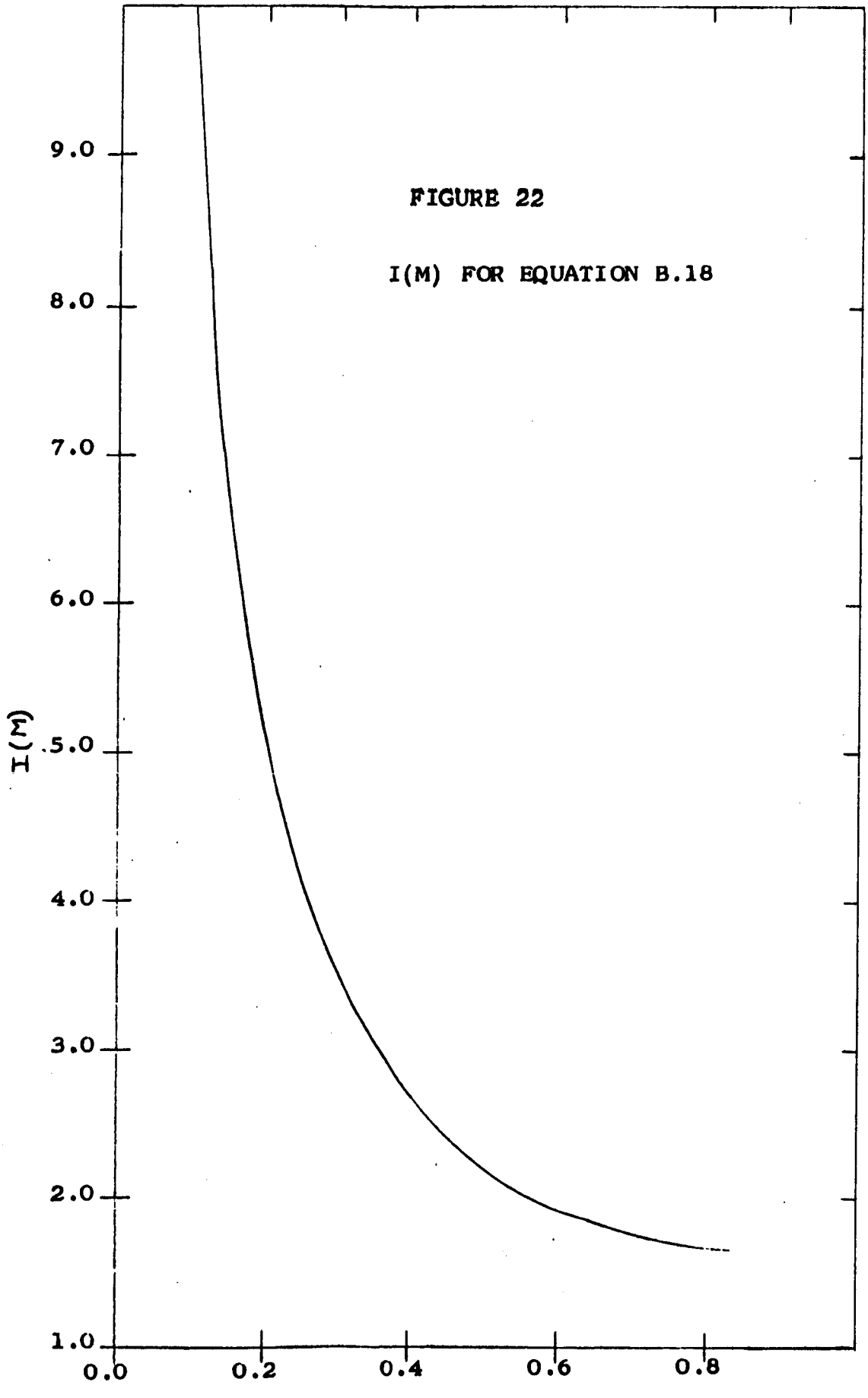

FIGURE 22

I(M) FOR EQUATION B.18

Results and Discussion

Here, we report the testing of the various interconversion formulas employing consistent sets of linear viscoelastic functions calculated in part A of this thesis. These functions will be referred to here as the correct viscoelastic functions.

We considered two cases, an unentangled polymer (Example I) and an extensively entangled polymer (Example II). See Appendix II for the physical constants associated with these two cases. We investigated the approximate interconversion formulas by examining the percent deviation between the log of the correct viscoelastic function and the log of the approximation.

Most approximate interconversion techniques require the evaluation of derivatives of the various viscoelastic functions. To obtain the needed derivatives, small segments of the appropriate viscoelastic function were fitted to a third order polynomial by least-squares analysis. These polynomials were used to evaluate the required derivatives.

Example I.

The correct linear viscoelastic functions for this

typical unentangled polymer are illustrated in Figures 31 through 36.

Calculation of $H(\tau)$

Several interconversion equations gave approximate representation of the relaxation spectrum from various moduli for this case. Figure 23 shows the percentage deviation of these equations from the correct relaxation spectrum. The maximum deviation of the log spectrum is 10%. Three of the formulas reproduced the correct curve within 3% for almost the entire range studied. The correct spectrum must be considered discrete at the longest relaxation times. All approximate equations predict a continuous spectrum for all times and they are, thus, inapplicable in the discrete relaxation time regime. Employment of Equation B.18 required the assumption of a slope and the calculation of a first approximation to the spectrum. We, then, measured its slope and computed a second approximation. We repeated this procedure until consistent results were obtained. For this example, the prediction of $\log(H)$ by this technique was in error by about 5%.

Calculation of G(t)

The relaxation modulus can be approximated from the

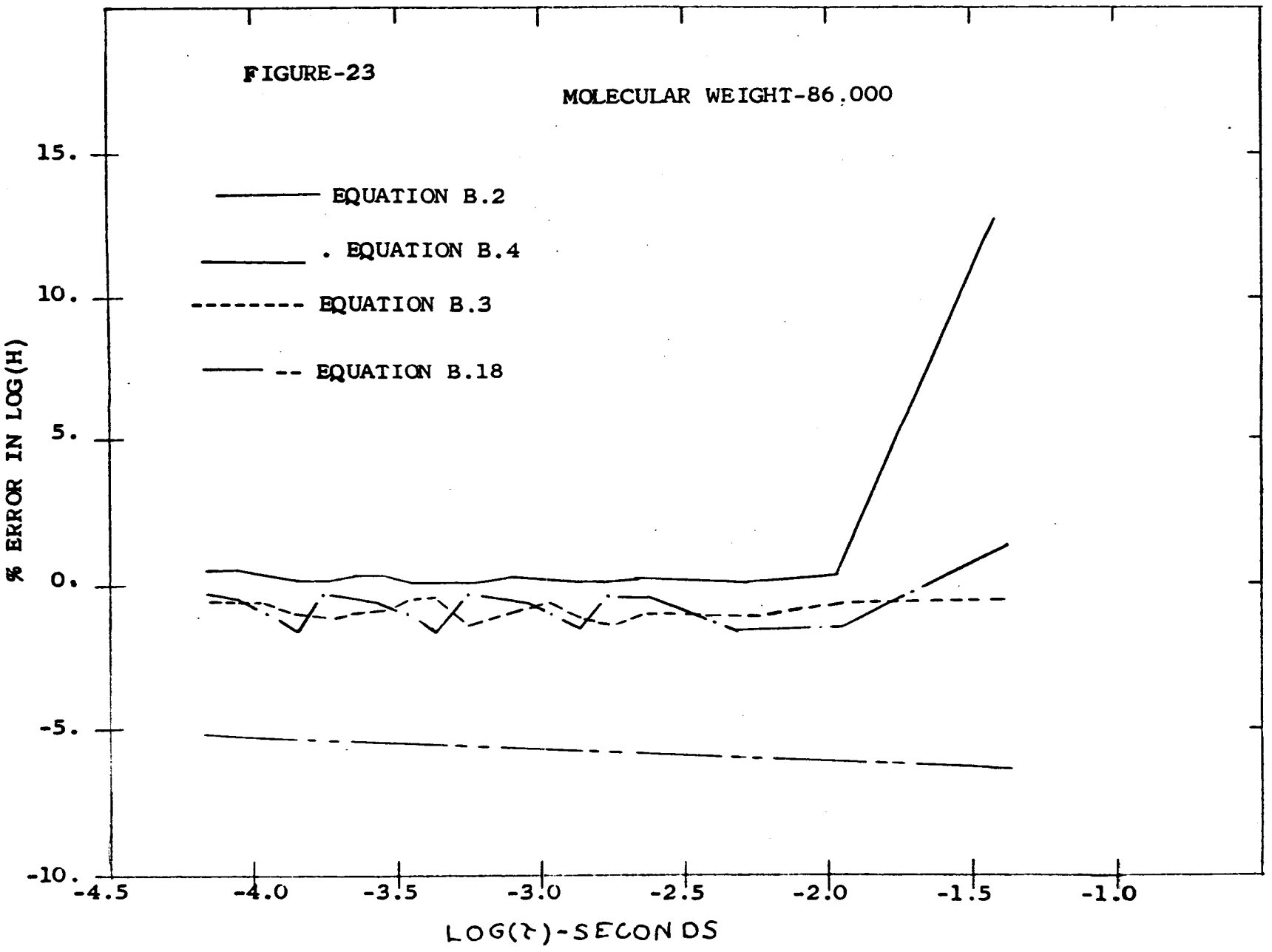
FIGURE-23
MOLECULAR WEIGHT-86.000
EQUATION B.2
. EQUATION B.4
EQUATION B.3
-- EQUATION B.18
% ERROR IN LOG(H)
15.
10.
5.
0.
-5.
-10.
-4.5
-4.0
-3.5
-3.0
-2.5
-2.0
-1.5
-1.0
LOG(τ)-SECONDS

dynamic modulus by using Equation B.5. Figure 24 shows the percentage error in log (G(t)) using this equation. The approximate formula gives less than half percentage deviation from the correct relaxation modulus except at the extremities of the range studied. The extrapolation of the data on the dynamic modulus necessary to evaluate relaxation modulus at the terminals of the time range causes this interconversion formula to break down.

Calculation of $G'(\omega)$

To obtain the storage modulus from the relaxation spectrum, we used the interconversion formula Equation B.18. The comparison of this approximate equation's prediction with the correct curve is illustrated in Figure 25. Since the relaxation times must be represented as discrete at the longest times, the approximate equation breaks down for the corresponding (smallest) frequencies. The relaxation spectrum for this case (see Figure 31) is continuous for $\log(\tau)$ shorter than -2.5. Therefore, our approximate equation is valid for $\log(\omega)$ greater than 2.5. This figure shows that Equation B.18 gives a percentage error in the log (G') less than 1% for $\log(\omega)$ in this range.

FIGURE 24 EXAMPLE I

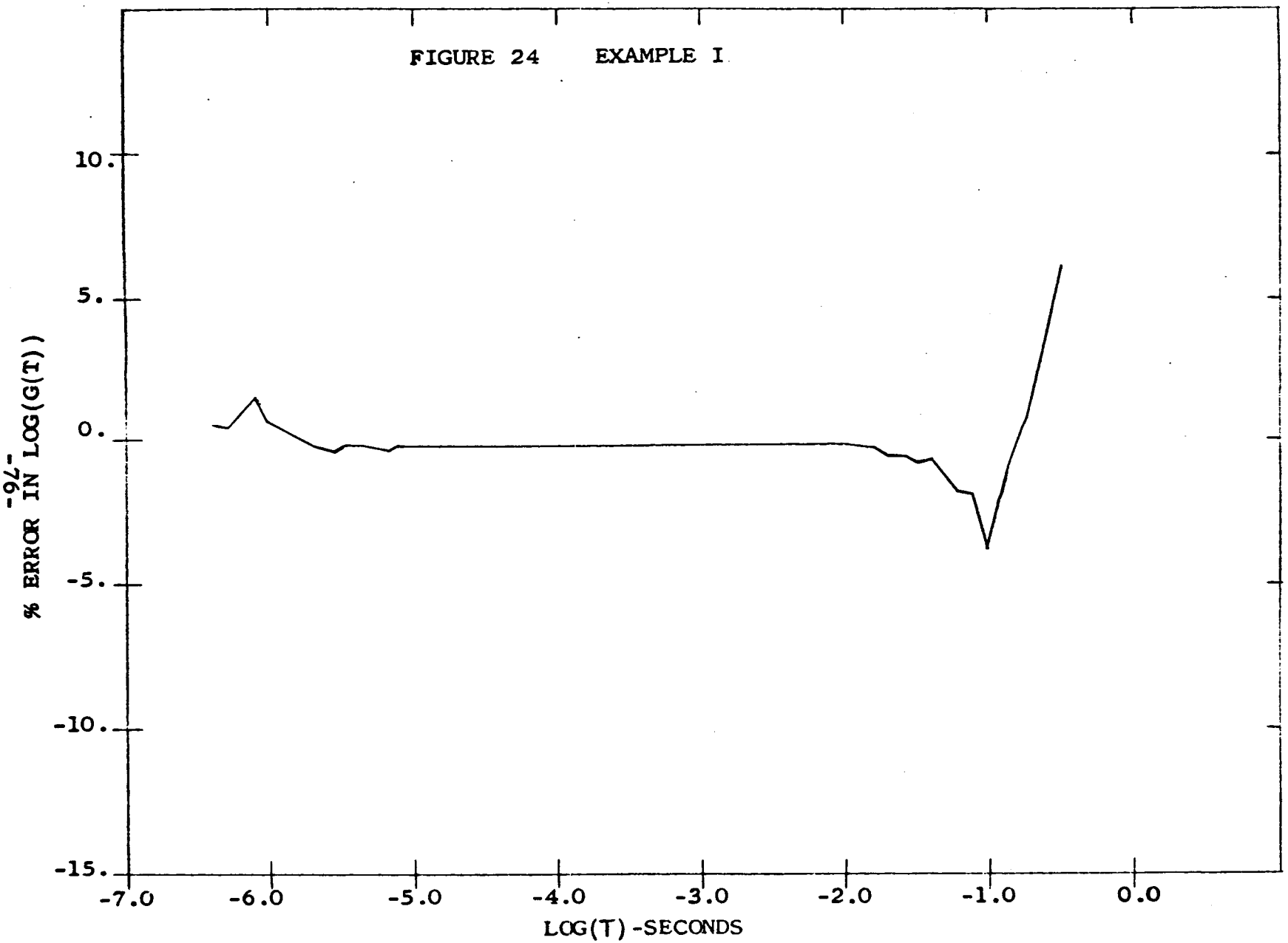

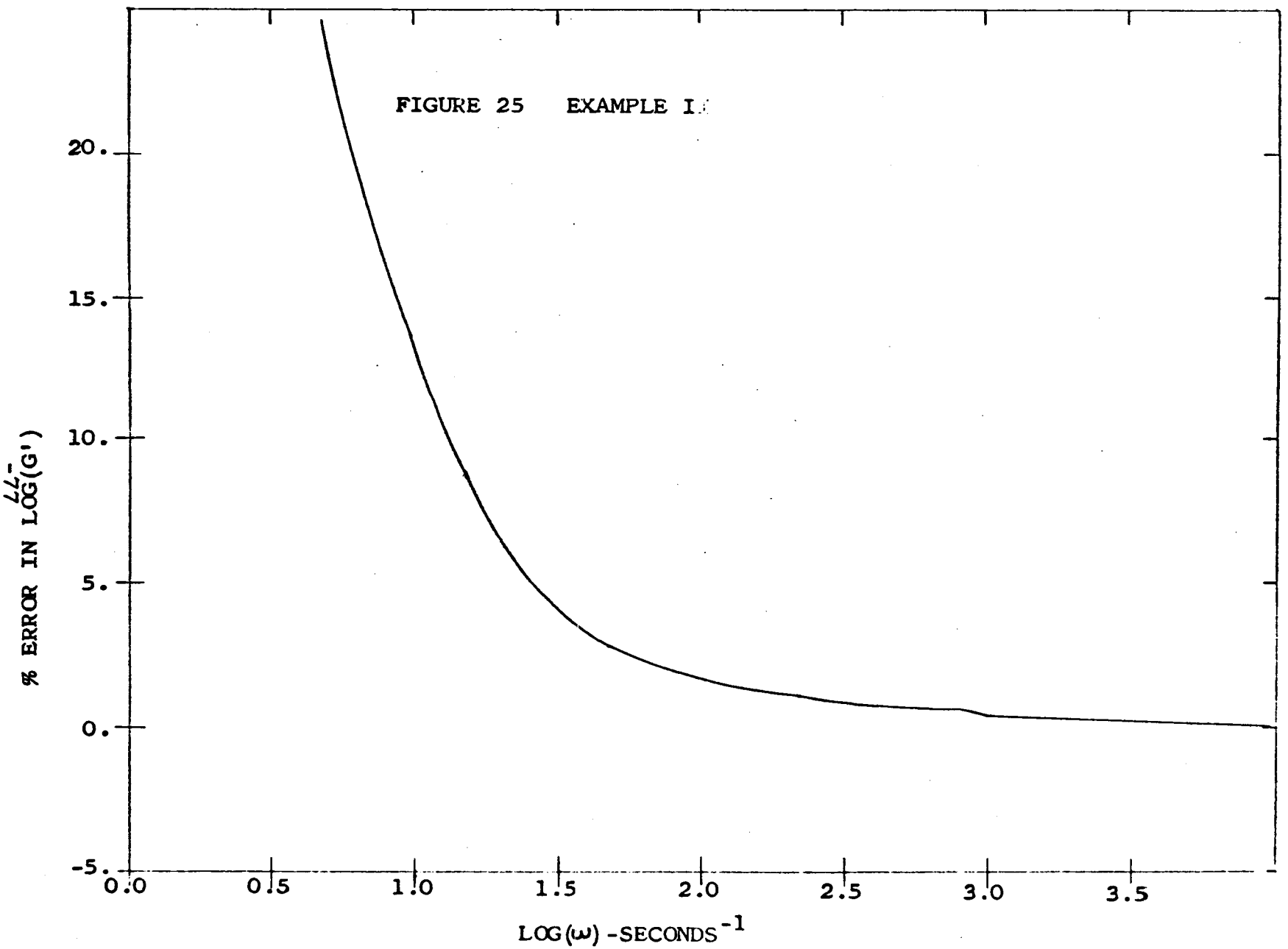

FIGURE 25 EXAMPLE I.

Calculation of $G''(\omega)$

Figure 26 displays the percentage error for the interconversion formulas in their prediction of the loss modulus from the relaxation spectrum. At low frequencies (i.e., long relaxation times), the approximate techniques show the greatest divergence from the correct curve because the relaxation spectrum is discrete at these times. Over a long range, the results of Equation B.6 are in error in predicting the correct modulus by a constant amount. If this equation is multiplied by 0.6, its results become nearly identical to the correct modulus except for the frequencies which correspond to the relaxation times where the spectrum is discrete and the interconversion formula does not apply. Equation B.7 predicts the correct curve similar to the corrected Equation B.6. The small error in approximating the correct curve from Equation B.7 was expected since it requires for its validity that $|m|$ be near 1/2. For this example, this condition was fulfilled for the correct relaxation spectrum except at the longest times.

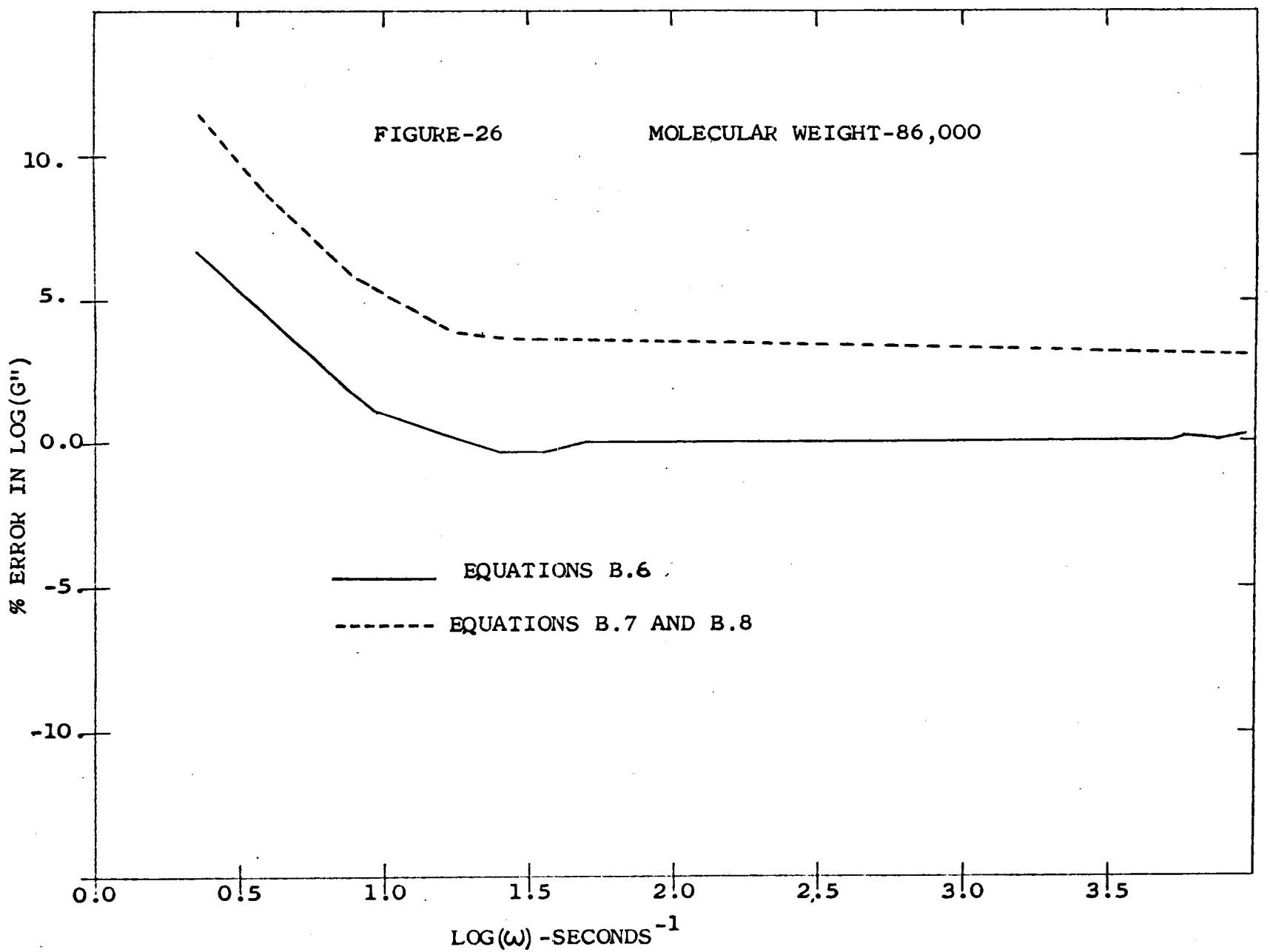
FIGURE-26
MOLECULAR WEIGHT-86,000
10.
5.
0.0
-5
-10
% ERROR IN LOG(G'')
EQUATIONS B.6
EQUATIONS B.7 AND B.8
0.0
0.5
1.0
1.5
2.0
2.5
3.0
3.5
LOG(ω) -SECONDS^{-1}

Example II

The correct viscoelastic functions for this typical entangled polymer, shown in Figures 10, 11, 16, 17, 18, and 19, were used to test the same approximate techniques as in Example I.

Calculation of $H(\tau)$

The relaxation spectrum (see Figure 10) can be divided into three zones, which are:

(1.) the completely unentangled modes of motion for log (τ) less than -7.0;

(2.) the partial entanglement or plateau region for log (τ) from -7.0 to -4.0;

(3.) the completely entangled modes of motion for log (τ) greater than -4.0..

Various approximate equations were used to calculate the relaxation spectrum with the results shown in Figure 27. The predicted spectra agree within ±5% of the correct value in the zone of completely unentangled modes of motion. The error in the prediction of the spectrum for Equations B.2 and B.4 is considerably higher for the longer relaxation times. These equations failed in the partial entanglement

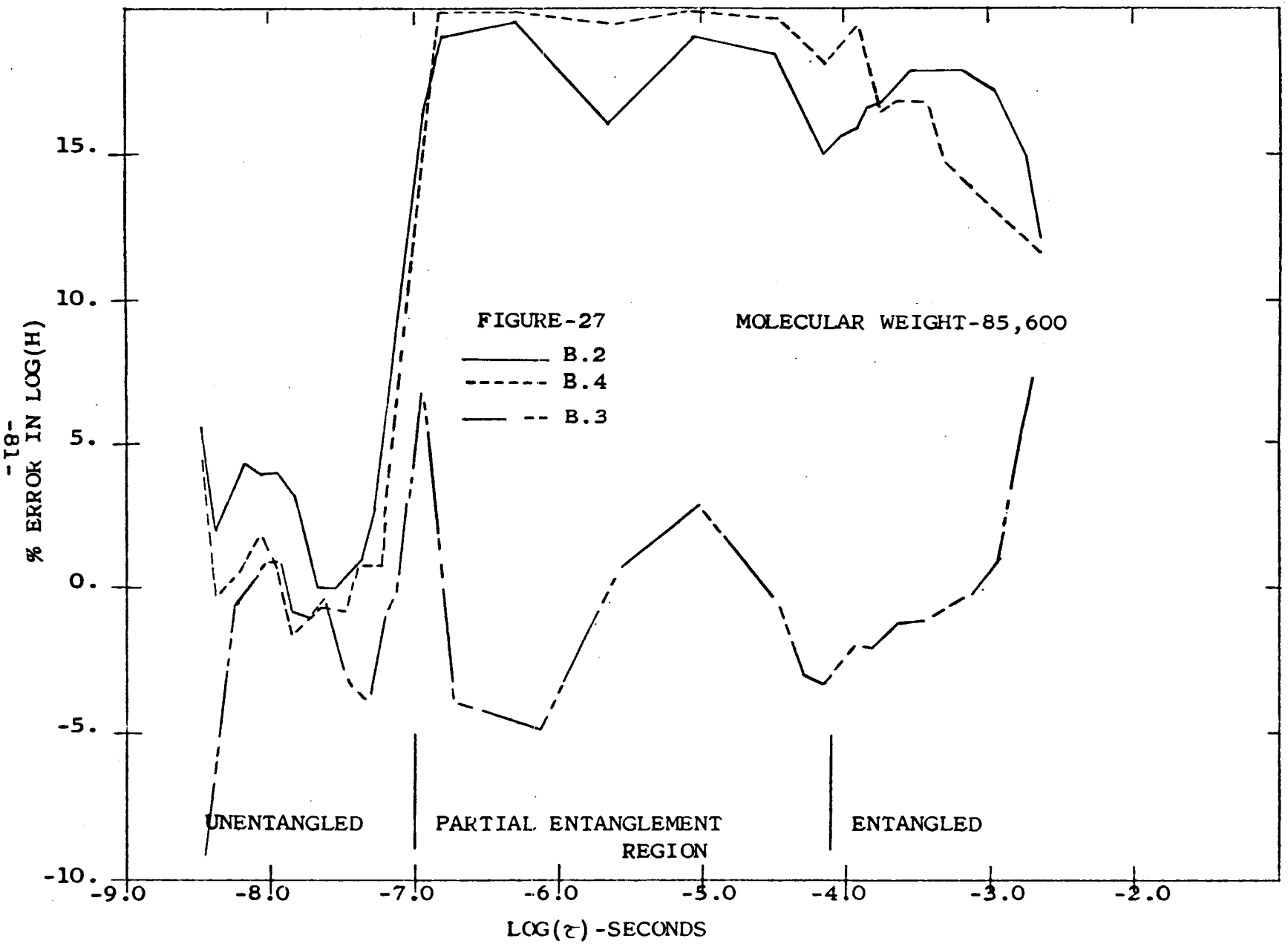
FIGURE-27
MOLECULAR WEIGHT-85,600
B.2
B.4
B.3
% ERROR IN LOG(H)
15.
10.
5.
0.
-5.
-10.
-9.0
-8.0
-7.0
-6.0
-5.0
-4.0
-3.0
-2.0
LOG(τ)-SECONDS
UNENTANGLED
PARTIAL ENTANGLEMENT REGION
ENTANGLED

region because $dG'/d(\ln\omega) \cong 0$ and the second term in each of these equations became significant. This term, which was intended to be only a correction factor, has a large error and here determined the value of the predicted spectrum. In the region of completely entangled modes of motion, the prediction in the log(H) by Equation B.2 is too large by nearly a constant amount. Equation B.3 maintained a prediction within 5% for the entire range of relaxation times studied. This is probably because this equation does not require the evaluation of derivatives to predict the spectrum.

Calculation of G(t)

The dynamic modulus predicted the relaxation modulus through the use of Equation B.5. Figure 28 shows that this equation yielded an approximate modulus correct to within 2% except at the longest times.

Calculation of $G'(\omega)$

The error in the approximation of the storage modulus from the relaxation spectrum by Equation B.18 is illustrated in Figure 29. As seen from this figure, the predicted modulus is in considerable error. This approximate

FIGURE 28 EXAMPLE II

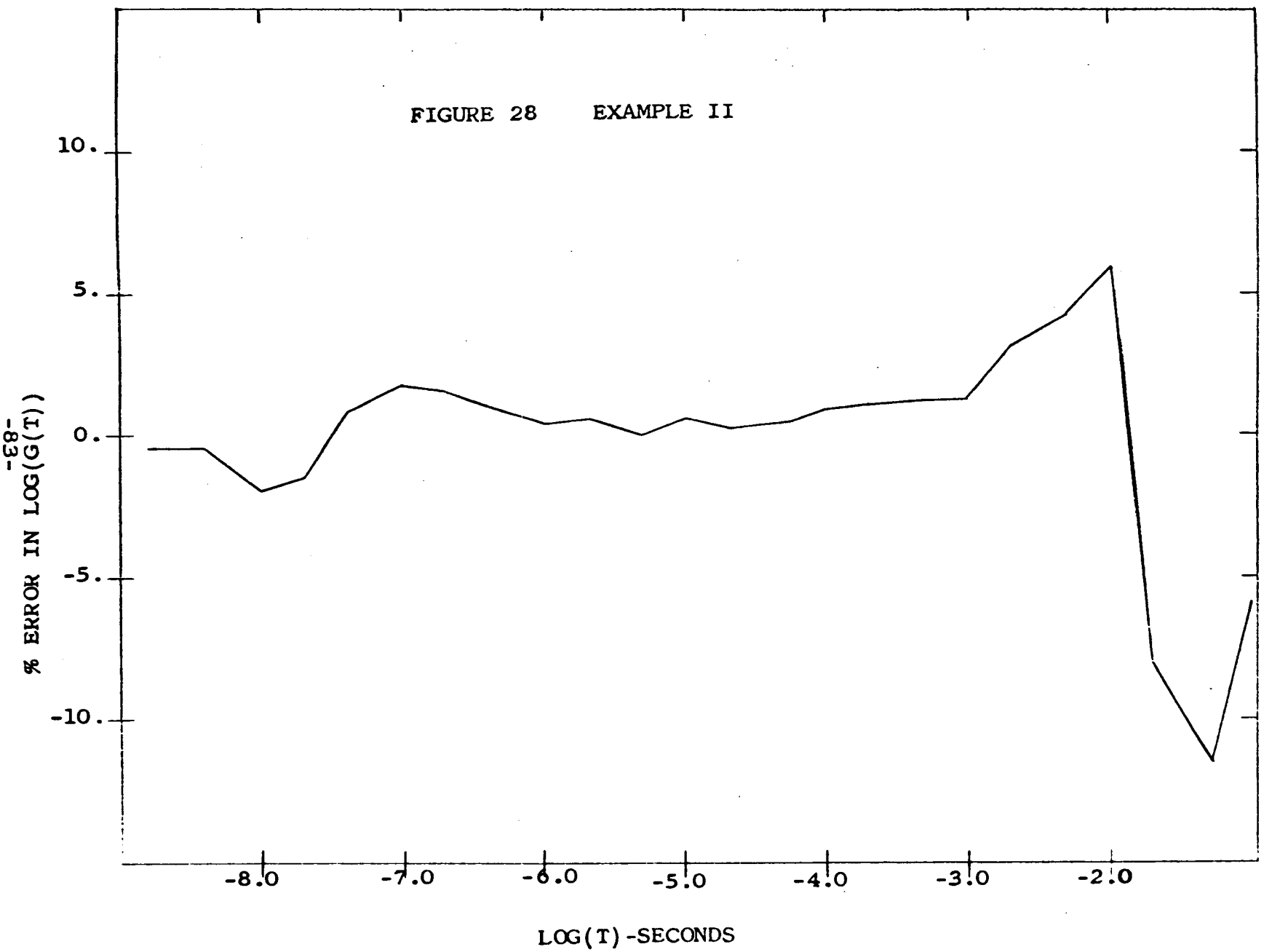

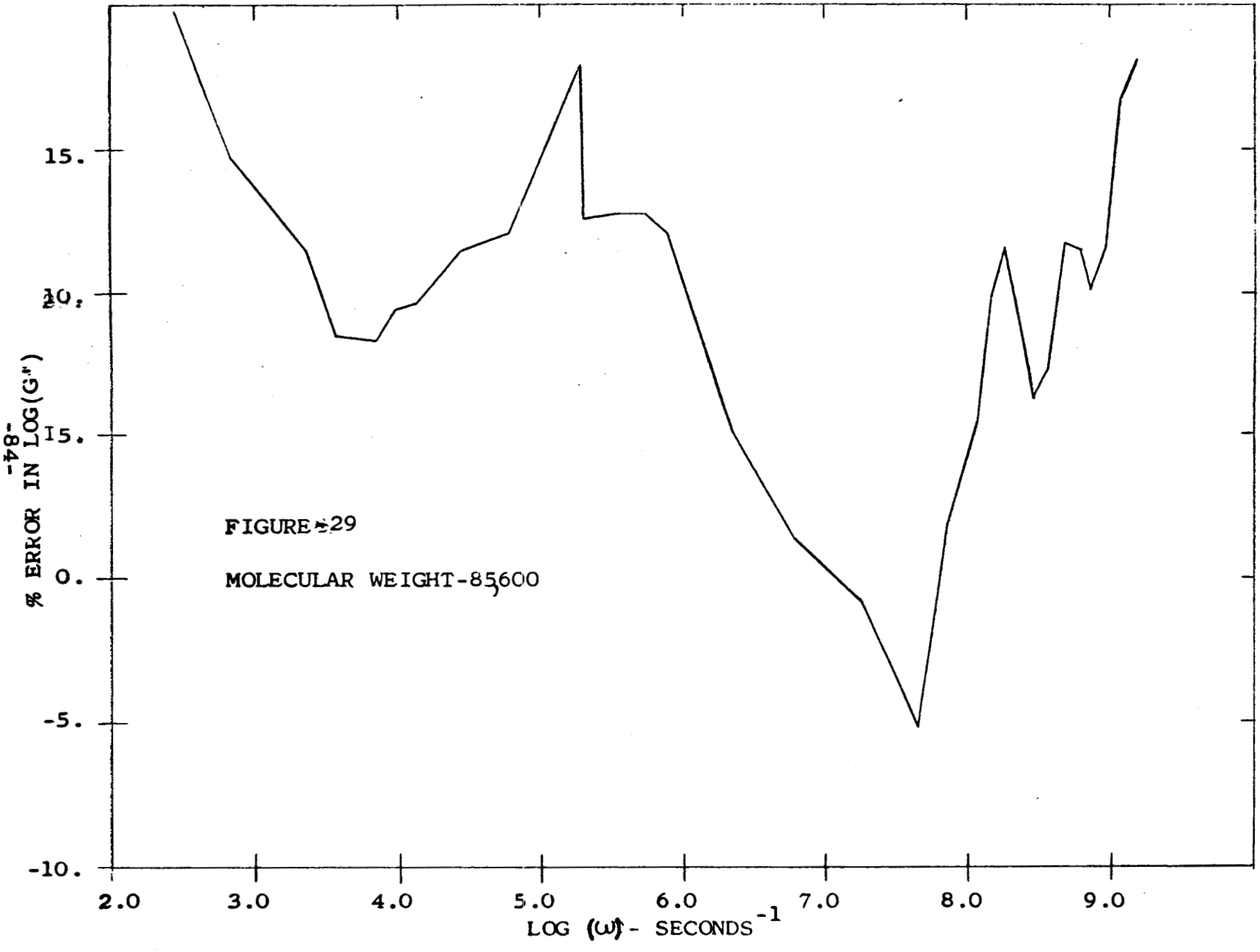

FIGURE 29

MOLECULAR WEIGHT-85600

interconversion formula gave poor results because the segments of the relaxation spectrum could not be sufficiently approximated by $\Theta \tau^{-m}$ with m between 0 and 2.

Calculation G"(ω)

Figure 30 shows the deviation of several approximate interconversion formulas in their prediction of the correct loss modulus. All of the equations predicted the log of the correct loss modulus within 10% for the entangled modes of motion (i.e., log(ω) less than 4.0). Considerable error in the prediction of these equations occurs in the region around log(ω) = 4.5 which corresponds to the region where the spectrum goes through a maximum. The slope of the spectrum changes rapidly in this region and this may have possibly caused the large discrepancy in predicting the log of the correct loss modulus. For the partial entanglement region and the region of unentangled modes of motion, the percentage error is within 10% for all of the formulas. In the region around log(τ) = -8.0, which corresponds to log(ω) = 8.0, the relaxation spectrum goes through a maximum and might be responsible for the large discrepancy noted here. This is the glassy region where Rouse's theory is no longer able to predict polymer behavior.

FIGURE-30 MOLECULAR WEIGHT-85,600

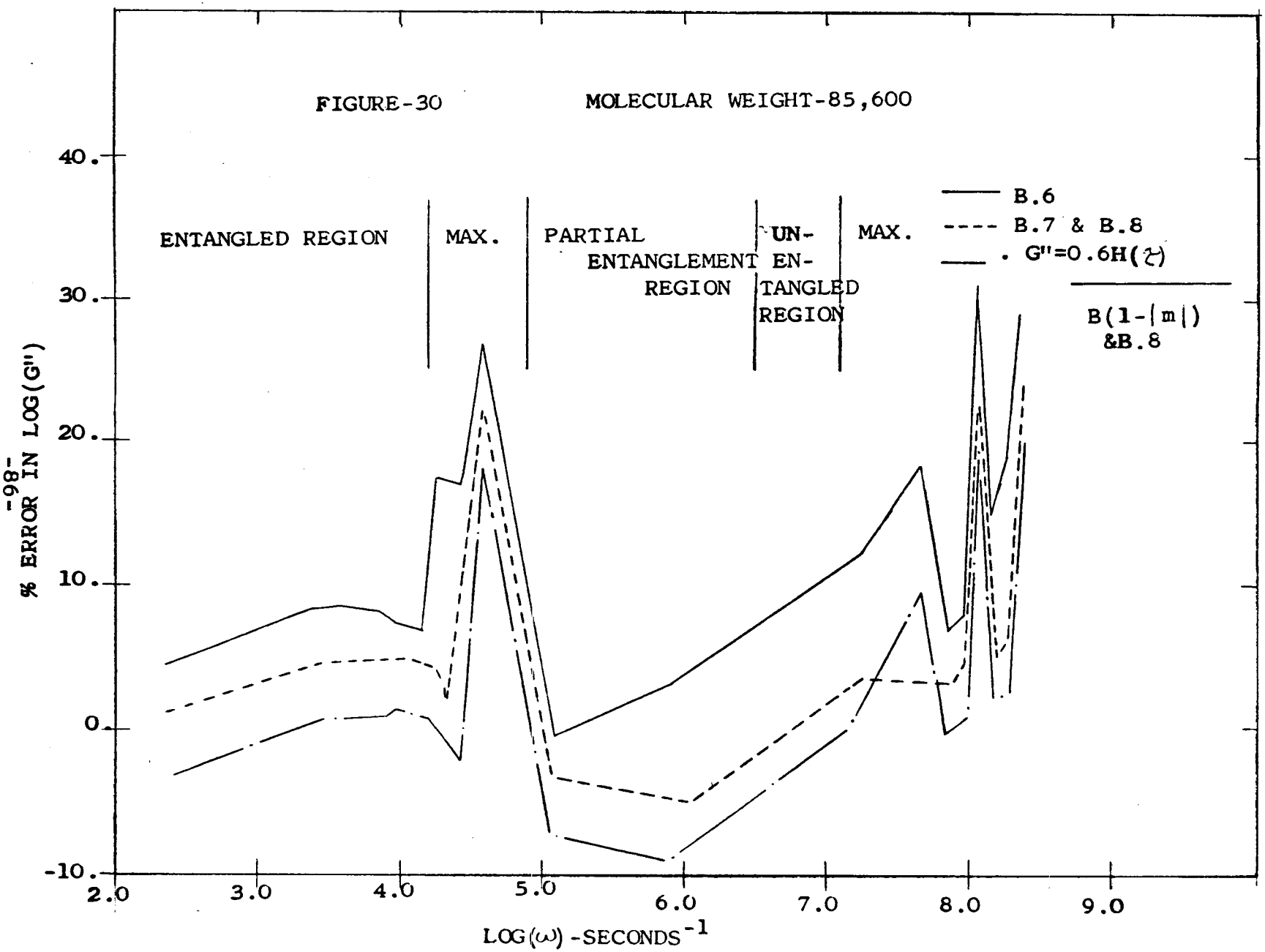

Conclusions

In employing the various approximate formulas to calculate $H(\tau)$, we conclude that:

(1.) the relationship of Marvin (Equation B.3) works well except where the relaxation spectrum is discrete;

(2.) the formulas of Okano and Fujita (Equation B.4) and Leaderman (Equation B.2) work well in the region of the relaxation spectrum where the slope is nearly -1/2 and give poor approximations to the spectrum in the region where the slope is nearly zero or is discrete.

The prediction of the relaxation modulus from the dynamic modulus using the relationship of Ferry and Ninomeya (Equation B.5) is excellent for both cases studied.

The approximation of the loss modulus from the relaxation spectrum using the expressions of Smith (Equation B.6) and Ferry (Equation B.7) is good when

the spectrum has a slope of nearly -1/2. Equation B.7, however, gave a 3% smaller error than Equation B.6. Neither relationship gave satisfactory predictions of the loss modulus where a plateau occurred in the relaxation spectrum.

Our approximate interconversion formula for calculating the storage modulus from the relaxation spectrum (Equation B.18) works well only when the spectrum can be well represented as a "wedge" with a slope of about -1/2. Considerable modification is required before this equation will apply where the slope of the spectrum is near zero.

Appendices

Appendix I: Viscosity-Molecular Weight Relationship

To be able to apply Equation A.39, the following equations are necessary to compute the radius of gyration and the monomeric friction factor for polystyrene (26):

$$(\langle S_o^2 \rangle_{av} / M) = 9.2 \times 10^{-18} (1 - 10^{-3}T) \qquad (C.1)$$

with T in degrees Centigrade and

$$1/Tg = 1/373 + 0.72/M \qquad (C.2)$$

$$\log (\xi_o) = \log \xi g - \epsilon (T-Tg)/(\lambda + T-Tg) \qquad (C.3)$$

with

$$\log(\xi g) = 3.0 \qquad (C.4)$$

$$\epsilon = 13.7 \qquad (C.5)$$

$$\lambda = 48^{o}K. \qquad (C.6)$$

We used the relationship of Fox and Flory (30.)

$$v = 1.040 + 72/M \qquad (C.7)$$

to calculate the required specific volume of polystyrene at 217°C.

Appendix II: Physical Constants for Various Cases

Tobolsky (6.) reports the relaxation spectrum for monodispersed polystyrene. The physical constants (6., 31.) for this case are listed in Table II.

Table II: Physical Constants for Case 1.

Polymer Viscosity (poises)	3.30×10^{14}
Solvent Viscosity (poises)	0.0
Temperature, ^{o}K	388
Number of Molecules per Cubic Centimeter	3.77×10^{18}
Molecular Weight	154,000
Molecular Weight between Entanglements	31,150
Critical Index	2.47
Number of Subchains	381
Parameter (E_1)	0.5
Entanglement Coupling Function	A.51

The physical constants for calculating the viscoelastic functions for Case II are listed in Table III.

Table III: Physical Constants for Case II.

Molecular Weight	750,000
Molecular Weight between Entanglements	31,500
Viscosity of Polymer (poises)	203,000
Viscosity of Solvent (poises)	0.0
Number of Subchains	288
Critical Index	12
Temperature (^{o}K)	490
Number of Molecules per Cubic Centimeter	7.73×10^{17}
Parameter (E_1)	10^{8}, 1.0, 0.5, 0.25
Entanglement Coupling Function	A.51

The physical constants for Case II (Example I for Part B of this thesis) are listed in Table IV.

Table IV: Physical Constants for Case III and Example I.

Molecular Weight	85,600
Molecular Weight between Entanglements	1,625
Viscosity of Polymer (poises)	10,000
Viscosity of Solvent (poises)	0.0
Number of Subchains	205
Critical Index	26
Temperature (^{o}K)	490
Number of Molecules per Cubic Centimeter	6.78×10^{18}
Parameter (E_1)	1.5, 1.0, 0.5
Entanglement Coupling Function	A.51

Table V lists physical constants for Example I.

Table V: Physical Constants for Example I.

Molecular Weight	86,000
Molecular Weight between Entanglements	___
Viscosity of Polymer (poises)	10,000
Viscosity of Solvent (poises)	0.0
Number of Subchains	209
Critical Index	___
Temperature (^{o}K)	500
Number of Molecules per Cubic Centimeter	6.74×10^{18}
Parameter	___

FIGURE-31 MOLECULAR WEIGHT-86,000

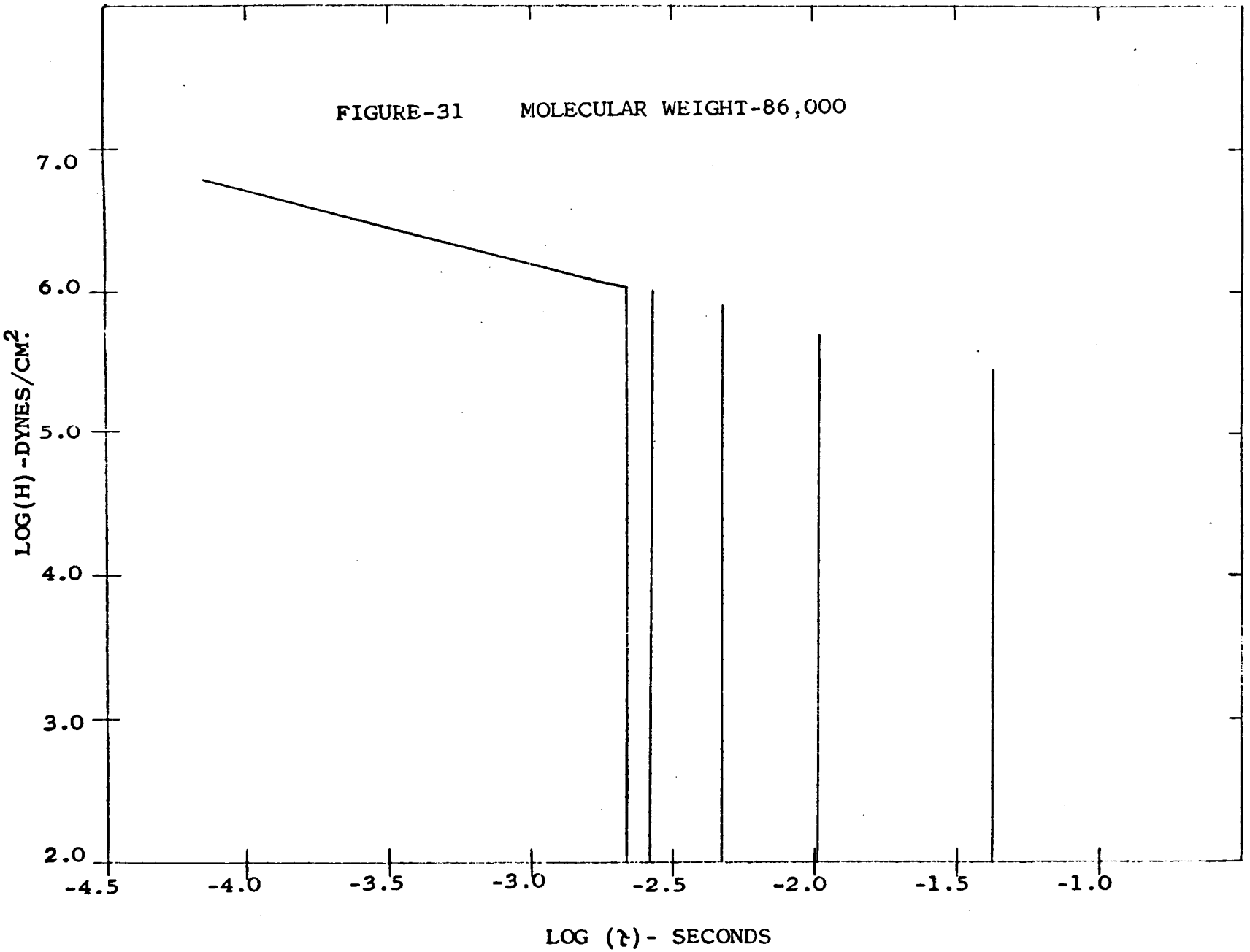

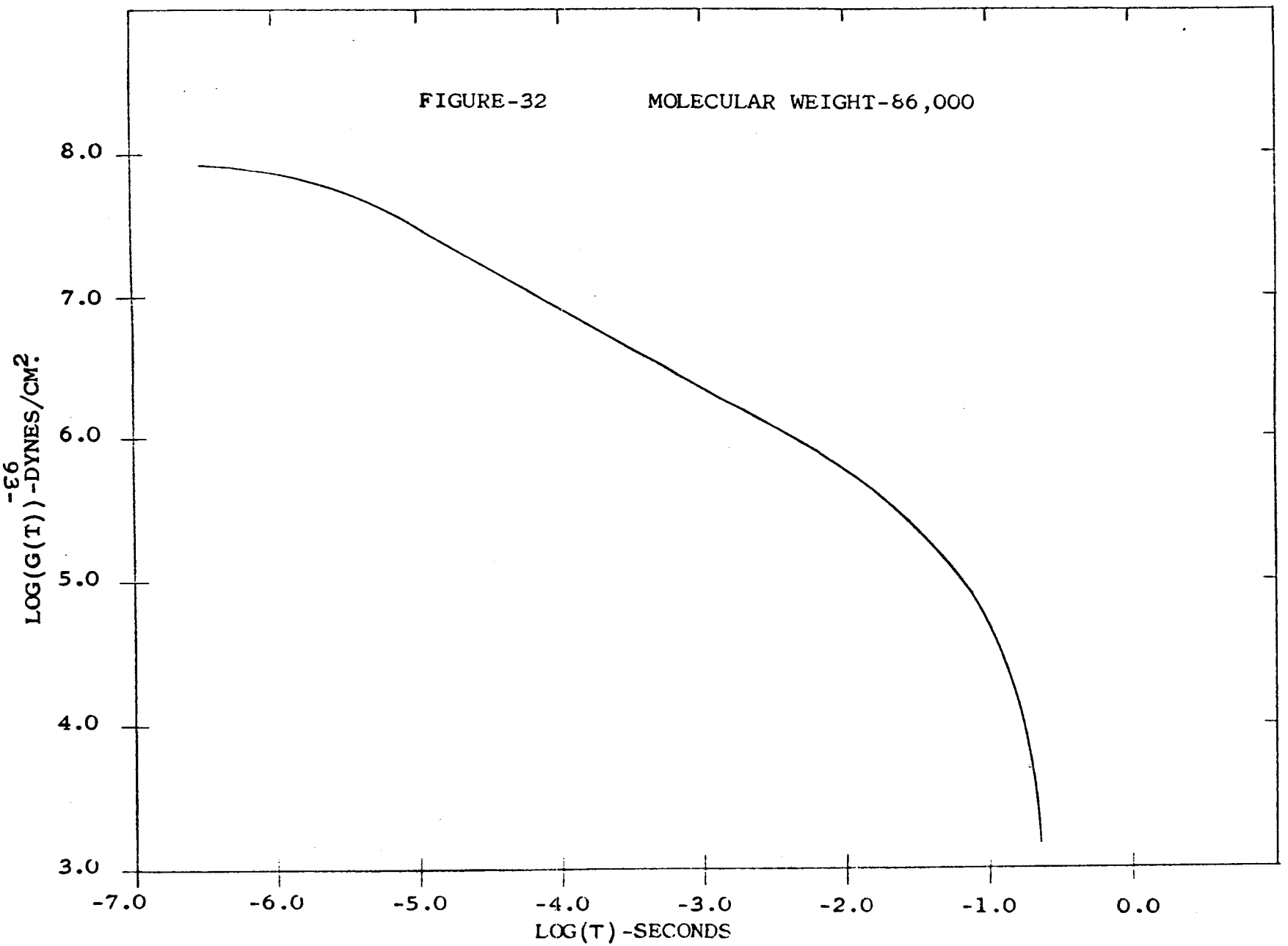
FIGURE-32 MOLECULAR WEIGHT-86,000
8.0
7.0
6.0
5.0
4.0
3.0
LOG(G(T))-DYNES/CM.2
-ε6
-7.0
-6.0
-5.0
-4.0
-3.0
-2.0
-1.0
0.0
LOG(T)-SECONDS

FIGURE-33 MOLECULAR WEIGHT-86,000

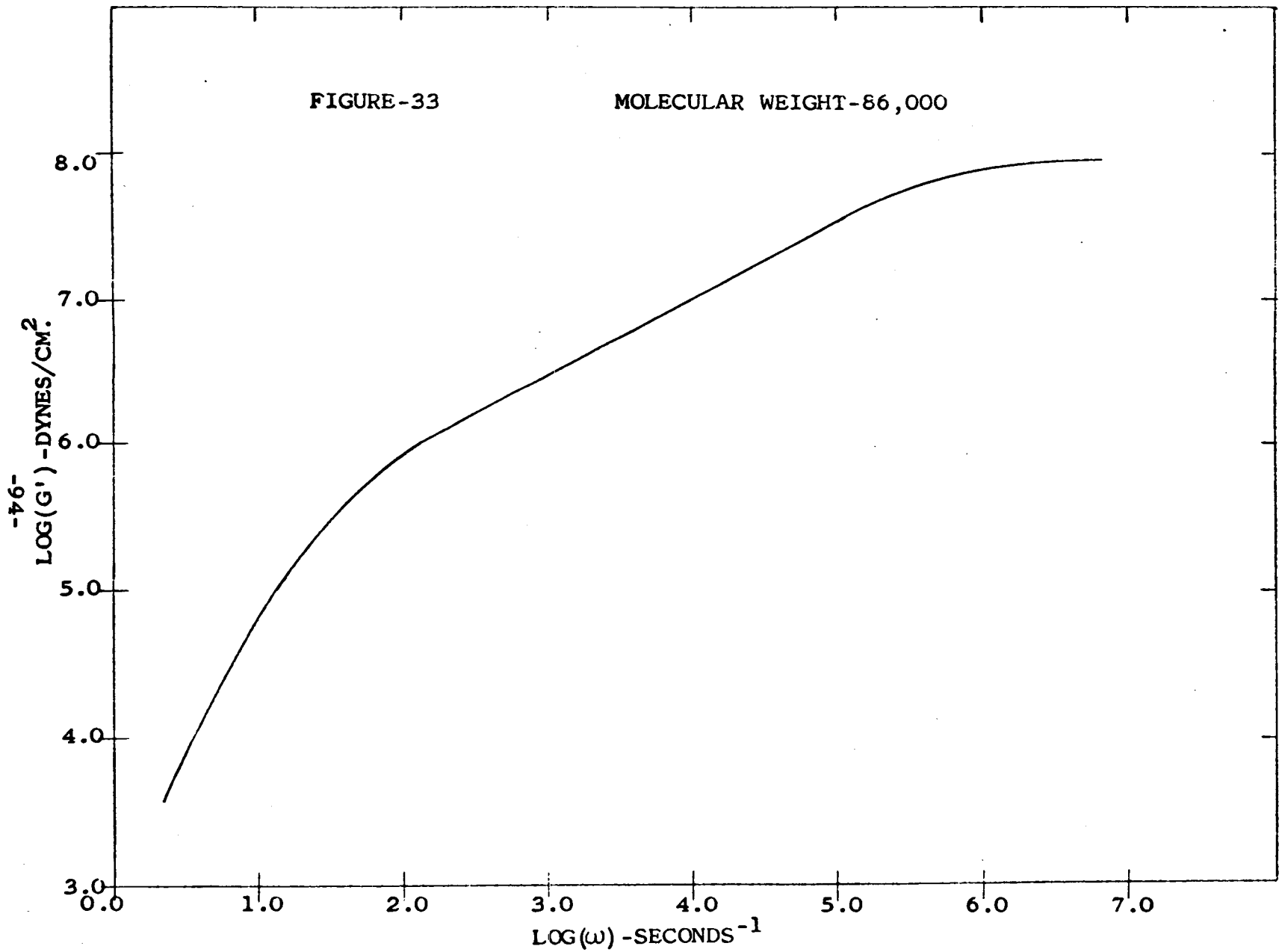

FIGURE-34 MOLECULAR WEIGHT-86,000

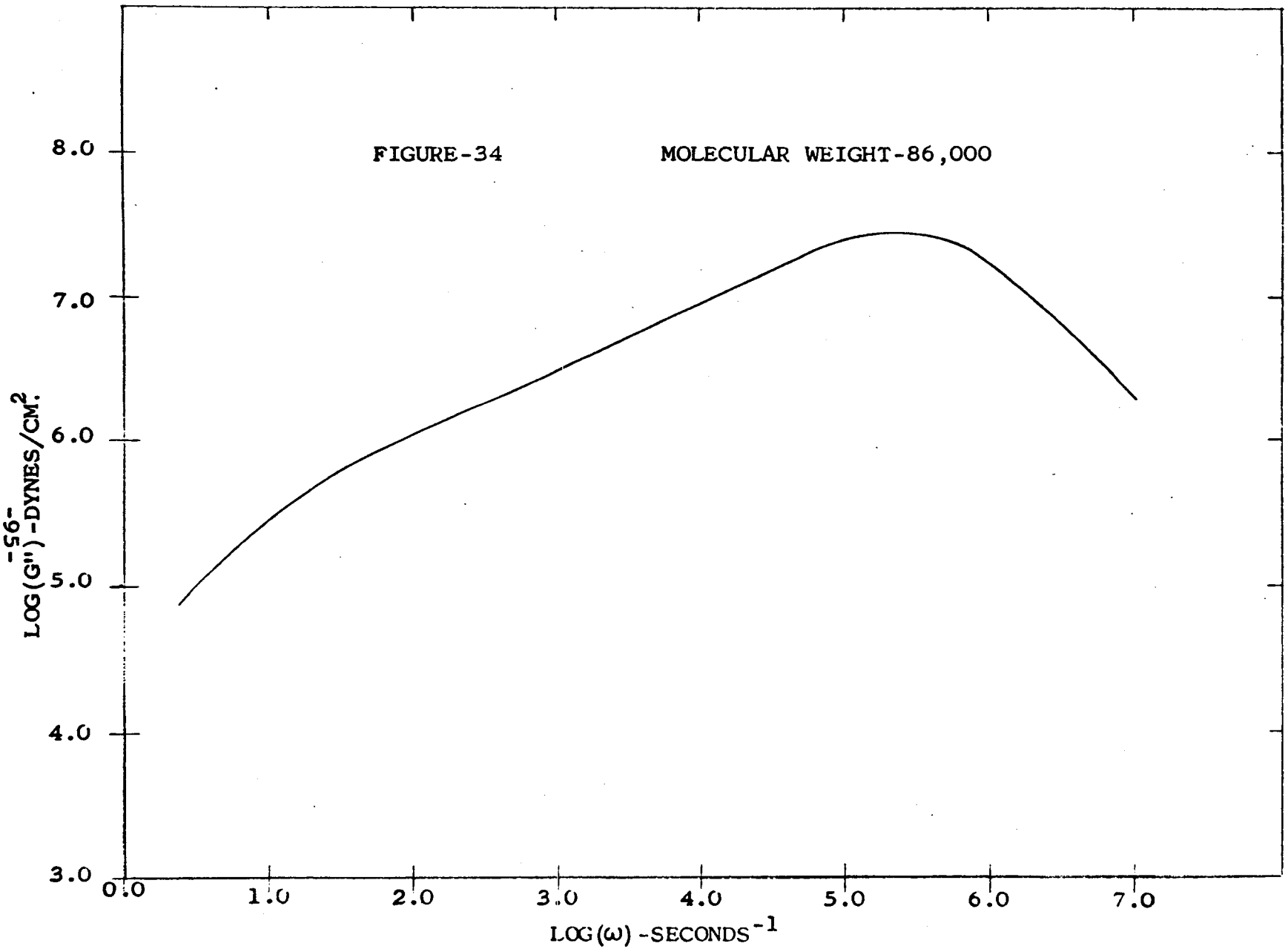

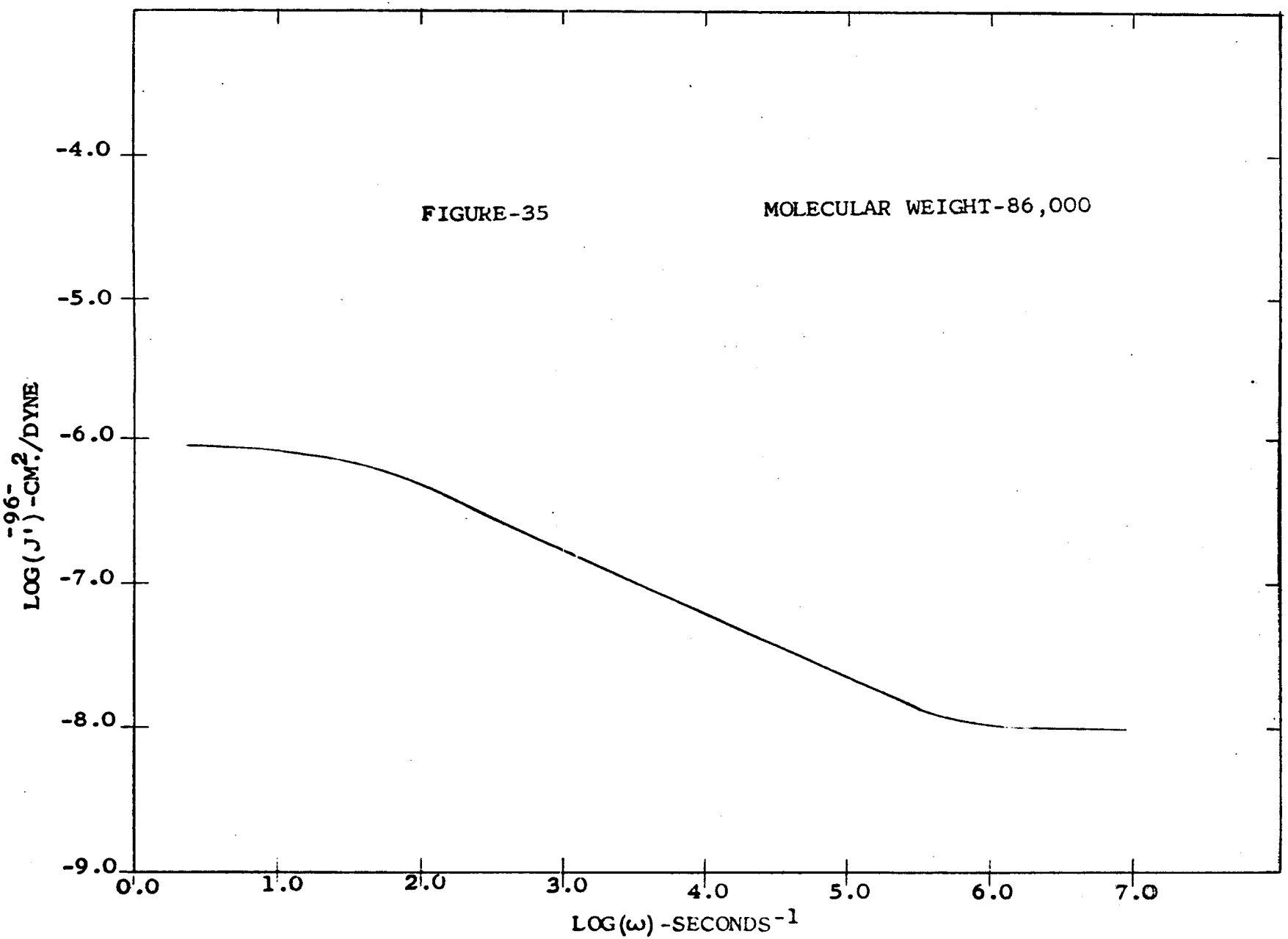
FIGURE-35
MOLECULAR WEIGHT-86,000
-4.0
-5.0
-6.0
-7.0
-8.0
-9.0
LOG(J') -96- -CM.2/DYNE
0.0
1.0
2.0
3.0
4.0
5.0
6.0
7.0
LOG(ω) -SECONDS-1

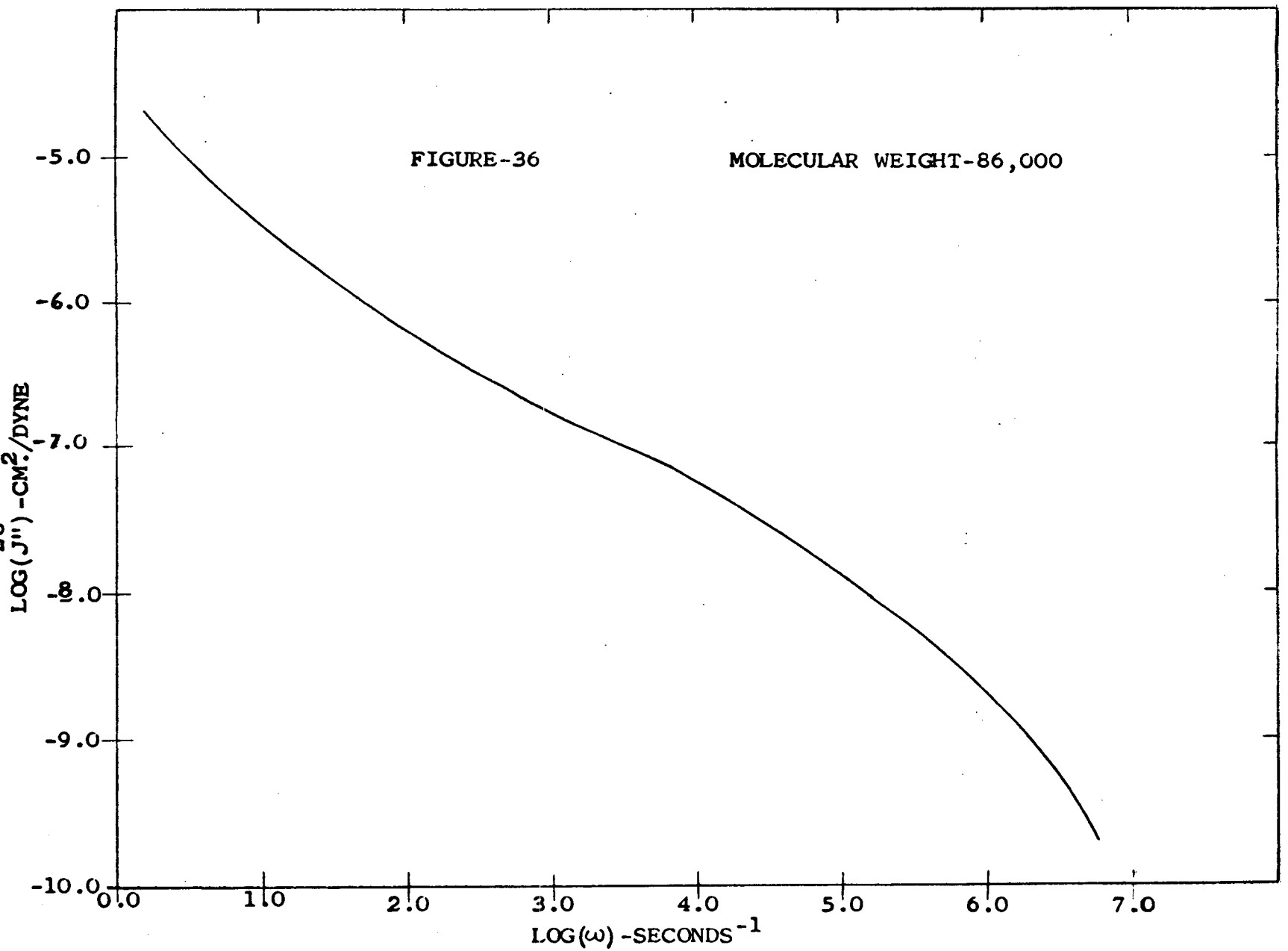
FIGURE-36
MOLECULAR WEIGHT-86,000
-5.0
-6.0
-7.0
-8.0
-9.0
-10.0
LOG(J'') -CM.2/DYNE
0.0
1.0
2.0
3.0
4.0
5.0
6.0
7.0
LOG(ω) -SECONDS-1

Appendix III: Outline of Computer Program to Calculate Linear Viscoelastic Functions.

The modification of Rouse's theory to include the effects of entanglements is

$$\zeta_p = \sigma_o^2 f_o \Big/ \left\{ 24\ n\ k\ T\ Qe\ SIN^2\left[P\pi/(2N+2) \right] \right\} \qquad (C.8)$$

where

$$\sigma_o\ f_o = 36(\eta - \eta_s)/N^2 \qquad (C.9)$$

and

$$Qe = \left[M/(2\ Me) \right]^{\kappa} \qquad (C.10)$$

$$\kappa = 2.4\ EXP\left[E_1(P-Pe) \right] \Big/ \left\{ 1 + EXP\left[E_1(P-Pe) \right] \right\} \qquad (C.11)$$

$$Pe = M/(2\ Me)\ . \qquad (C.12)$$

The relaxation times characterize the system entirely and yield directly the viscoelastic functions. They are given by (2.a, 2.b)

$$G(t) = n\ k\ T \sum_{p=1}^{N} EXP(-t/\zeta_p) \qquad (C.13)$$

$$G'(\omega) = n\ k\ T \sum_{p=1}^{N} \left[\omega^2 \zeta_p^2 / (1 + \omega^2 \zeta_p^2) \right] \qquad (C.14)$$

$$G''(\omega) = n\ k\ T \sum_{p=1}^{N} \left[\omega\ \zeta_p / (1 + \omega^2 \zeta_p^2) \right] \qquad (C.15)$$

$$J'(\omega) = G'(\omega) \Big/ \left[G'(\omega)^2 + G''(\omega)^2 \right] \qquad (C.16)$$

$$J''(\omega) = G''(\omega) \Big/ \left[G'(\omega)^2 + G''(\omega)^2 \right] \qquad (C.17)$$

$$\eta'(\omega) = G''(\omega)/\omega \qquad (C.18)$$

$$\eta''(\omega) = G'(\omega)/\omega\ . \qquad (C.19)$$

The relaxation spectrum is given exactly by

$$H(\zeta) = n\ k\ T \sum_{p=1}^{N} \zeta_p \delta(\zeta - \zeta_p)\ . \qquad (C.20)$$

We approximated the delta-function with a sharp Gaussian and evaluated the relaxation spectrum by

$$H(\tau) = n\,k\,T \sum_{p=1}^{N} (C/\sqrt{\pi})\,EXP\left\{\left[(\tau/\tau_p) - 1\right]^2 C^2\right\}. \quad (C.21)$$

The constant,C, was set equal to 4 for our calculation.

Appendix IV: The Physical Constants for Figure 6.

Table VI lists the physical constants required to calculate the Entanglement Coupling Function using the arc tangent modification (Equation A.51).

Table VI: Physical Constants for Figure 6.

Molecular Weight	85,600
Molecular Weight between Entanglements	1,650
Number of Subchains	205
Critical Index	26
Parameter Value (E_2)	0.001, 0.1, 0.5, 10
Entanglement Coupling Function	A.52

Appendix V: Use of Chiakahisa's Theory

Chiakahisa (24.) derives

$$\eta = b_1 M + b_2 M^3 \quad (C.22)$$

for relating viscosity to molecular weight. The constants b_1 and b_2 were used as adjustable parameters to obtain the

best fit of the data by a least-square analysis below Mc to evaluate b_1 and above Mc to evaluate b_2. The determination of these constants yielded the equation

$$\eta = 9.053 \times 10^{-4} M + 4.103 \times 10^{-12} M^3 \qquad (C.23)$$

with the viscosity given in poises. This satisfies the criteria developed by Chiakahisa that

$$b_1 \gg b_2 . \qquad (C.24)$$

We note that these constants cannot yet be calculated from first principles.

Appendix VI: The Influence of Length of Subchain on Viscoelastic Functions.

Two cases were compared where the subchain length of one was double the subchain length of the other having other identical physical constants. Table VII shows the data employed to calculate the viscoelastic function for the two cases.

Table VII: Data for Testing the Influence of Subchain Length

Case Number	II.a	II.b
Molecular Weight	750,000	750,000
Molecular Weight between Entanglements	31,500	31,500
Viscosity of Polymer (poises)	203,000	203,000
Viscosity of Solvent (poises)	0.0	0.0
Number of Subchains	288	144
Critical Index	12	12
Temperature (^{o}K)	490	490
Number of Molecules per Cubic Centimeter	7.73×10^{17}	7.73×10^{17}
Parameter (E_1)	0.5	0.5
Entanglement Coupling Function	A.51	A.51

The relaxation spectra for these two cases are shown in Figure 37. They do not deviate until they approach glassy response for the system. Here, the theory of Rouse is invalid. Thus, the spectrum is independent of the number of subchains in the region where the theor is valid.

Appendix VII: The Continuous Relaxation Spectrum from Rouse's Theory

The general viscoelastic function is written as

$$F(\xi) = \int_{o}^{\infty} \left[H(\tau)/\tau\right] f(\xi\tau) \, d\tau \qquad (C.25)$$

FIGURE-37 MOLECULAR WEIGHT-750,000

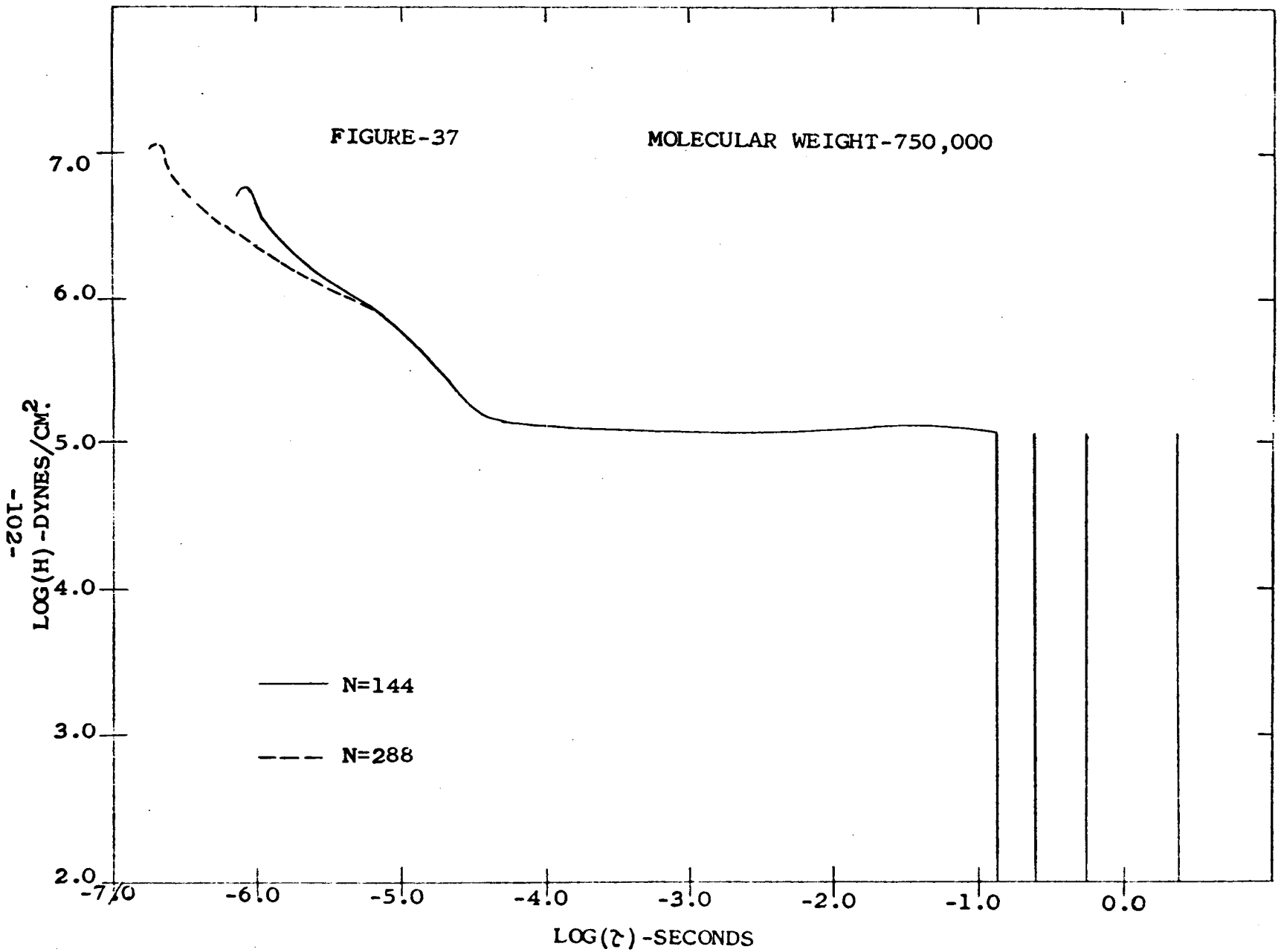

or

$$F(\tau) = \sum_i G_i f(\xi\tau) \qquad (C.26)$$

where ξ is a dummy variable equal to either $1/t$ or ω. If the relaxation times are sufficiently close, the term $G_i f(\xi\tau)$ can be replaced by $\rho(\tau) f(\xi\tau) d\tau$ with $\rho(\tau)$ considered a density of τ and the summation replaced by integration. Then, from Equation C.26, it follows that:

$$\sum_i G_i f(\xi\tau) = \int_0^\infty \rho(\tau) f(\xi\tau)\, d\tau \qquad (C.27)$$

and

$$H(\tau) = \tau \rho(\tau). \qquad (C.28)$$

The relaxation times for Rouse's theory may be written as

$$\tau_p = \tau_1 / p^2 \qquad (C.29)$$

with

$$\tau_1 = a^2 Z_1^2 \xi_0 / (6\pi^2 kT) \qquad (C.30)$$

from Equation A.27. The Rouse theory assumes that

$$G_i = nkT. \qquad (C.31)$$

With the density of relaxation times given by

$$\rho(\tau) = G_i \left| dP/d\tau \right| \qquad (C.32)$$

and with

$$dP/d\tau = -(1/2) (\tau_1)^{1/2} / (\tau)^{3/2}, \qquad (C.33)$$

substituting these into Equation C.28 yields

$$H(\tau) = nkT(\tau_i)^{1/2}/(2\tau^{1/2}). \qquad (C.34)$$

Thus, Rouse's theory for closely spaced relaxation times predicts that the log (H) versus log (τ) plot is a wedge with a slope of -1/2 which corresponds approximately to the experimentally determined slope of the wedge (3., 4., 5.).

Notation

A - Constant.

B - Constant.

C - Constant.

D - Constant.

E_1 - Constant of Equation A.51.

E_2 - Constant of Equation A.52.

$F(\tau)$ - Function of shear stress.

G(t) - Shear relaxation modulus.

G^* - Complex dynamic shear modulus.

G' - Shear storage modulus.

G'' - Shear loss modulus.

$(G'')_{max}$ - Maximum in loss modulus.

G_i - Spring constant of Maxwell element.

G_e - Equilibrium modulus.

H - Relaxation spectrum.

I(m) - Tabulated function of m.

J^* - Complex dynamic compliance.

J_e - Pseudo-equilibrium compliance.

J' - Shear storage compliance.

J'' - Shear loss compliance.

$(J'')_{max}$ - Maximum in loss compliance.

K_T - Constant this is a function of temperature.

L - Retardation spectrum.

M - Molecular Weight.

Mc - Critical Molecular Weight.

Me - Molecular Weight between entanglements.

Mo - Monomer molecular weight.

N - Number of submolecules in a macromolecule.

NA - Avogradro's number.

P - Index.

Pe - Index for entanglements.

Qe - Entanglement coupling function.

R - Gas constant.

$\langle S_o^2 \rangle_{AV.}$ - Average square end-to-end distance of an unperturbed macromolecule.

T - Temperature.

Tg - Glass transition temperature.

Z - Number of backbone atoms in a polymer chain.

Zc - Critical number of backbone atoms in a polymer chain.

Z_1 - Degree of polymerization.

a_T - Temperature shift factor.

a - Effective root-mean-square end-to-end distance of one repeat unit.

b_1, b_2 - Constants of Equation A.42.

c_1^g, c_2^g - Coefficients in WLF equation referred to T_g as reference.

c_1^o, c_1^o - Coefficients in WLF equation referred to T_o as reference.

f - Fractional free volume.

f_g - Fractional free volume at T_g .

f_o - Transitional friction coefficient of a submolecule.

k - Boltzmann's constant.

m - Negative slope of log-log plot of relaxation spectrum versus relaxation time.

n - Number of molecules per Cubic Centimeter.

t - Time.

v - Free volume.

α - Function of molecular weight.

α_f - Thermal expansion of free volume relative to total volume.

β - Constant.

γ_o - Constant shear stress.

$\gamma(t)$ - Time varying shear strain.

γ^* - Sinusoidally time varying shear strain at an angular frequency of ω radians per second.

$\dot{\gamma}$ - Rate of strain.

δ - Dirac delta function.

Δ - Logarithmic decrement of plateau region of the relaxation spectrum.

ϵ - Constant.

η^* - Complex dynamic viscosity.

η' - Real part of the complex dynamic viscosity.

η'' - Imaginary part of the complex dynamic viscosity.

η_g - Steady-state viscosity at T_g .

η - Steady-state viscosity at zero shear rate.

η_s - Solvent viscosity.

κ - Exponential function in the entanglement.

λ - Constant.

ξ_o - Translational friction coefficient per monomer unit.

ρ - Density.

$\rho(\gamma)$ - Density of γ .

τ_o - Constant shear stress.

$\tau(t)$ - Time varying shear stress.

τ^* - Sinusoidally time varying shear stress at an angular frequency of radius per second.

σ - Root-mean-square end-to-end distance of a submolecule.

τ_p - Relaxation time.

ω - Frequency.

$u(t)$ - Step function.

References

1.a Eirich, Frederich R.(ed): Rheology: Theory and Applications, Vol. II, Chapter II, New York; Academic Press, 1960.

1.b Eirich, Frederich R. (ed.): Rheology: Theory and Applications, Vol. I, Chapter I, New York; Academic Press, 1960.

1.c Eirich, Frederich R. (ed.): Rheology: Theory and Applications, Vol. I, Chapter XII, New York; Academic Press, 1960.

2.a Ferry, John D.: Viscoelastic Properties of Polymers, Chapter X, New York; John Wiley and Sons, Inc., 1961.

2.b Ferry, John D.: Viscoelastic Properties of Polymers, Chapter III, New York; John Wiley and Sons, Inc., 1961.

2.c Ferry, John D.: Viscoelastic Properties of Polymers, Chapter IV, New York; John Wiley and Sons, Inc., 1961.

3. Porter, Roger S. and Johnson, Julian F.: Chemical Reviews, 66: 1; 1966.

4. Haijah, Shizuo: Journal of the Physical Society of Japan, 19: 2306, 1964.

5. Tobolsky, Arthur V., Mercurio, A. and Murakami, A.: Journal of Colloid Science, 13: 196, 1958.

6. Murakami, Kenkichi, Nakamura, Shiga, and Sobue, Hiroshi: Zairyo, 14: 316, 1965.

7. Tobolsky, Arthur V. and Aklonsis, J. J.: Journal of Physical Chemistry, 68: 1970, 1964.

8. Flory, Paul J.: Principle of Polymer Chemistry, Ithaca: Cornell University Press, 1953.

9. Boon, J., Challa, G., and Hermans, P. H.: Makromolecular Chemie, 74: 129, 1964.

10. Malkin, A. Ya. and Vinogradov, G. V.: Polymer Science (U.S.S.R.), 7: 1252, 1965.

11. Johnson, Julian F. and Porter, Roger S.: Journal of Applied Physics, 32: 2326, 1961.

12. Fox, Thomas G. and Flory, Paul J.: Journal of Polymer Science, 14: 315, 1954.

13. Cox, W. P. and Ballman, R. S.: Journal of Applied Polymer Science, 4: 121, 1960.

14. Tobolsky, Arthur V., Schoffhauser, R., and Bohme, R.: Journal of Polymer Science, Pt.B2: 103, 1964.

15. Rudd, John F.: Journal of Polymer Science, 44: 459, 1960.

16. Rouse, Prince E.: The Journal of Chemical Physics, 21: 1272, 1953.

17. Nakada, Osamu: The Journal of the Physical Society of Japan, 10: 804, 1955.

18. Bueche, F.: The Journal of Chemical Physics, 22: 603, 1954.

19. Williams, Malcolm L.: Journal of Polymer Science, 62: S7, 1962.

20. Bueche, F.: The Journal of Chemical Physics, 20: 1959, 1952.

21. Bueche, F.: The Journal of Chemical Physics, 25: 603, 1956.

22. Ferry, John D., Landel, R. F., and Williams, Malcolm L.: Journal of Applied Physics, 26: 359, 1955.

23. Bueche, F. and Kelley, Frank N.: Journal of Polymer Science, 45: 267, 1960.

24. Chikahisa, Yosiaki: Journal of the Physical Society of Japan, 19: 92, 1964.

25. Bueche, F.: Physical Properties of Polymers, New York: Interscience Publishing, 1962.

26. Fox, Thomas G. and Allen, Vernon R.: Journal of Chemical Physics, 41: 337, 1967.

27. Bergen, John T.(ed.): Viscoelasticity: Phenomenological Aspects. New York; Academy Press, 1960.

28. Smith, Thor L.: Transactions of the Society of Rheology, 2: 131, 1958.

29. Boon, M. and Green, H. S.: Proceedings of the Royal Society, A 188: 10, 1946.

30. Flory, Paul J. and Fox, Thomas G.: Journal of Applied Physics, 21: 581, 1950.

31. Tobolsky, Arthur V., Aklonsis, J. J., and Akovali, G.: Journal of Chemical Physics, 42: 723, 1965.